May 2016

Effects of substrate stiffness on bacterial biofilm formation

Fangchao Song
Syracuse University

Effects of Substrate Stiffness on Bacterial Biofilm Formation

Abstract

Biofilms are communities of microbial cells attached on surfaces and embedded in a self-produced extracellular matrix comprised of polysaccharides, DNA, and proteins. Biofilms of pathogenic bacteria cause serious chronic infections due to high tolerance to antibiotics and host immune systems compared to their planktonic compartments. Biofilm formation is known to be influenced by many properties of substrate materials, such as surface chemistry, hydrophobicity, roughness, topography, and charge. However, few studies have been conducted to investigate the effects of substrate stiffness. In this study, *Escherichia coli* RP437 and *Pseudomonas aeruginosa* PAO1 were used as model strains to investigate the early stage biofilm formation on poly(dimethylsil-oxane) (PDMS) with varying stiffness of 0.1 MPa to 2.6 MPa, which were prepared by controlling the degree of crosslinking.

An inverse correlation between cell adhesion and substrate stiffness was observed for both *E. coli* and *P. aeruginosa*. Interestingly, it was found that the cells attached on relatively stiff substrates were significantly shorter than those on relatively soft substrates, and the distribution of cell length was narrower on stiff substrates. In addition to the difference in size, the cells on stiff substrates were also found to be less susceptible to antimicrobials, such as ofloxacin, ampicillin, tobramycin and lysozyme, than the cells attached on soft substrates. The cell tracking results revealed that the *E. coli* cells on stiff surfaces were more mobile than those on soft surfaces, suggesting that the cells attached on soft surfaces may enter biofilm stage faster.

Consistently, the intracellular level of c-di-GMP (an important signal for biofilm formation) in the cells on soft surfaces was higher than that of cells on stiff surfaces.

Comparison of the wild-type strains and isogenic mutants revealed that the *motB* mutant of *E. coli* RP437 has defects in response to the stiffness of PDMS, which was rescued by complementation of the *motB* gene. Additionally, the cell tracking results indicate that the mutation of *motB* rendered the cells much less mobile compared to wild type *E. coli* RP437 strains, and the decrease in the velocity of motility is higher on stiff surfaces than on soft surfaces. Those results suggest that *motB* may play a role in mechanosensing of material stiffness by *E. coli*. Similarly, mutation of *oprF* in *P. aeruginosa* also caused major defects in response to PDMS stiffness and abolished the difference in adhesion, growth, morphology and antibiotic susceptibility of attached cells between soft and stiff PDMS surfaces. These defects were rescued by genetic complementation of *oprF*, suggesting that *oprF* is involved in mechnosensing of *P. aeruginosa*.

In summary, the findings from this study indicate that material stiffness has potent effects on bacterial adhesion and the physiology of attached cells. To our best knowledge, this is the first study on the effects of material stiffness of silicon-based polymers on biofilm formation, and the first report of the effects of material stiffness on the physiology of attached cells. These results are helpful for designing better anti-fouling and anti-microbial materials.

EFFECTS OF SUBSTRATE STIFFNESS ON BACTERIAL BIOFILM FORMATOIN

By

Fangchao Song

B.S. Chemical Engineering, Shandong University, 2007
M.S. Chemical Engineering, Zhejiang University, 2010

DISSERTATION

Submitted in partial fulfillment of the requirements for the
degree of Doctor of Philosophy in Chemical Engineering
in the Graduate School of Syracuse University

May 2016

In memory of

my beloved grandfather, Zeqin Song

&

my beloved grandmother, Lianying Zhang

Acknowledgements

I would like to express my gratitude to my research advisor, Prof. Dacheng Ren, for his generous supports, constructive advice and encouragement during my Ph.D. research. I really appreciate the countless time he spent on my research and writing, and the invaluable knowledge he taught me.

I would also like to thank the committee members in my proposal and dissertation defense, Prof. Anthony Garza, Prof. Patrick Mather, Prof. James Henderson, Prof. Shikha Nangia, Prof. Pranav Soman, and Prof. Ashok Sangani to their invaluable discussions and suggestions to my research.

This work cannot be accomplished without so many generous helps. I want to thank Megan Brasch for her help with the ACT*IV*E tracking code, Huiyu Shi and Dr. Shiril Sivan for their help with phagocytosis, Robert Smith and Dr. Qiong Song at SUNY-ESF for helping with SEM and DMA, respectively. I want also to acknowledge Dr. John Parkinson at the University of Utah, Dr. Thomas Wood at Pennsylvania State University, Dr. Arne Heydorn and Søren Molin at the Technical University of Denmark, Dr. Jeremy Gilbert at Syracuse University, and Dr. Gary Chan at SUNY-Upstate, for sharing the bacterial strains and macrophage cell lines. And I also appreciate the advice given by Dr. Gary Winslow and Dr. Steven Taffet at SUNY-Upstate for phagocytosis.

My grateful thanks also go out to all the group members in Ren lab. I am pleasure to work with Dr. Jianchuan Pan, Dr. Tagbo Roland Herman Niepa, Dr. Huan Gu, Dr. Geetika Choudhary, Dr. Ali Adem Bahar, Dr. Xiangyu Yao, Grace Altimus, Li Zhang, Nicholas Kelly, Hao Wang, Xuan Cheng, Bo Peng, Sang Won Lee, Yanrui Zhao, Shuyuan Ma, Xinran Song, Huiqing Zheng, Xi Chen, Jing Wang, Chanokpon Yongyat, Kris Kolewe, Daxi Li, Plansky Hoang, Robert Neiberger, Gregory Bassani, Tyler Bender, Henry Peterson, Ginger Star Gunnip, Meagan Garafalo, Laura Snepenger, Jennifer Puthota, Haseeba Syed, and Srujana Govindarajulu. I sincerely appreciate your helps in my daily lab work.

I would also like to acknowledge the kind helps provided by Dawn Long, Sabina Redington, Kristin Lingo, Lynore de la Rosa, Karen Low, Barbara Walton, Jason Markle, Richard Chave, William Dossert, Neil Jasper, Jim Spoelstra, Chris Stathatos, and Mario Montesdeoca. And I want to express my thanks to the financial supports from the U.S. National Science Foundation and the Department of Biomedical and Chemical Engineering at Syracuse University.

Finally, I wish to thank my family and my friends for their love, support and encouragements. Special thanks are given to my parents Chanjun Song, Dongling Zhang, and my wife, Xiaole Sunny Ni, for your endless love, support, encouragement, and patience.

Table of Contents

List of Figures

of *E. coli* RP437 cells on PDMS surfaces. Cells were stained with acridine orange. Top: green fluorescence images indicating the amount of DNA in attached cells. Middle: red fluorescence images indicating the amount of RNA in attached cells. Bottom: DIC images (Bar = 2 μm). (B) Average lengths of *E. coli* RP437 cells attached on PDMS surfaces with different moduli. The cell length was found to be inversely correlated with surface stiffness ($r = -0.44$, $p < 0.001$, Pearson correlation analysis). (C) Distribution of the length of attached *E. coli* RP437 cells on PDMS surfaces with varying stiffness. (D) Bright field images of detached *E. coli* RP437 biofilm cells (Bar = 2 μm). (E1&2) Representative SEM images of *E. coli* RP437 cells attached to 40:1 PDMS (E1) and 5:1 PDMS (E2) (Bar = 1 μm). (E3) Average length of attached cells calculated from SEM images. ***$p < 0.001$, versus 40:1 PDMS (*t* test).

Figure 2.5 Length of *E. coli* RP437 cells on 40:1 PDMS and 5:1 PDMS surfaces. Biofilm cultures were inoculated with 4 × 107 cells/mL and incubated for 2 h for attachment. Then the PDMS surfaces were transferred to LB medium (at t = 0 h) for biofilm growth. The lengths of biofilm cells were found to be significantly different between 40:1 PDMS and 5:1 PDMS surfaces during 24 h of growth ($p < 0.001$, *t* test, for all time points up to 24 h except for t = 0 h).

Figure 2.6 Effects of PDMS stiffness on the susceptibility of *E. coli* RP437 to antibiotics. (A) Number of cells before and after treatment with 5 μg/mL ofloxacin (Ofl). The bars represent the number of cells based on CFU. The red dots represent the percentage of cells that survived the treatment, which increased with surface stiffness ($r = 0.58$, $p < 0.001$, Pearson correlation analysis). (B) Susceptibility of detached biofilm cells to 0.5 and 1 μg/mL ofloxacin. Biofilm cells on 40:1 PDMS and 5:1 PDMS surfaces were detached by sonication before being treated with ofloxacin. (C) Relative number of biofilm cells that survived the treatment with 100 μg/mL ampicillin (Amp) or 20 μg/mL tobramycin (Tob). (D) Effects of PDMS stiffness on the susceptibility of *E. coli* RP437 to 1.5 mg/mL lysozyme. *$p < 0.05$, versus 40:1 PDMS (*t* test).

Figure 2.7 Effects of surface stiffness on biofilm formation, cell length, and antibiotic susceptibility of *P. aeruginosa* PAO1 cells. (A) Effects of inoculum cell density and PDMS stiffness on attachment. (B) Number of attached *P. aeruginosa* PAO1 cells on 40:1 PDMS

List of Tables

Chapter 1
Introduction

1.1 Antimicrobial resistant infections, biofilms and persisters

Antimicrobial resistant infection is one of the biggest challenges to the public health. As reported by the Center for Disease Control and Prevention (CDC) in 2013, at least 2 million people suffer antimicrobial resistant infection annually in the U.S. with more than 23,000 death each year.[1] World Health Organization (WHO) stated in 2014 that "the resistance to common antibiotics has reached alarming levels in many parts of the world and that in some setting, few, if any, of the available treatments options remains effective for common infections."[2] There are two primary mechanisms of antimicrobial resistance: the acquired mechanism based on drug resistant genes that could be shared by different bacterial species and the intrinsic mechanism due to the formation of multicellular structure known as biofilm.

Biofilms are complex structures comprised of surface attached bacterial cells embedded in an extracellular matrix consisting of polysaccharides, proteins, DNA, and lipids. With high-level tolerance to antimicrobials and disinfectants, biofilm infections associated with indwelling

medical devices normally are chronic with recurring symptoms. As the development of biofilm research, two fundamental mechanisms which cause biofilm-associated antimicrobial-resistant infection have been proposed.[3]

One mechanism of biofilm-associated antibiotic tolerance arises from the failure of the antimicrobial agent to fully penetrate the biofilm. Biofilm matrix is a three dimensional highly complex hydrated extracellular polymeric substance containing both proteins, nucleic acids, lipids, and enzymes produced by bacteria, as well as ions and other substances from the environment.[4] Antimicrobial agents could be either hindered or neutralized by the biofilm matrix components. This mechanism has been demonstrated with experimental data of the penetration of hydrogen peroxide into a catalase-positive biofilm.[5] Consistently, a reactive diffusion model has been successful developed to describe the diffusion of antibiotics through biofilm matrix.[6]

Another cause of antibiotic tolerance is nutrient depletion and environmental stress within the biofilm leading to slow growth, dormancy and highly tolerant subpopulation called persister cells. Persister cells are a small population of bacteria, which is highly tolerant to antibiotics due to phenotype variations rather than genetic mutations. The first description of persisters was made by Joseph Bigger in 1944 when he studied the killing of *Staphylococcus* spp. by penicillin.[7] It was found that there were always a small amount of bacterial cells that cannot be killed by penicillin even when the majority of population was lysed. Such surviving cells are not mutants with ampicillin resistant genes, because when they are treated with ampicillin after re-grown in the absence of ampicillin, a similar number of cells survive like the first treatment.

Although the mechanism is not fully understood, a number of conditions have been found to induce persister formation such as the lack of nutrients and the abundance of toxin.[8]

Biofilm are up to 1000 times more tolerant to antimicrobial agents than planktonic cells of the same makeup. Biofilm associated infections are normally chronic, recurrent, and very difficult to eradicate. Thus, biofilms are involved in 80% of all bacterial infections in humans which result in around 100,000 deaths and 28-45 billion dollars of cost each year in the U.S. alone.[9,10] Although increasing use of intravenous catheters, prosthetic heart valves, joint prostheses, peritoneal dialysis catheters, cardiac pacemakers, cerebrospinal fluid shunts and endotracheal tubes have saved millions of lives, the intrinsic risk of biofilm associated infections have been increasing every year, posing an urgent need for new control methods and non-fouling materials. Besides the vital diseases, biofilm formed on tooth surfaces, called dental plaque, is responsible for major dental diseases, such as periodontitis, caries, and dental implant failure. Biofilms also play an important role in eye infections causing vision impairment and even blindness. In addition to medical problems, biofilm on ship hulls and heat exchangers etc. causes increased energy consumption and equipment damage, which put a heavy burdon on our economy.

Given the broad spectrum of problems caused by biofilms, it is important to understand the mechanism of biofilm formation. As shown in Figure 1.1, biofilm formation is a dynamic process including attachment, micro-colony formation, maturation, and dispersion. Since biofilm formation is based on bacteria-surface interaction, the properties of the substrate material are critical to biofilm formation, especially the initial attachment and micro-colony

formation. After bacterial cells are brought to the surface by fluid stream and motility, these cells use extracellular organelles, such as flagella, fimbriae and outer membrane proteins to sense and overcome the repel force between bacteria and the surface. After the attachment, pili or outer membrane proteins, as well as the polysaccharides produced by attached cells, will enhance the binding of bacteria to the surface. This process enables the transition from reversible attachment to irreversible attachment. Many genes are involved in the regulation of biofilm formation, such as flagella genes, *motA*, *motB*, *fliC*; fimbriae genes, *fimA*, *pilA*; Wsp pathway genes, *fleQ*, *wspR*, *wspC*, as well as coding for surface proteins, *sadC*, *oprF*, *oprE*. A number of signaling molecules have been shown to be involved in the biofilm formation, such as the quorum sensing signals Autoinducer I (AI) and the messenger molecule cyclic di-GMP (c-di-GMP).

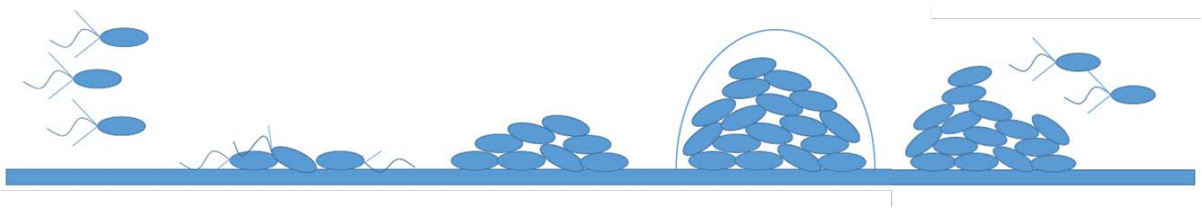

Figure 1.1 The dynamic process of biofilm formation.

1.2 Effects of material properties on biofilm formation

As a process of bacteria-surface interaction, biofilm formation is known to be influenced by many factors of the surface (Figure 1.2), such as surface chemistry,[11-14] hydrophobicity,[15,164] roughness,[17,18] topography,[19-22] and charge.[11,23] and some theories and models have been proposed to explain the observed phenomena. Here, we summarize the major effects of surface properties on biofilm formation known to date.

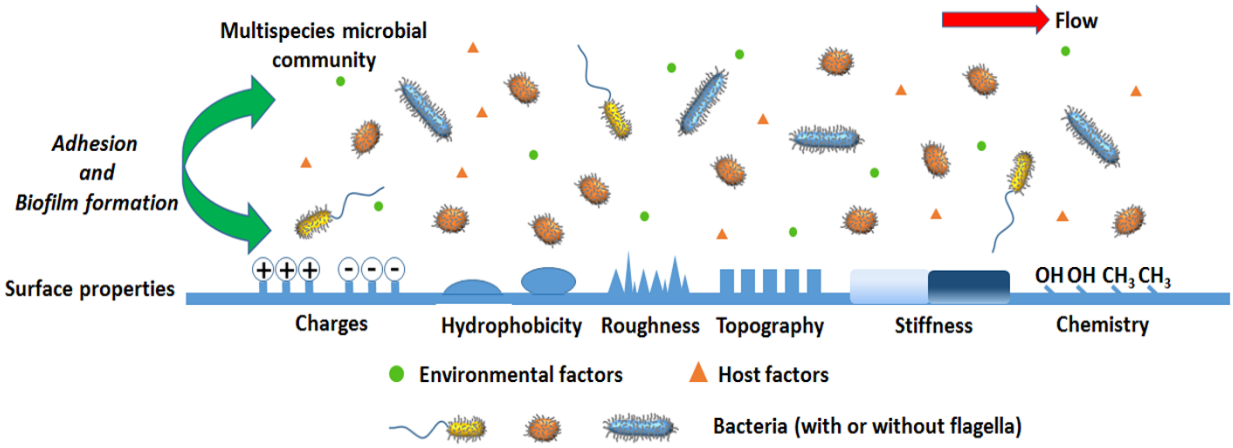

Figure 1.2 Schematic illustration of bacterial adhesion and the effects of material properties in complex environments. Reprinted with permission from Song et al. (2015).[24]

1.2.1 Surface charges

Surface charge plays an important role in determining the binding force between bacteria and the surface, and it has long been known to affect biofilm formation. Most bacterial cells are negatively charged; thus, in general, a positively charged surface is more prone to bacterial adhesion and a negatively charged surface is more resistant to bacterial adhesion. Meanwhile, surfaces presenting certain cationic groups, such as quaternary ammonium and polyethylenimines, have antimicrobial activities and thus can kill the attached cells [25]. In principle, controlling bacterial adhesion with surface charge may not work in static systems because the dead cells present a barrier which reduces the charge and facilitates the adhesion of other bacterial cells. However, if there are continuous shear force readily applied to remove dead cells, the positive charged surface could be effective to kill and repel biofilms, such as those in oral and ocean environments.

Recently, Terada et al.[26] introduced glycidyl methacrylate(GMA) as a linking agent to modify Polyethylene (PE) sheets with sodium sulfite (SS) and diethylamine (DEA), which create the negatively charged and positively charged surfaces respectively. It was found that *Escherichia coli* (*E. coli*) cell density on positively charged surfaces is much higher than that on negatively charged surfaces (10 times after 0.25 h incubation and 3 times after 8 h incubation). The biofilms on positively charged surfaces are also more difficult to remove by 5000 s^{-1} shear force (Reynolds number 666) compared to those on negatively charged surfaces. Both results indicate that the affinity of bacterial cells to positively charged surfaces is higher than that to negatively charged surfaces. Interestingly, it was also found that the biofilm structure on these surfaces are different; e.g., biofilms on positively charged surfaces are dense, homogeneous and uniform; while biofilms on negatively charged surfaces are sparse, heterogeneous and mushroom shaped. This finding is consistent with the results of *Pseudomonas aeruginosa* PAO1 reported by Rzhepishevska et al.[27], which showed that the mushroom shaped biofilms on negatively charged Poly(3-sulphopropylmethacrylate) (SPM) surfaces have enhanced c-di-GMP level compared to the uniform biofilms on positively charged poly(2-(methacryloyloxy)-ethyl trimethyl ammonium chloride) (METAC) surfaces. Because the c-di-GMP level is positively correlated with the production of biofilm matrix exopolysaccharides, these results suggest that *P. aerugionsa* PAO1 enhanced the attachment on negatively charge surfaces. Furthermore, Rzhepishevska et al.[27] found that the *ΔwbpA* mutant of *P. aerugionsa* PAO1, which has defects in lipopolysaccharide (LPS) synthesis, has reduced interaction with negatively charged SPM surfaces compared to the positively charged METAC surfaces. This suggested LPS is important for biofilm formation on negatively charged surfaces. In the other

hand, the charged surfaces can also kill bacteria.[28] For example, Terada et al.[26] showed that the viability of attached *E. coli* biofilm cells is dramatically reduced on positively charged surfaces, Similar results were also reported by Carmona-Ribeiro and Carrasco,[29] whose study showed that multiple cationic polymers could be assembled on surfaces to exhibit antimicrobial properties, such as quaternary ammonium, polyhexamethylene biguanide, and polyethylenimines. However, because of the electrostatically attractive nature of positively charged material surfaces, the dead cells on positively charged surfaces will stay on the surfaces, which could be favorable for the attachment of other bacterial cells.[26] Therefore, the antimicrobial property of positively charged surfaces is likely limited to the initial adhesion.

1.2.2 Hydrophobicity

Hydrophobicity is an important property of surface material which defines the affinity of the surface with water. Inspired by the lotus leaves, super hydrophobic materials can be obtained to repel water, proteins and bacteria, and thus are non-wetting and non-fouling. Based on this principle, self-cleaning surfaces have been developed.[30-40] The first method to achieve superhydrophobic surfaces is based on hydrophobic particles or film coating. Chung et al.[30] reported that the surface coverage of 9 h *P. aeruginosa* PAO1 biofilm on hydrophobic silver-perfluorodecanethiolate (AgSF) film on polystyrene coated silicon wafer was 10 time less than those on hydrophilic UV-treated AgSF film. Pernites et al.[33] made a superhydrophobic surfaces by electrodepositing a polythiophene layer on a 0.5 μm PS particle coated Au surfaces. The surface showed good repellant to fibrinogen and *E. coli* for 2 h adhesion. Another method to obtain a superhydrophobic surfaces is by controlling the microstructure of the surface. Freschauf et al.[35] made a microscale structured surface on PDMS, polystyrene, polycarbonate,

and polyethylene. The surface showed superhydrophobicity compared to their flat counterparts, which led to a significant reduction of *E. coli* DH5α attachment. Verho et al.[36] created superhydrophobic surfaces by creating microtopography on silicon surfaces to achieve Cassie wetting state, which has air trapped by the surface topography. The surfaces were shown to reduce biofouling. Loo et al.[39] used ethanol or methanol treated polyvinyl chloride (PVC) films to obtain microstructured superhydrophobic surfaces, which reduced the colonization of *P aeruginosa* PAO1. Zhang et al.[37] also reported that *staphylococcus aureus* attached more on superhydrophobic topographic TiO_2 surfaces compared to hydrophobic as well as hydrophilic TiO_2 surfaces. Super hydrophilic surfaces can also repel bacteria and resist biofouling.[41,42] It has been demonstrated that a dense layer of water molecules is formed on such surfaces, which can reduce the interaction force between cell surface and material surface. This theory, known as water layer theory, has guided the design of non-fouling materials. Brambilla et al.[38] created a hydrophilic surface of a resin blend 2,2-bis[4-(2-hydroxy-3-methacryloylpropoxy)]-phenyl propane (bisGMA), bis[2-(methacryloyloxy)ethyl]phosphate (BisMP) and 2-hydroxyethel methacrylate (HEMA), which showed a 8 time reduction of *Streptococcus mutans* biofilm formation after 24 h incubation compared to the hydrophobic resin. Treter et al.[43] found that hydrophilic Pluronic F127 coated polystyrene surfaces can inhibit 24 h *Staphylococcus epidermidis* biofilm formation by up to 90%. In addition, zwitterionic polymers, which are neutral molecules with both positive and negative charge groups, could be coated on a material surface to obtain superhydrophilicity with great non-fouling property. For example, Jiang et al.[44] used multiple zwitterionic polymers, such as polysulfobetaine and polycarboxybetaine, to obtain super hydrophilic surfaces. All of these surfaces exhibited ultra-low fouling by either

protein or bacteria. In summary, both superhydrophobic and superhydrophilic surfaces could inhibit biofilm formation but the effects are based on different mechanisms.

1.2.3 Roughness

The effects of surface roughness on bacterial adhesion and biofilm formation vary significantly with the size and shape of bacterial cells and the level of surface roughness. Thus, there is no "one-size-fits-all" rule between the surface roughness and bacterial attachment.[11] The basic understanding is that increase of surface roughness promotes bacterial attachment due to the increase in contact area between surface and bacterial cells.[45] For example, Bohinc et al.[46] reported that the biofilm formation of *E. coli*, *P. aeruginosa*, and *S. aureus* on glass was all reduced with the decrease of surface roughness from 5.8 μm to 0.7 μm. Yoda et al.[47] investigated the effect of less than 30 nm scale roughness of 5 implant biomaterials including oxidized zirconium-niobium alloy (Oxinium), cobalt-chromium-molybdenum alloy (Co-Cr-Mo), titanium alloy (Ti-6Al-4 V), commercially pure titanium (Cp-Ti) and stainless steel (SUS316L). The results indicate that bacterial attachment is faster on rough surfaces than on smooth surfaces. However, because bacterial cells are normally a few μm long and relatively rigid, there is expected to be an optimal feature size on nm scale which can reduce bacterial attachment by decreasing the contact area.[45] For example, Seddiki et al.[48] showed that the nanorough titanium surface obtained by a combination of mechanical polishing and chemical etching can reduce *E. coli* attachment by 20 times. The reduction was attributed to the decrease in the contact area due to the presence of surface features consisting of tips that had a high aspect ratio of peak height to peak width. Traditionally, roughness is calculated from the average of the amplitudes of the peak and valley on the surfaces. However, Siegismund et al.[49]

showed that such description is not sufficient to describe the 3D feature of a surface at nm scale. Poncin-Epaillard et al.[40] also found the importance of the distribution of peaks and valleys in deciding the non-fouling properties when polypropylene and polystyrene treated by RF or CF_4 plasma were used to test the adhesion of *Listeria monocytogenes*, *P. aeruginosa* and *Hafnia alvei*. Furthermore, Webb et al.[50] characterized sub-nanometrically smooth titanium surfaces using nine parameters which describe the height, shape, and distribution of the surface features in multiple ways. The results demonstrated that the roughness calculated from the amplitude of the peak and valley is not the only determinant of bacterial attachment. *S. aureus* was found to preferentially attach to less ordered surfaces with peak heights and valley depths evenly distributed. In addition to adhesion, surface roughness has been found to influence bacterial physiology. Singh et al.[51] investigated the effects of nanostructured titanium oxide on *P. aeruginosa* attachment. Besides the increase in bacterial attachment with roughness, they also found that *P. aeruginosa* cells lose their flagella on the nanostructured titanium oxide but not on smooth titanium oxide.

1.2.4 Topography

Recent advances in material and surface engineering have brought exciting opportuniites to develop sufaces with well-defined topographic patterns. These materials can be used to study bioflm formaton and help the design of non-fouling surfaces. Using PDMS with 10 μm tall square shape patterns, Hou et al.[22] revealed that *E. coli* adhesion to the top of these patterns was significant only if patterns are 20 × 20 μm or bigger for face-up surfaces and 40 × 40 μm or bigger for face-down surfaces. Also, by testing the antimicrobial property of nanopatterned surfaces of Clager cicada wings, Pogodin et al.[52] found that the wing surface covered by an

array of nano scale pillars with 200 nm heighth and 60 nm diameter has good antimicrobial properties. They also proposed a mechanism that the cell membrane stretches in the regions suspended between the pillars, if the degree of stretching is sufficient, this will lead to cell rupture and finally cell death. In addition to pattern size, different shapes of topographic patterns have also been compared. Perni et al.[20] found that cone shaped μm scale patterns of silicone could affect the adhesion of *E. coli* and *S. epidermidis*. The results showed that the patterns with 20 μm diameter and 1 μm height, and with 40 μm diameter and 9 μm height cone have less bacteria attached in 5 h compared to the pattern with 25 μm diameter and 2 μm height, and 30 μm diameter and 6 μm height cone patterns. Chebolu et al.[53] also reported ridge shaped PDMS surfaces with 60 μm width, 20 μm height and 170 μm spaces have less *E. coli* colonization in 36 h incubation compared to the smooth PDMS surfaces. Inspired by the nonfouling skins of echinoderms, Epstein et al.[54] found that the wrinkled surface could also prevent biofilm formation. By using wrinkle PDMS surfaces induced by a strain after O_2 plasma treatment, the team found that wrinkled surfaces with 1 μm valley width could reduce *P. aeruginosa* biofouling by 80% after 24 hour growth. Perera-Costa et al.[55] also investigated the effects of PDMS surfaces with topological patterns, such as protruding and receding square, circular with 5 or 10 μm length and 21 or 117 nm height, and parallel channels with 5 nm pitch and 21 or 117 nm height. Results showed that all of the features could cause 30-40% reduction in *P. aeruginosa* adhesion compared to the smooth surfaces after 30 min attachment in PBS. Manabe et al.[56] used porous polystyrene surfaces to test *P. aeruginosa* bacterial attachment. It was found that when the arrayed pores size is from 5 to 11 μm, the surface has the optimal prohibition of bacterial attachment. It was speculated that contact area is highly affected by the size of the pore. If the pore size is smaller than 3.5 μm or bigger than 11 μm, bacterial cells

have more area to attach. In addition to the aforementioned structures, some well-defined nanostructures can also lead to superhydrophobicity and reduce biofouling.[57] Xu et al.[58] showed that the submicro-size textured pillar patterns can reduce the adhesion of *S. epidermidis* on polyurethane urea (PUU) surfaces under shear stress of 2.2-13.2 dyn/cm^2, which is attributed to the super hydrophobicity afforded by the air trapped between the pillars. The size of pillar played an important role in trapping air and the results showed the inhibition of bacterial attachment only occurr on submicro-sized patterns, but not on micro-sized patterns which actually promote bacterial attachment. Graham et al.[59] introduced the concept of Engineered Roughness Index (ERI) which is based on three parameters associated with the geometry, spatial arrangement and size of topographical features. Attachment of *E. coli* TOP 10 to PDMS, glass, and titanium was found to be negatively correlated with ERI when it is less than 10. Also, all the engineered topographic surfaces reduced the bacterial adhesion compared to the smooth surfaces, and 1 μm-spaced holes exhibited the most significant reduction of 2 h *E. coli* adhesion. Besides the attachment, some surface topology can also affect the viability of attached cells. Jansson et al.[60] found the surfaces with ZnO nanorods can reduce the adhesion of *P. aeruginosa*, but not *S. epidermidis* on glass. However, ZnO showed bactericidal effects on both strains; e.g., 15 % of the attached *S. epidermidis* on ZnO nanorods was killed, which is 30 folds higher compared to the killing of cells attached on glass. In terms of the location of bacterial attachment on topographical surfaces, it has been shown that the cells prefer the valley than the top of PDMS surfaces.[20,22] Using well defined silicon nanowire array with 10 μm pitch and 300 nm height on Si (111) substrate, Jeong et al.[61] found that the majority of *Shewandla oneidensis* MR-1 cells attached directly to Si nanowires rather than the bottom of substrate after 12 h biofilm formation in minimal media; and the cells prefer to align with the Si

nanowires. Similar phenomenon was also found by Jahed et al.[62]. It was found that *S. aureus* cells could attach to the bottom of nickel nanostructures on Au surfaces and partially or fully in the holes in the nanostructured nickel pillar, which has comparable size with bacteria, showed a great success in adhesion to the pillars. In addition, Mehdi et al.[63] found that the position of attached *P. aeruginosa* cells may change as the geometry changes of the nanofiber textured surfaces. Increase in fiber diameter promotes the adhesion along the nanofibers. If the diameter of fiber is shorter than the diameter of bacteria, more bacteria lie on the nanofiber orthogonally.

2.5 Surfaces chemistry

Surfaces chemistry affects bacterial adhesion and biofilm formation by either changing the surface charge, hydrophobicity, or exhibiting antimicrobial properties. For example, Al-Radha et al.[64] found that polished partially stabilized zirconia and titanium blasted with zirconia have less adhesion of *Streptococcus mitis* and *Prevotella nigrescens* than titanium blased with zirconia, acid etched and polished titanium. Moreover, Loskill et al.[65] showed that fluoride treated hydroxyapatite have less colonizationing oral bacteria. To better understand the effects of surface chemistry, Hook et al.[66] screened the 72-h biofilm formation of *P. aeruginosa*, *S. aureus*, and *E. coli* on hundreds of the polymeric materials in a high throughput microarray format. The screening results suggest that material comprising ester and cyclic hydrocarbon moieties have good potential for reducing the attachment of pathogenic bacteria.

2.6 Bacterial response to surface properties

The results discussed above and some others in the literature suggest that bacteria have complex systems to sense and respond to environmental challenges. For example, by studying *E. coli* cells attached on 2.7 μm height hexagon topographical surfaces, it was found that *E. coli* cells use flagella to attach to the surface and overcome unfavorable surface topography [67]. However, the genetic basis of surface sensing is still poorly understood except for some studies on the general sensing of surface wetness[68] and surface contact[69]. For instance, two systems have been reported for surface sensing by *P. aeruginosa*. In the first system, the sensing of surface contact by *Sad C* leads to increase in the production of c-di-GMP, which binds to the transcriptional regulator FleQ. This interaction releases the inhibition of *pel* by FleQ and thus activates polysaccharide synthesis to form biofilm matrix.[70] Another system for surface sensing, known as the Wsp regulatory circuit, was discovered in *P. aeruginosa* recently. In this system, a membrane-bound chemoreceptor homolog WspA senses unknown surface signals (postulated to be related to mechanical stress) and phosphorylates WspR, causing an increase in c-di-GMP production and thus biofilm formation[69]. However, these studies are based on sensing of general surface contact. The mechanisms of bacterial response to specific material properties remain to be revealed.

1.3 Effects of surface stiffness on biofilm formation

1.3.1 Material stiffness.

Stiffness or rigidity, is an integrated property of object which represents the deformation of the material to an applied force. Sometimes, the inverse of stiffness is used as compliance or flexibility. The stiffness is mathematically defined as $\frac{F}{\delta}$, where F is the force applied on the material and δ is the displacement produced by the force. A more commonly used definition is

$\frac{A\,E}{L}$, where A is the surface area; L is the height; and E is the material modulus. Based on the definition, two factors influence the surface stiffness. One is intensive property E (material modulus); and another is extensive property (A and L). For flat surfaces, the surface stiffness is only related to the material modulus E.

Young's modulus is the most common used material modulus, which is defined as the ratio of stress to strain. Figure 1.3 shows a standard stress-strain curve of materials. When the strain is small, the correlation between stress and stain is linear following the Hooke's law. Young's modulus is defined as the proportionality in this zone by $k = \frac{\sigma}{\varepsilon}$, where σ is the tensile stress on the objective, and ε is the extensional strain of the objective. Therefore, the unit of Young's modulus is N/m^2, psi or Pa.

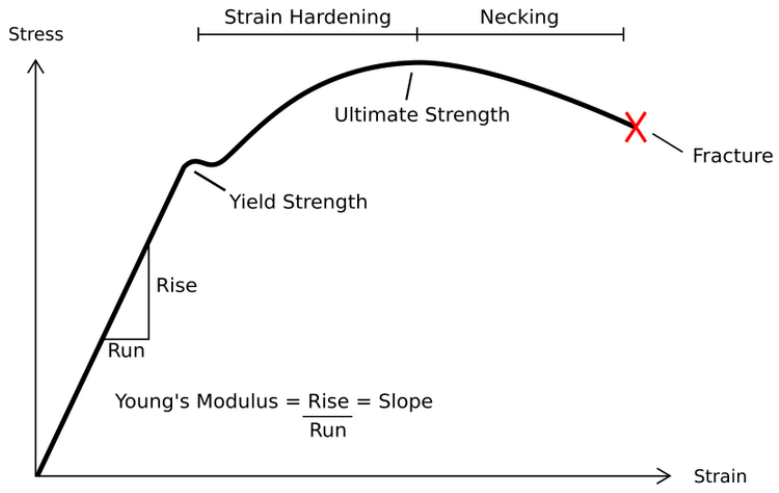

Figure 1.3 Standard stress-strain curve of materials.

(https://commons.wikimedia.org/wiki/File:Stress_Strain_Ductile_Material.pdf)

1.3.2 Effects of material stiffness on biofilm formation

As one of the mechanical properties of materials, substrate stiffness has been found to affect the shape, adhesion, proliferation, and migration of eukaryotic cells. However, compared to these well-known effects on eukaryotic cells and effects of surface chemistry, roughness, hydrophobicity on biofilm formation, the role of stiffness in biofilm formation is the least explored and only scare reports are available in the literature (Table 1.2). Bakker et al. [71] first speculated that surface stiffness may affect bacterial attachment based on the observation that *Marinobacter hydrocarbonoclasticus* attached more on glass surface with 2.2 GPa of Young's modulus than fluoridated polyurethane coated glass surface with 1.5 GPa of Young's modulus, although these two surfaces are also different in material composition. Using polyelectrolyte multilayer thin films comprised of poly(allylamine) hydrochloride and poly(acrylic acid) as a model, Lichter et. al [72] reported that the adhesion of *S. epidermidis* is positively correlated with the stiffness of this material with Young's modulus of 0.8 MPa to 80 MPa, independent of surface roughness and charge density. In addition to adhesion, *E. coli* and *Lactococcus lactis* [73] were found to grow faster on soft (Young's modulus 30 kPa) than hard (Young's modulus 150 kPa) polyelectrolyte multilayer thin films. Guegan et al.[74] also reported the increase of the stiffness of agar hydrogels from 6.6 kPa to 110 kPa promoted the biofilm formation of *Pseudoalteromonas sp. D41*. In addition to bacterial adhesion, it is also reported that there are more cell clusters formed on the soft agar surfaces (6.6 kPa) than on the stiff agar surfaces (110 kPa), and the production of outer membrane proteins (OMPs) was induced by the increase in surface stiffness.[74] The mechanism of how surface stiffness affects biofilm formation is still unclear, however, understanding these effects is important for the design of non-fouling

surfaces, which can find applications in the dental material, contact lenses, and other implanted materials.

Table 1.1 Literatures on effects of surface stiffness on biofilm formation.

Authors	Material	Strains	Process	Modulus
K.J.van Vliet et al.	Layer by layer PAA/PAH polyelectrolytes	*S. epidermidis*, *E. coli* W3100	Attachment	0.8-100MPa
Karine Glinel et al.	Layer by layer PLL/HAVB polyelectrolytes	*L. lactis* NZ3900, *E. coli* TOP10, *E. coli* MG1655E.	Growth	30 and 150kPa
J. Aizenberg et al.	Polyepoxy and polyurethanes nano pillar	*P. aeruginosa*	biofilm	20M,500M,2GPa
Henry C. van de Mei et al.	Polyurethane coating w/ or w/o F	*H. pacifica* & *M. hydrocarbonoclasticus*	Attachment	1.5GPa, 2.2GPa
C. Guegan et al.	Agarose hydrogel	*Bacillus* sp. 4J6 & *Pseudoalteromonas* sp. D41	Attachment	7kPa, 110kPa
K. Kolewe et al.	PEGDMA and agar hydrogels	*E. coli and S. aureus*	Attachment	0.1, 2, and 6MPa

1.4 Bacterial virulence and phagocytosis.

To engineer new materials for medical application, it is important to evaluate bacterial persistence, production of virulence factors and the response to host immune systems. Virulence is the degree of a pathogenicity of pathogen, which indicates the ability to invade human tissues and fatality rate. Virulence is determined by virulent factors which are important molecules produced by pathogens during infection. For example, virulence factors may help a pathogen invade or inhibit the host immune system, colonize the niche of tissues, enter host cells, and obtain nutrients from the host cells. Each pathogen produces a wide array of virulence factors, such as toxins, hemolysins, and the factors that promote colonization. The

production of virulence factors is regulated by complex systems in response to environmental conditions.

Phagocytosis is a process that phagocytes, such as macrophages, internalizes particles or pathogens and form phagolysozyme, in which the pathogen or cell debris will be digested by enzymes. Phagocytosis is an important mechanism used by the host to remove pathogen and cell debris. When an infection occurs, the virulence factors produced by the microbes stimulate the production of immune factors which could attract phagocytes to the infection site to remove the pathogens.

1.5 Materials and techniques in this study.

1.5.1 Strains.

Escherichia coli and *Pseudomonas aeruginosa* were used as the bacterial models in this study. Both of them are gram negative strains. As the most investigated strains in the field of microbiology, the physiology of *Escherichia coli* is well-known, so this strain could help us to better understand the mechanism of effect of surface. *Pseudomonas aeruginosa* is one of the most concern pathogen in hospital, which is a common cause of healthcare associated infections including pneumonia, bloodstream infections, urinary tract infections, and surgical site infections. As reported by CDC in 2013, there were estimated 51,000 persons infected by *Pseudomonas aeruginosa* in United State each year, with roughly 440 persons died per year due to this infection. To understand the biofilm formation of *Pseudomonas aeruginosa* could be directly benefit on the severe *Pseudomonas aeruginosa* infections.

Monocyte U-937 (ATCC^{R} CRL-1593.2^{TM}) was used as the macrophage model in our research. This is a macrophage like cell line originally from pleura effusion or lymphocyte or myeloid of a 37 years old male histiocytic lymphoma patient. This cell suspends in the culture and will attached on surfaces while differentiated.

1.5.2 Poly(dimethylsilloxane) (PDMS).

Previous research used polyelectrolyte multilayer (PEM). However, there are limitations of PEM about the effect of material stiffness on the biofilm formation. First, PEM is a charged surface. In particular, the PEM used in Lichter's research[72] is about 3 mC/m^2. Because the electrostatic force caused by surface charge can also affect biofilm formation, this presents a confounding factor. Second, the PEM used in previous research is a 9 nm coating on a glass substrate. In this case, the substrate under PEM may also affect the surface stiffness. Although there is no results of how deep bacteria can sense the surface mechanical properties, 9 nm thickness is relatively thin compared to the size of bacteria cells (normally 2 μm long).

Poly(dimethylsilloxane) (PDMS) is used as the model of material in this study. We chose PDMS (silicone) surfaces since it is broadly used in medical devices, such as catheters, contact lenses, and finger joint implants.[75-77] Also, unlike polyelectrolyte surface, PDMS has negligible charge;[78] thus, using this material allows the effects of surface stiffness to be specifically studied. Moreover, thickness is not a problem in this study because bulk material is used instead of thin film. Furthermore, using PDMS allows us to compare with our other biofilm studies.[22,79] In addition, the surface roughness and chemistry could also be ignored. In our study, the surfaces were polymerized in flat petri dishes. The SEM images in Chapter 2 indicate

that both soft and stiff surfaces are flat in μm scale. This is consistent with previous reports that such PDMS surfaces only have nm or sub-nm scale roughness. Eroshenoko et al.[2] reported that the roughness of 20:1 PDMS, 10:1 PDMS, and 5:1 PDMS are very similar, e.g., 0.8 nm, 0.8 nm, and 1 nm, respectively. In comparison, Wala et al. reported a slightly different result that the roughness of 20:1 PDMS (soft) and 5:1 PDMS (stiff) are 2.6 nm and 1 nm, respectively. Increase in roughness of glass surfaces in this range (from 1.6 nm to 2.8 nm) was found to cause minor inhibition of bacterial adhesion (by up to 2 fold). Thus, if the differences in our study were caused by changes in surface roughness, we would expect slightly more cell adhesion on 5:1 PDMS than on 20:1 PDMS. Jiang et al.5 measured the composition of the soft and stiff PDMS surfaces including the ones with the same base : curing agent ratios used in this study with XPS; and showed that the composition of the main elements C, O, and Si are essentially the same and the change in surface chemistry is negligible. To confirm that the difference in adhesion on the surfaces was not caused by toxicity of any leftover base or curing agent, we also conducted an additional experiment to compare the 5-h planktonic growth of E. coli RP437 at 37°C in LB medium supplemented with different concentrations of base and curing agents (0, 0.1%, 1%, and 2% tested for both). The results showed that the growth yield was not affected by either the base or curing agent ($p > 0.1$ for both, one-way ANOVA), confirming that the observed results were not caused by killing.

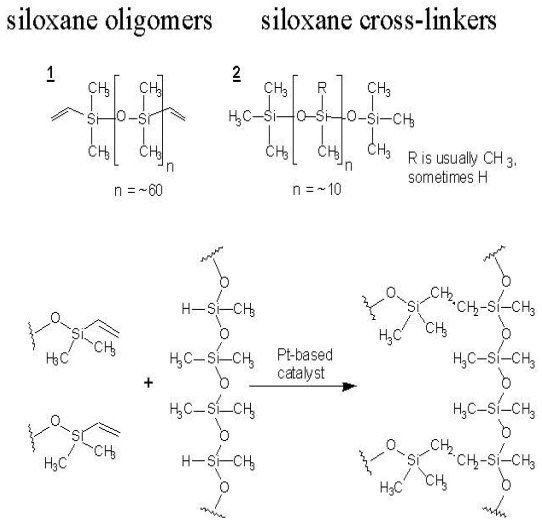

Figure 1.4 Material PDMS used in this study.

(http://education.mrsec.wisc.edu/background/PDMS)

PDMS surfaces were prepared using SYLGARD184 Silicone Elastomer Kit (Dow Corning Corporation, Midland, MI). Because the normal range of stiffness of commercial contact lenses is between 0.3-3 MPa, we chose this range of stiffness in this study. The stiffness was adjusted by varying the mass ratio of base to curing agent by following a protocol described previously.[80-82] The base:curing agent ratios (wt/wt) of 5:1, 10:1, 20:1, and 40: 1 were tested (Table 1.2). For each given ratio, elastomer base and curing agent were thoroughly mixed and degased under vacuum for 30 min. Then, the mixture was poured into a petri-dish, cured at 60^{o}C for 24 h, and incubated at room temperature for another 24 h to fully polymerize. The PDMS surface was then peeled off the petri-dish and cut into 1.0 cm by 0.6 cm pieces (1.5 mm thick), which were sterilized by soaking in 190 proof ethanol for 20 min and dried with sterile air. All of the sterilized PDMS substrates were stored at room temperature until use. The Young's moduli of PDMS surfaces were measured using dynamic mechanical analysis (DMA)

(Q800, TA instrument, DE, USA). The results indicated that the Young's moduli of 5:1 PDMS, 10: 1 PDMS, 20: 1 PDMS, and 40:1 PDMS were 2.6 ± 0.2 MPa, 2.1 ± 0.1 MPa, 1.0 ± 0.1 MPa and 0.1 ± 0.02 MPa, respectively (Table 1.2), which are similar to the values reported by Evans et al.[80] and Wang et al.[81]

Table 1.2 Material modulus used in this study.

Ratio of base:curing agent	40:1 PDMS (soft)	20:1 PDMS	10:1 PDMS	5:1 PDMS (stiff)
Young's modulus	0.1 ± 0.02 MPa	1.0 ± 0.1 MPa	2.1 ± 0.1 MPa	2.6 ± 0.2 MPa

1.5.3 Scanning Electron Microscopy (SEM)

Scanning Electron Microscopy (SEM) is an imaging technique which uses a focused beam of electron to scan the sample. Because the wavelength of electron is much shorter in comparison to photon, SEM could image as small as 1 nanometer. To image the specimens, the specimens should be dry and coated by a conductive metal such as Pt or Ag. Then electron beam will be shot on the surface by a high voltage in high vacuum environment. The secondary electrons emitted by atoms excited by the electron beam will be detected. Based on the number of secondary electrons in different angle, the surface topography will be described.

1.5.4 Flow cytometry

Flow cytometry is a technique to count the cell number based on the different properties of cells, such as size, shape, or fluorescence. As shown in Figure 1.5, the nozzle will create a single cell flow to the channel. As a laser shoot on the cell, the different scatter will tell us the

size and shape of the cell. If an excitation light was shot on the cell, the detector will get the emission light, and differentiate cells with different properties.

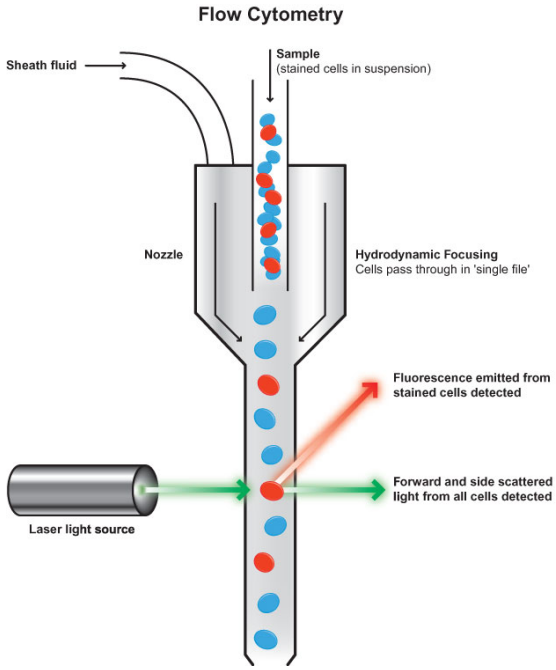

Figure 1.5 Scheme of flow cytometer. (flowcytometry.med.ualberta.ca)

1.6 Motivation and hypothesis

As shown in Introduction, the effects of surface stiffness on biofilm formation have only been scarcely explored. And previous studies[72,83] only investigated the effect of surface stiffness on bacterial attachment and growth. It is still unknown if and how surface stiffness affects the physiology of attached cells such as motility, cell morphology, antimicrobial susceptibility, and gene expression in these cells. This knowledge gap motivated us to investigate the effects of surface stiffness on biofilm formation.

We hypothesize that bacteria have complex systems to sense and respond to material stiffness during biofilm formation and interaction with host cells and tissues. In this thesis research, we conducted multidisciplinary studies to investigate the role of material stiffness in bacterial adhesion and the physiology of attached cells. Specifically, this dissertation explores the effects of material stiffness on biofilm formation of *E. coli* and *P. aeruginosa*, as well as the cell motility and phagocytosis of attached cells. The role of important genes in bacterial response to material stiffness is also explored.

An overall introduction on biofilm and known effects of material properties on biofilm formation are given in *Chapter 1*. The effects of material stiffness on biofilm formation are investigated in *Chapter 2*, including the effects on bacterial adhesion, growth, transcriptional activity, cell morphology, antimicrobial susceptibility, and phagocytosis. *Chapter 3* further investigates the cell motility on soft and stiff surfaces and reveal the role of key genes of *E. coli* in response to the material stiffness. *Chapter 4* focus on the mechanism of *P. aeruginosa* sensing surface stiffness and reveals the possible pathway of bacterial mechnosensing. The major findings of this thesis research is summarized in *Chapter 5* along with suggested further work.

1.7 References:

(1) Health, U. D. o.; Services, H. Antibiotic resistance threats in the United States, 2013. *Centers for Disease Control and Prevention, Atlanta, GA: http://www. cdc. gov/drugresistance/threat-report-2013* **2013**.

(2) Organization, W. H., *Antimicrobial resistance: global report on surveillance*. World Health Organization: 2014.

(3) Stewart, P. S.; Costerton, J. W. Antibiotic resistance of bacteria in biofilms. *The lancet* **2001,** *358*, 135-138.

(4) Flemming, H.-C.; Wingender, J. The biofilm matrix. *Nature Reviews Microbiology* **2010,** *8*, 623-633.

(5) Stewart, P. S.; Roe, F.; Rayner, J.; Elkins, J. G.; Lewandowski, Z.; Ochsner, U. A.; Hassett, D. J. Effect of catalase on hydrogen peroxide penetration into Pseudomonas aeruginosa biofilms. *Applied and Environmental Microbiology* **2000,** *66*, 836-838.

(6) Chen, X.; Stewart, P. S. Chlorine penetration into artificial biofilm is limited by a reaction-diffusion interaction. *Environmental science & technology* **1996,** *30*, 2078-2083.

(7) Bigger, J. Treatment of staphylococcal infections with penicillin by intermittent sterilisation. *The Lancet* **1944,** *244*, 497-500.

(8) Lewis, K., Multidrug tolerance of biofilms and persister cells. In *Bacterial Biofilms*, Springer: 2008; pp 107-131.

(9) Klevens, R. M.; Edwards, J. R.; Richards, C. L.; Horan, T. C.; Gaynes, R. P.; Pollock, D. A.; Cardo, D. M. Estimating health care-associated infections and deaths in US hospitals, 2002. *Public health reports* **2007,** *122*, 160.

(10) Klevens, R. M.; Morrison, M. A.; Nadle, J.; Petit, S.; Gershman, K.; Ray, S.; Harrison, L. H.; Lynfield, R.; Dumyati, G.; Townes, J. M. Invasive methicillin-resistant Staphylococcus aureus infections in the United States. *Jama* **2007,** *298*, 1763-1771.

(11) Renner, L. D.; Weibel, D. B. Physicochemical regulation of biofilm formation. *MRS bulletin* **2011,** *36*, 347-355.

(12) Cheng, G.; Zhang, Z.; Chen, S.; Bryers, J. D.; Jiang, S. Inhibition of bacterial adhesion and biofilm formation on zwitterionic surfaces. *Biomaterials* **2007,** *28*, 4192-4199.

(13) Nejadnik, M. R.; van der Mei, H. C.; Norde, W.; Busscher, H. J. Bacterial adhesion and growth on a polymer brush-coating. *Biomaterials* **2008,** *29*, 4117-4121.

(14) Hou, S.; Burton, E. A.; Wu, R. L.; Luk, Y.-Y.; Ren, D. Prolonged control of patterned biofilm formation by bio-inert surface chemistry. *Chemical Communications* **2009**, 1207-1209.

(15) Packham, D. E. Surface energy, surface topography and adhesion. *International journal of adhesion and adhesives* **2003,** *23*, 437-448.

(16) Oliveira, R.; Azeredo, J.; Teixeira, P.; Fonseca, A. The role of hydrophobicity in bacterial adhesion. **2001**.

(17) Singh, A. V.; Vyas, V.; Patil, R.; Sharma, V.; Scopelliti, P. E.; Bongiorno, G.; Podestà, A.; Lenardi, C.; Gade, W. N.; Milani, P. Quantitative characterization of the influence of the nanoscale morphology of nanostructured surfaces on bacterial adhesion and biofilm formation. *PloS one* **2011,** *6*, e25029.

(18) Díaz, C.; Cortizo, M. C.; Schilardi, P. L.; Saravia, S. G. G. d.; Mele, M. A. F. L. d. Influence of the nano-micro structure of the surface on bacterial adhesion. *Materials Research* **2007,** *10*, 11-14.

(19) Scheuerman, T. R.; Camper, A. K.; Hamilton, M. A. Effects of substratum topography on bacterial adhesion. *Journal of colloid and interface science* **1998,** *208*, 23-33.

(20) Perni, S.; Prokopovich, P. Micropatterning with conical features can control bacterial adhesion on silicone. *Soft Matter* **2013,** *9*, 1844-1851.

(21) Crawford, R. J.; Webb, H. K.; Truong, V. K.; Hasan, J.; Ivanova, E. P. Surface topographical factors influencing bacterial attachment. *Advances in Colloid and Interface Science* **2012**.

(22) Hou, S.; Gu, H.; Smith, C.; Ren, D. Microtopographic patterns affect Escherichia coli biofilm formation on poly (dimethylsiloxane) surfaces. *Langmuir* **2011,** *27*, 2686-2691.

(23) An, Y. H.; Friedman, R. J. Concise review of mechanisms of bacterial adhesion to biomaterial surfaces. *Journal of biomedical materials research* **1998,** *43*, 338-348.

(24) Song, F.; Koo, H.; Ren, D. Effects of material properties on bacterial adhesion and biofilm formation. *Journal of dental research* **2015**, 0022034515587690.

(25) Campoccia, D.; Montanaro, L.; Arciola, C. R. A review of the biomaterials technologies for infection-resistant surfaces. *Biomaterials* **2013,** *34*, 8533-54.

(26) Terada, A.; Okuyama, K.; Nishikawa, M.; Tsuneda, S.; Hosomi, M. The effect of surface charge property on Escherichia coli initial adhesion and subsequent biofilm formation. *Biotechnology and bioengineering* **2012,** *109*, 1745-1754.

(27) Rzhepishevska, O.; Hakobyan, S.; Ruhal, R.; Gautrot, J.; Barbero, D.; Ramstedt, M. The surface charge of anti-bacterial coatings alters motility and biofilm architecture. *Biomaterials Science* **2013,** *1*, 589-602.

(28) Kügler, R.; Bouloussa, O.; Rondelez, F. Evidence of a charge-density threshold for optimum efficiency of biocidal cationic surfaces. *Microbiology* **2005,** *151*, 1341-1348.

(29) Carmona-Ribeiro, A. M.; de Melo Carrasco, L. D. Cationic antimicrobial polymers and their assemblies. *International journal of molecular sciences* **2013,** *14*, 9906-9946.

(30) Chung, J.-S.; Kim, B. G.; Shim, S.; Kim, S.-E.; Sohn, E.-H.; Yoon, J.; Lee, J.-C. Silver-perfluorodecanethiolate complexes having superhydrophobic, antifouling, antibacterial properties. *Journal of colloid and interface science* **2012,** *366*, 64-69.

(31) Truong, V.; Webb, H.; Fadeeva, E.; Chichkov, B.; Wu, A.; Lamb, R.; Wang, J.; Crawford, R.; Ivanova, E. Air-directed attachment of coccoid bacteria to the surface of superhydrophobic lotus-like titanium. *Biofouling* **2012,** *28*, 539-550.

(32) Nishimoto, S.; Bhushan, B. Bioinspired self-cleaning surfaces with superhydrophobicity, superoleophobicity, and superhydrophilicity. *Rsc Advances* **2013,** *3*, 671-690.

(33) Pernites, R. B.; Santos, C. M.; Maldonado, M.; Ponnapati, R. R.; Rodrigues, D. F.; Advincula, R. C. Tunable protein and bacterial cell adsorption on colloidally templated superhydrophobic polythiophene films. *Chemistry of Materials* **2011,** *24*, 870-880.

(34) Zhang, X.; Liu, X.; Laakso, J.; Levänen, E.; Mäntylä, T. Easy-to-clean property and durability of superhydrophobic flaky γ-alumina coating on stainless steel in field test at a paper machine. *Applied Surface Science* **2012,** *258*, 3102-3108.

(35) Freschauf, L. R.; McLane, J.; Sharma, H.; Khine, M. Shrink-induced superhydrophobic and antibacterial surfaces in consumer plastics. *PloS one* **2012,** *7*, e40987.

(36) Verho, T.; Korhonen, J. T.; Sainiemi, L.; Jokinen, V.; Bower, C.; Franze, K.; Franssila, S.; Andrew, P.; Ikkala, O.; Ras, R. H. Reversible switching between superhydrophobic states on a hierarchically structured surface. *Proceedings of the National Academy of Sciences* **2012,** *109*, 10210-10213.

(37) Zhang, X.; Wang, L.; Levänen, E. Superhydrophobic surfaces for the reduction of bacterial adhesion. *RSC Advances* **2013,** *3*, 12003-12020.

(38) Brambilla, E.; Ionescu, A.; Mazzoni, A.; Cadenaro, M.; Gagliani, M.; Ferraroni, M.; Tay, F.; Pashley, D.; Breschi, L. Hydrophilicity of dentin bonding systems influences< i> in vitro Streptococcus mutans</i> biofilm formation. *Dental Materials* **2014,** *30*, 926-935.

(39) Loo, C.-Y.; Young, P. M.; Lee, W.-H.; Cavaliere, R.; Whitchurch, C. B.; Rohanizadeh, R. Superhydrophobic, nanotextured polyvinyl chloride films for delaying< i> Pseudomonas aeruginosa</i> attachment to intubation tubes and medical plastics. *Acta biomaterialia* **2012,** *8*, 1881-1890.

(40) Poncin-Epaillard, F.; Herry, J.; Marmey, P.; Legeay, G.; Debarnot, D.; Bellon-Fontaine, M. Elaboration of highly hydrophobic polymeric surface—a potential strategy to reduce the adhesion of pathogenic bacteria? *Materials Science and Engineering: C* **2013,** *33*, 1152-1161.

(41) Chen, S.; Li, L.; Zhao, C.; Zheng, J. Surface hydration: principles and applications toward low-fouling/nonfouling biomaterials. *Polymer* **2010,** *51*, 5283-5293.

(42) Zheng, J.; Li, L.; Chen, S.; Jiang, S. Molecular simulation study of water interactions with oligo (ethylene glycol)-terminated alkanethiol self-assembled monolayers. *Langmuir* **2004,** *20*, 8931-8938.

(43) Treter, J.; Bonatto, F.; Krug, C.; Soares, G. V.; Baumvol, I. J. R.; Macedo, A. J. Washing-resistant surfactant coated surface is able to inhibit pathogenic bacteria adhesion. *Applied Surface Science* **2014,** *303*, 147-154.

(44) Mi, L.; Jiang, S. Integrated Antimicrobial and Nonfouling Zwitterionic Polymers. *Angewandte Chemie International Edition* **2014,** *53*, 1746-1754.

(45) Anselme, K.; Davidson, P.; Popa, A.; Giazzon, M.; Liley, M.; Ploux, L. The interaction of cells and bacteria with surfaces structured at the nanometre scale. *Acta biomaterialia* **2010,** *6*, 3824-3846.

(46) Bohinc, K.; Dražić, G.; Fink, R.; Oder, M.; Jevšnik, M.; Nipič, D.; Godič-Torkar, K.; Raspor, P. Available surface dictates microbial adhesion capacity. *International Journal of Adhesion and Adhesives* **2014,** *50*, 265-272.

(47) Yoda, I.; Koseki, H.; Tomita, M.; Shida, T.; Horiuchi, H.; Sakoda, H.; Osaki, M. Effect of surface roughness of biomaterials on Staphylococcus epidermidis adhesion. *BMC microbiology* **2014,** *14*, 234.

(48) Seddiki, O.; Harnagea, C.; Levesque, L.; Mantovani, D.; Rosei, F. Evidence of antibacterial activity on titanium surfaces through nanotextures. *Applied Surface Science* **2014,** *308*, 275-284.

(49) Siegismund, D.; Undisz, A.; Germerodt, S.; Schuster, S.; Rettenmayr, M. Quantification of the interaction between biomaterial surfaces and bacteria by 3-D modeling. *Acta biomaterialia* **2014,** *10*, 267-275.

(50) Webb, H.; Boshkovikj, V.; Fluke, C.; Truong, V. K.; Hasan, J.; Baulin, V.; Lapovok, R.; Estrin, Y.; Crawford, R.; Ivanova, E. Bacterial attachment on sub-nanometrically smooth titanium substrata. *Biofouling* **2013,** *29*, 163-170.

(51) Singh, A. V.; Galluzzi, M.; Borghi, F.; Indrieri, M.; Vyas, V.; Podestà, A.; Gade, W. Interaction of bacterial cells with cluster-assembled nanostructured titania surfaces: An atomic force microscopy study. *Journal of nanoscience and nanotechnology* **2013,** *13*, 77-85.

(52) Pogodin, S.; Hasan, J.; Baulin, V. A.; Webb, H. K.; Truong, V. K.; Phong Nguyen, T. H.; Boshkovikj, V.; Fluke, C. J.; Watson, G. S.; Watson, J. A. Biophysical model of bacterial cell interactions with nanopatterned cicada wing surfaces. *Biophysical journal* **2013,** *104*, 835-840.

(53) Chebolu, A.; Laha, B.; Ghosh, M. Investigation on bacterial adhesion and colonisation resistance over laser-machined micro patterned surfaces. *Micro & Nano Letters, IET* **2013,** *8*.

(54) Epstein, A. K.; Hong, D.; Kim, P.; Aizenberg, J. Biofilm attachment reduction on bioinspired, dynamic, micro-wrinkling surfaces. *New Journal of Physics* **2013,** *15*, 095018.

(55) Perera-Costa, D.; Bruque, J. M.; González-Martín, M. a. L.; Gómez-García, A. C.; Vadillo-Rodriguez, V. Studying the Influence of Surface Topography on Bacterial Adhesion using Spatially Organized Microtopographic Surface Patterns. *Langmuir* **2014,** *30*, 4633-4641.

(56) Manabe, K.; Nishizawa, S.; Shiratori, S. Porous surface structure fabricated by breath figures that suppresses pseudomonas aeruginosa biofilm formation. *ACS applied materials & interfaces* **2013,** *5*, 11900-11905.

(57) Roach, P.; Shirtcliffe, N. J.; Newton, M. I. Progess in superhydrophobic surface development. *Soft Matter* **2008,** *4*, 224-240.

(58) Xu, L.-C.; Siedlecki, C. A. Staphylococcus epidermidis adhesion on hydrophobic and hydrophilic textured biomaterial surfaces. *Biomedical Materials* **2014,** *9*, 035003.

(59) Graham, M. V.; Mosier, A. P.; Kiehl, T. R.; Kaloyeros, A. E.; Cady, N. C. Development of antifouling surfaces to reduce bacterial attachment. *Soft Matter* **2013,** *9*, 6235-6244.

(60) Jansson, T.; Clare-Salzler, Z. J.; Zaveri, T. D.; Mehta, S.; Dolgova, N. V.; Chu, B.-H.; Ren, F.; Keselowsky, B. G. Antibacterial effects of zinc oxide nanorod surfaces. *Journal of nanoscience and nanotechnology* **2012,** *12*, 7132-7138.

(61) Jeong, H. E.; Kim, I.; Karam, P.; Choi, H.-J.; Yang, P. Bacterial recognition of silicon nanowire arrays. *Nano letters* **2013,** *13*, 2864-2869.

(62) Jahed, Z.; Lin, P.; Seo, B. B.; Verma, M. S.; Gu, F. X.; Tsui, T. Y.; Mofrad, M. R. K. Responses of Staphylococcus aureus bacterial cells to nanocrystalline nickel nanostructures. *Biomaterials* **2014,** *35*, 4249-4254.

(63) Kargar, M.; Wang, J.; Nain, A. S.; Behkam, B. Controlling bacterial adhesion to surfaces using topographical cues: a study of the interaction of Pseudomonas aeruginosa with nanofiber-textured surfaces. *Soft Matter* **2012,** *8*, 10254-10259.

(64) Al-Radha, A. S. D.; Dymock, D.; Younes, C.; O'Sullivan, D. Surface properties of titanium and zirconia dental implant materials and their effect on bacterial adhesion. *Journal of dentistry* **2012,** *40*, 146-153.

(65) Loskill, P.; Zeitz, C.; Grandthyll, S.; Thewes, N.; Müller, F.; Bischoff, M.; Herrmann, M.; Jacobs, K. Reduced Adhesion of Oral Bacteria on Hydroxyapatite by Fluoride Treatment. *Langmuir* **2013,** *29*, 5528-5533.

(66) Hook, A. L.; Chang, C.-Y.; Yang, J.; Luckett, J.; Cockayne, A.; Atkinson, S.; Mei, Y.; Bayston, R.; Irvine, D. J.; Langer, R. Combinatorial discovery of polymers resistant to bacterial attachment. *Nature biotechnology* **2012,** *30*, 868-875.

(67) Friedlander, R. S.; Vlamakis, H.; Kim, P.; Khan, M.; Kolter, R.; Aizenberg, J. Bacterial flagella explore microscale hummocks and hollows to increase adhesion. *Proceedings of the National Academy of Sciences* **2013,** *110*, 5624-5629.

(68) Wang, Q.; Suzuki, A.; Mariconda, S.; Porwollik, S.; Harshey, R. M. Sensing wetness: a new role for the bacterial flagellum. *EMBO J* **2005,** *24*, 2034-42.

(69) Belas, R. Biofilms, flagella, and mechanosensing of surfaces by bacteria. *Trends in microbiology* **2014,** *22*, 517-527.

(70) Hickman, J. W.; Harwood, C. S. Identification of FleQ from Pseudomonas aeruginosa as a c-di-GMP-responsive transcription factor. *Mol Microbiol* **2008,** *69*, 376-89.

(71) Bakker, D. P.; Huijs, F. M.; de Vries, J.; Klijnstra, J. W.; Busscher, H. J.; van der Mei, H. C. Bacterial deposition to fluoridated and non-fluoridated polyurethane coatings with different elastic modulus and surface tension in a parallel plate and a stagnation point flow chamber. *Colloids and Surfaces B: Biointerfaces* **2003,** *32*, 179-190.

(72) Lichter, J. A.; Thompson, M. T.; Delgadillo, M.; Nishikawa, T.; Rubner, M. F.; Van Vliet, K. J. Substrata mechanical stiffness can regulate adhesion of viable bacteria. *Biomacromolecules* **2008,** *9*, 1571-1578.

(73) Saha, N.; Monge, C.; Dulong, V.; Picart, C.; Glinel, K. Influence of Polyelectrolyte Film Stiffness on Bacterial Growth. *Biomacromolecules* **2013,** *14*, 520-528.

(74) Guégan, C.; Garderes, J.; Le Pennec, G.; Gaillard, F.; Fay, F.; Linossier, I.; Herry, J.-M.; Fontaine, M.-N. B.; Réhel, K. V. Alteration of bacterial adhesion induced by the substrate stiffness. *Colloids and Surfaces B: Biointerfaces* **2014,** *114*, 193-200.

(75) Kim, S. H.; Moon, J.-H.; Kim, J. H.; Jeong, S. M.; Lee, S.-H. Flexible, stretchable and implantable PDMS encapsulated cable for implantable medical device. *Biomedical Engineering Letters* **2011,** *1*, 199-203.

(76) Crnich, C. J.; Halfmann, J. A.; Crone, W. C.; Maki, D. G. The effects of prolonged ethanol exposure on the mechanical properties of polyurethane and silicone catheters used for intravascular access. *Infection control and hospital epidemiology* **2005,** *26*, 708-714.

(77) Habal, M. B. The biologic basis for the clinical application of the silicones: a correlate to their biocompatibility. *Archives of Surgery* **1984,** *119*, 843.

(78) Sabri, F.; Marchetta, J. G.; Sinden-Redding, M.; Habenicht, J. J.; Chung, T. P.; Melton, C. N.; Hatch, C. J.; Lirette, R. L. Effect of Surface Plasma Treatments on the Adhesion of Mars JSC 1 Simulant Dust to RTV 655, RTV 615, and Sylgard 184. *PloS one* **2012,** *7*, e45719.

(79) Gu, H.; Hou, S.; Yongyat, C.; De Tore, S.; Ren, D. Patterned Biofilm Formation Reveals a Mechanism for Structural Heterogeneity in Bacterial Biofilms. *Langmuir* **2013,** *29*, 11145-11153.

(80) Evans, N. D.; Minelli, C.; Gentleman, E.; LaPointe, V.; Patankar, S. N.; Kallivretaki, M.; Chen, X.; Roberts, C. J.; Stevens, M. M. Substrate stiffness affects early differentiation events in embryonic stem cells. *Eur Cell Mater* **2009,** *18*, 13-14.

(81) Wang, Z. Polydimethylsiloxane Mechanical Properties Measured by Macroscopic Compression and Nanoindentation Techniques. University of South Florida, 2011.

(82) Fuard, D.; Tzvetkova-Chevolleau, T.; Decossas, S.; Tracqui, P.; Schiavone, P. Optimization of poly-di-methyl-siloxane (PDMS) substrates for studying cellular adhesion and motility. *Microelectronic Engineering* **2008,** *85*, 1289-1293.

(83) Saha, N.; Monge, C.; Dulong, V.; Picart, C.; Glinel, K. Influence of Polyelectrolyte Film Stiffness on Bacterial Growth. *Biomacromolecules* **2013**.

Chapter 2

Effects of material stiffness on bacterial adhesion, biofilm formation and the physiology of attached cells

Adapted (in part) with permission from Fangchao Song et al., *Langmuir*, 2014, 30, 10354-10362.

2.1 Abstract

In this study, *Escherichia coli* RP437, *Pseudomonas aeruginosa* PAO1, *Pseudomonas aeruginosa* PA14 and were used as model strains to investigate the early stage biofilm formation on poly(dimethylsiloxane) (PDMS) surfaces with varying stiffness, which were prepared by controlling the degree of crosslinking (base : curing agent ratios of 5:1, 10:1, 20:1, and 40:1 were tested). An inverse correlation between cell adhesion and substrate stiffness was observed for both species. Interestingly, it was found that the cells that attached on relatively stiff substrates (5:1 PDMS) were significantly smaller than those on relatively soft substrates (40:1 PDMS). In addition to the difference in size, the cells on 5:1 PDMS substrates were also found to be less susceptible to antibiotics, such as ofloxacin, ampicillin, and tobramycin, than the cells attached on 40:1 PDMS substrates. These results reveal that surface stiffness is an important material property that influences the attachment, growth, and stress tolerance of biofilm cells.

2.2 Introduction

Biofilms are multicellular structures formed by microorganisms attached to surfaces. Due to the high level tolerance to antibiotics,[1] biofilms are considered as the leading cause of persistent infections, which result in 98,987 deaths and 28-45 billion dollars of cost each year in the U.S. alone.[2-4] Biofilm formation is a dynamic process including initial attachment, microcolony formation, maturation, and detachment. Among these steps, initial attachment plays an important role in biofilm formation and is known to be influenced by many factors of the surface such as surface chemistry,[5-8] stiffness,[9-11] hydrophobicity,[12,13] roughness,[14,15] topography,[16-19] and charge.[5,20]

As one of the mechanical properties of materials, substrate stiffness has been found to affect the shape, adhesion, proliferation, and migration of eukaryotic cells.[21-27] However, compared to these well documented effects on eukaryotic cells, few studies have been conducted to investigate the effects of stiffness on bacterial attachment. Lichter et al.[10] reported that the adhesion of *Staphylococcus epidermidis* and *Escherichia coli* W3100 is positively correlated with the stiffness (around 1, 10, 40, and 100 MPa tested) of polyelectrolyte multilayer (PEM) thin films consisting of poly(allylamine) hydrochloride (PAH) and poly(acrylic acid) (PAA). Saha et al.[9] showed that the growth of *E. coli* MG1655 biofilm colonies is faster on 30 kPa PEM than on 150 kPa PEM, which are thin films consisting of poly(L-lysine) (PLL) and a hyaluronan derivative modified with photoreactive vinylbenzyl groups (HAVB). These pioneering studies presented promising data indicating that surface stiffness may affect bacterial adhesion and biofilm formation, although the effects on the physiology of attached cells is unknown. To better understand the role of stiffness and the underlying mechanism, we

conducted this study to investigate the effects of surface stiffness on early stage biofilm formation including attachment, cell morphology, and antibiotic tolerance. We chose PDMS (silicone) surfaces since it is broadly used for medical devices, such as catheters, contact lenses, and finger joint implants.[28-30] Unlike polyelectrolyte surfaces, PDMS has negligible charge;[31] thus, using this material allows the effects of surface stiffness to be more specifically studied. It also allows us to compare with our other biofilm studies using this material.[2019,323] We prepared cross-linked PDMS with varying Young's modulus (between 0.1 MPa and 2.6 MPa tested). The range of 0.1-2.6 MPa was selected because similar moduli are found in biomaterials for medical applications (e.g., contact lenses).[33]

2.3 Materials and Methods

2.3.1 Bacterial strains and Growth medium

Escherichia coli RP437 [345] and *Pseudomonas aeruginosa* PAO1 [35] were used in this study. Both strains were routinely grown at 37^{o}C in Lysogeny Broth (henceforth LB medium) containing 10 g/L tryptone, 5 g/L yeast extract, and 10 g/L NaCl in DI water.[19,36]

2.3.2 Preparation of PDMS surfaces

PDMS surfaces were prepared using SYLGARD184 Silicone Elastomer Kit (Dow Corning Corporation, Midland, MI). The stiffness was adjusted by varying the mass ratio of base to curing agent by following a protocol described previously.[37-39] The base : curing agent ratios (wt/wt) of 5:1, 10:1, 20:1, and 40: 1 were tested. For each given ratio, elastomer base and curing agent were thoroughly mixed and degased under vacuum for 30 min. Then, the mixture was poured into a petri-dish, cured at 60^{o}C for 24 h, and incubated at room temperature for

another 24 h to fully polymerize. The PDMS surface was then peeled off the petri-dish and cut into 1.0 cm by 0.6 cm pieces (1.5 mm thick), which were sterilized by soaking in 200 proof ethanol for 20 min and dried with sterile air. All of the sterilized PDMS substrates were stored at room temperature until use. The Young's moduli of PDMS surfaces were measured using dynamic mechanical analysis (DMA) (Q800, TA instrument, DE, USA) by following a previously described protocol.[39]

2.3.3 Bacterial adhesion on PDMS

Bacterial cells from overnight cultures were harvested by centrifugation at 8,000 rpm for 3 min at 4ºC, washed with phosphate buffered saline (PBS) (pH 7.3) three times, and then used to inoculate LB medium to desired cell density. This cell suspension (30 mL) was transferred to a petri-dish containing sterilized PDMS surfaces. After incubation at 37ºC for 2 h without shaking, the PDMS surfaces were gently washed by dipping in PBS three times (changed to clean PBS for each step). The viability of cells was determined using the drop plate assay as described previously.[40] Briefly, the attached cells were harvested by gentle sonication for 1 min and vortexing for 30 s, which was tested for effectively detaching more than 92% of the attached cells. Then the cell suspension was dropped on a LB plate after a series of 10× dilution (10 μL in each drop). The plate was included at 37°C overnight to count colony forming units (CFU).

Meanwhile, some PDMS surfaces were examined using an Axio Imager M1 fluorescence microscope (Carl Zeiss Inc., Berlin, Germany) to directly visualize the cells attached on PDMS surfaces. The live/Dead BacLight bacterial viability kit (Invitrogen Corporation, Carlsbad, CA,

USA) was used to stain *E. coli* RP437. To achieve this, the washed surfaces were soaked in a 12 well plate; each well contained 2 mL PBS supplemented with 1.5 µL/mL SYTO 9 and 1.5 µL/mL propidium iodide, and the plate was kept in the dark for 20 min. At least five images were randomly taken from each sample, and the surface coverage by attached cells was calculated using COMSTAT.[41] The data of surface coverage and CFU were analyzed with *t* test, Pearson correlation analysis, and one-way ANOVA followed by Tukey test using SAS 9.2 software (SAS Institute, Cary, NC, USA).

2.3.4 Biofilm growth

After attachment, the surfaces were washed three times with PBS to remove the planktonic cells. The washed surfaces with attached cells were transferred to a new petri-dish containing 30 mL LB medium, and incubated at 37^{o}C without shaking for 5 h. After incubation, the PDMS surfaces were gently washed and analyzed as described above. Surface coverage was determined using COMSTAT. The length of attached cells was measured directly from microscope images. At least 300 cells were analyzed for each condition. To understand if surface stiffness affects the growth of attached cells, the biofilm cells after 5 h of growth were stained with 500 µg/mL acridine orange (Sigma-Aldrich, St. Louis, MO, USA) in PBS for 2 min, and imaged with fluorescence microscopy. The same cells were also imaged using DIC (differential interference contrast) as control. Biofilm growth was also tested in 96-well plates. Briefly, a 96 well plate containing either 5:1 PDMS or 40:1 PDMS substrates coated on the bottom of the wells were inoculated using an overnight culture of *E. coli* RP437 to a density of 10^5 cells/mL, and the plate was incubated at 37°C for 72 h. Samples were analyzed

throughout the incubation period. The attached cells were harvested by sonication for 1 min; and the cell number was determined by counting CFU.

2.3.5 Antibiotic susceptibility of attached cells

The washed surfaces after 5-h growth were transferred to a 12 well plate containing 2 mL PBS in each well supplemented with antibiotics, e.g., 5 μg/mL ofloxacin, 100 μg/mL ampicillin, or 20 μg/mL tobramycin, and incubated at 37^{o}C without shaking for 3.5 h. The control surfaces were incubated in the same condition without antibiotic. After incubation, the number of viable cells was determined by counting CFU as described above.

2.3.6 Scanning electron microscopy (SEM)

Surface-attached *E. coli* cells were also imaged with SEM (JEOL JSM-5800 LV, JEOL, Peabody, MA, USA). Briefly, PDMS surfaces after 5 h of biofilm growth were stored in 2.5% glutaraldehyde/PBS solution to fix the cells on the surfaces. Then, the surfaces were stained with 2% osmium tetroxide solution for 45 min, and dehydrated by soaking in ethanol/water solutions with increasing ethanol content (in the order of 70%, 80%, 90%, and 95% wt) for 30 min each. Finally, the samples were dehydrated in 100% ethanol for 30 min (repeated twice). Tetramethylsilane (TMS) was added on PDMS surfaces for further dehydration. After TMS evaporated completely, the dry PDMS surfaces were coated with platinum in a sputter coater (DESK II, Denton vacuum, Moorestown, NJ, USA) before SEM analysis.

2.3.7 Phagocytosis

Macrophage U-937 was used as the model cell line in this study, which is cultured in RPMI supplemented in 10% BSA at 37% with 5% CO_2. U-938 was used by differentiated type and non-differentiated type in this study. For the assay of phagocytosis by differentiated macrophage, U-937 was differentiated by 230 nmol/mL PMA for 1 day in 24 well plate, and the bacteria cell isolated from 5 h biofilm (cultured as the procedure above), were added in to the U-937 culture. For the assay of phagocytosis by non-differentiated macrophage, U-937 was added into the 5 h biofilm (cultured as the procedure above). For both assay, the co-culture was incubated at 37^{o}C with 5% CO_2 for 1 h, and the CFU was tested for calculating the killing.

2.4 Results

2.4.1 Effects of surface stiffness on *E. coli* biofilm formation

To understand the effects of surface stiffness on bacterial attachment and biofilm formation, PDMS surfaces with different stiffness were prepared by varying the base : curing agent ratio (5:1, 10:1, 20: 1, and 40:1). Because different values have been reported for Young's modulus of PDMS prepared with the same base : curing agent ratio,[38-40] we also measured our samples using dynamic mechanical analysis (DMA). The results indicated that the Young's moduli of 5:1 PDMS, 10: 1 PDMS, 20: 1 PDMS, and 40:1 PDMS were 2.6 ± 0.2 MPa, 2.1 ± 0.1 MPa, 1.0 ± 0.1 MPa and 0.1 ± 0.02 MPa, respectively, which are similar to the values reported by Evans et al.[38] and Wang et al.[3937,3837,38]

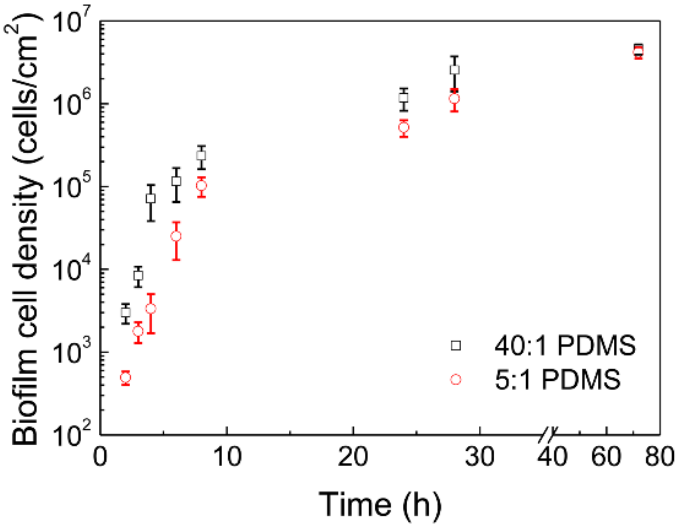

Figure 2.1 Effect of PDMS stiffness on *E. coli* RP437 biofilm formation. Biofilms were grown in LB medium with 4×10^5 cells/mL at inoculation. Biofilm cell densities were found to be significantly different between 40:1 PDMS and 5:1 PDMS surfaces up to 24 h after inoculation. $p < 0.01$ for all time points up to 24 h (*t* test).

We first compared the biofilms of *E. coli* RP437 on 40:1 PDMS and 5:1 PDMS substrates over 72 h after inoculation using the 96 well plate assay described in Method section. As shown in Figure 2.1, biofilm formation in the first 6 h was faster on 40:1 PDMS surfaces than that on 5:1 PDMS surfaces. The biggest difference in the density of biofilm cells between 40:1 PDMS and 5:1 PDMS substrates was observed at 4 h after inoculation: e.g. 7×10^4 cells/cm^2 and 3×10^3 cells/cm^2 biofilm cells were found on 40:1 PDMS and 5:1 PDMS surfaces, respectively. When the cell density reached around 10^5 cells/cm^2, biofilm formation on both 40:1 PDMS and 5:1 PDMS surfaces slowed down. However, there were still more cells on the 40:1 PDMS substrates until 38 h after inoculation. At 72 h, the cell numbers were about equal on 40:1 PDMS and 5:1 PDMS substrates. To confirm that the difference in biofilm formation on these

surfaces was not caused by toxicity of any leftover base or curing agent, we also grew *E. coli* RP437 in planktonic cultures for 5 h at 37°C in LB medium supplemented with different concentrations of base or curing agents (0, 0.1%, 1%, and 2% tested for both). The results showed that the growth yield was not affected by either the base or curing agent ($p > 0.1$ for both, one-way ANOVA), confirming that the observed results were not caused by killing and surface stiffness does affect biofilm formation on PDMS surfaces.

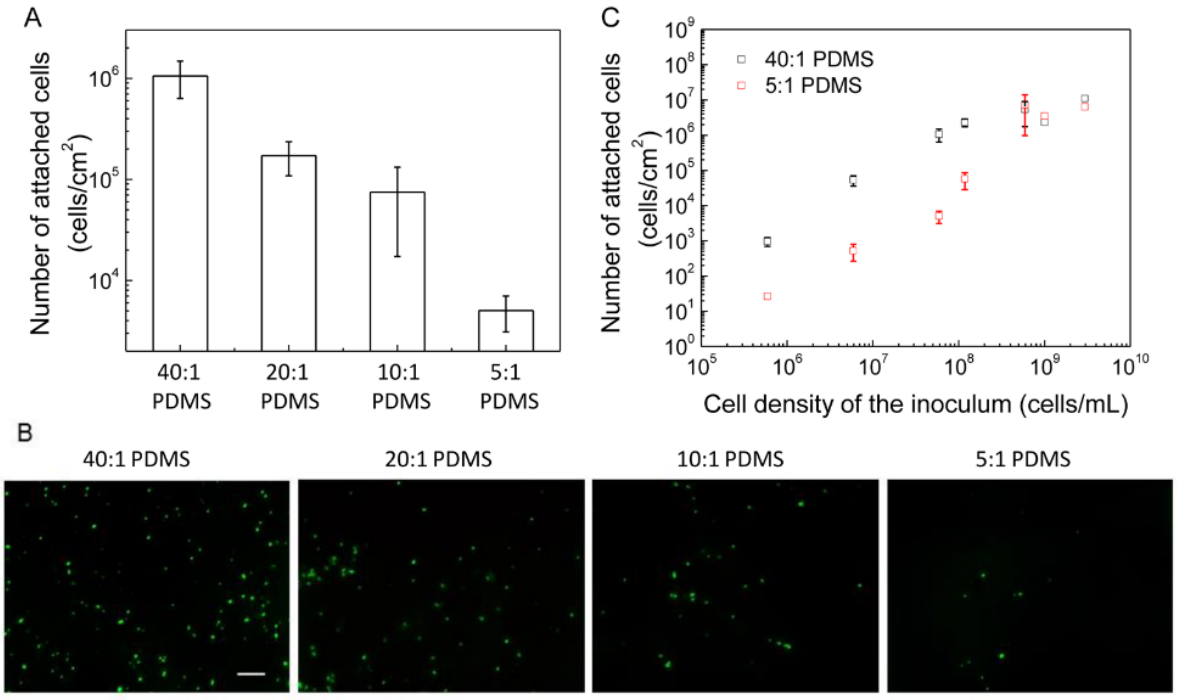

Figure 2.2 Effects of PDMS stiffness on the attachment of *E. coli* RP437 cells. (A) Number of attached *E. coli* RP437 cells. *E. coli* RP437 with a density of 4×10^7 cells/mL was used to inoculate the biofilm cultures. Attachment of *E. coli* RP437 cells was found to be inversely correlated with substrate stiffness ($r = -0.61$, $p < 0.05$, Pearson correlation analysis). (B) Representative images of attached *E. coli* RP437 cells (Bar = 10 µm). The cells were stained

with the Live/dead BacLight bacterial viability kit. (C) Effects of cell density of the inoculum and the stiffness of PDMS on the attachment of *E. coli* RP437 cells.

2.4.2 Effects of surface stiffness on *E. coli* adhesion

To understand if the effects of stiffness observed above were on the initial attachment, biofilm growth, or both, further experiments were conducted to study these processes more specifically. First, to understand the effects on attachment, the inoculum was washed three times with PBS and the adhesion (for 2 h) was carried out in PBS in the absence of any carbon source so that no growth is supported. Attachment of *E. coli* RP437 cells was found to be inversely correlated with substrate stiffness ($r = -0.61$, $p = 0.012$; Pearson correlation analysis). As shown in Figures 2A&B, when the stiffness increased from 0.1 MPa (40:1 PDMS) to 2.6 MPa (5:1 PDMS), the number of attached cells decreased from $(1.0 \pm 0.4) \times 10^6$ cells/cm^2 to $(5.0 \pm 2.0) \times 10^3$ cells/cm^2, corresponding to a 200-fold decrease in adhesion ($p = 0.016$, one-way ANOVA adjusted by Tukey test). Interestingly, the number of attached cells increased with cell density at inoculation. For example, the number of attached *E. coli* RP437 cells on 40:1 PDMS surfaces increased drastically from 1.1×10^3 to 1.4×10^7 cells/cm^2 when the cell density at inoculation was increased from 5.8×10^5 to 2.9×10^9 cells/mL (Figure 2.2C). When the cell density at inoculation was between 5.8×10^5 and 1.2×10^8 cells/mL, there were constantly 10 times or more cells on 40:1 PDMS than on 5:1 PDMS surfaces ($p < 0.001$ for all cell densities between 5.8×10^5 and 1.2×10^8 cells/mL, *t* test). However, when the culture concentration was higher than 10^9 cells/mL, the numbers of attached cells were about the same on 40:1 PDMS and 5:1 PDMS surfaces (Figure 2.2C). Thus, cell density in the inoculum also affected *E. coli* adhesion.

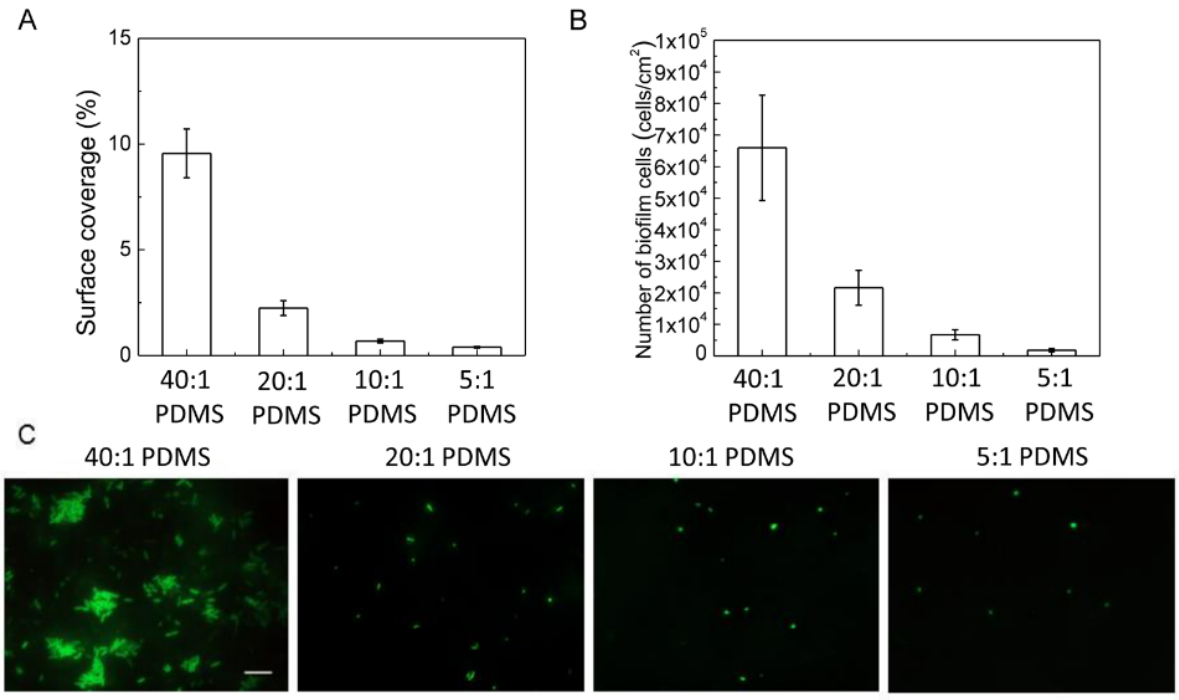

Figure 2.3 Effect of PDMS stiffness on the growth of attached *E. coli* RP437 cells. (A) Surface coverage of attached cells calculated using COMSTAT. The surface coverage after 5-h growth was found to be inversely correlated with surface stiffness ($r = -0.71$, $p < 0.001$, Pearson correlation analysis). (B) Number of attached cells based on CFU count. The cell number after 5-h growth was found to be inversely correlated with surface stiffness ($r = -0.66$, $p < 0.001$, Pearson correlation analysis). (C) Representative Live/Dead images of attached cells (Bar = 10 μm).

Table 2.1 Effects of PDMS stiffness on biofilm formation of *E. coli* RP437.

Number of initially attached cells ($cells/cm^2$)	Number of *E. coli* RP437 biofilm cells after 5 h of biofilm growth ($cells/cm^2$)	
	On 40:1 PDMS surfaces	On 5:1 PDMS surfaces
9×10^2	$(3.6 \pm 0.4) \times 10^2$	$(2.8 \pm 1.2) \times 10^1$
7×10^4	$(4.9 \pm 0.6) \times 10^3$	$(2.7 \pm 0.8) \times 10^3$
1×10^6	$(7.1 \pm 1.7) \times 10^4$	$(9.1 \pm 1.4) \times 10^3$

2.4.3 Effects of surface stiffness on the growth of attached *E. coli* cells

To understand if surface stiffness affects the early stage biofilm formation, we compared the biofilms of *E. coli* RP437 on 40:1 PDMS, 20:1 PDMS, 10:1 PDMS, and 5:1 PDMS surfaces. The surfaces were incubated in PBS with 4×10^7 cells/mL for 2 h to allow the cells to attach, and then transferred to LB medium to allow the biofilms to grow for 5 h. The surfaces were washed three times with PBS to remove planktonic cells before transfer. As shown in Figure 2.3A, after 5-h growth, the surface coverage appeared to decrease as the stiffness of PDMS increased. For example, the surface coverage on 40:1 PDMS surfaces was 9.6 ± 1.2%; while the surface coverage on 20:1 PDMS, 10:1 PDMS, and 5:1 PDMS surfaces was 2.2 ± 0.4%, 0.7 ± 0.08%, and 0.4 ± 0.04%, respectively. These imaging results are corroborated by the CFU data (Figure 2.3B), which indicate that the cell number after 5-h growth is also inversely correlated with surface stiffness ($r = -0.66$, $p < 0.01$; Pearson correlation analysis). The number of attached cells on 40:1 PDMS, 20:1 PDMS, 10:1 PDMS, and 5:1 PDMS surfaces were $(6.7 \pm 1.6) \times 10^4$, $(2.3 \pm 0.7) \times 10^4$, $(7.9 \pm 1.7) \times 10^3$, and $(2.2 \pm 0.9) \times 10^3$ CFU/cm^2, respectively (Figure 2.3B). The results of surface coverage and CFU are consistent with the biofilm images shown in Figure 2.3C.

As described above, the number of initially attached cells varied with surface stiffness when the biofilm cultures were inoculated with the same density of planktonic cells. In order to study biofilm growth specifically, the cell density of inoculum was adjusted to obtain the same number of cells attached on 40:1 PDMS and 5:1 PDMS substrates. Three cell densities of initial attachment were tested for biofilm growth on 40:1 PDMS and 5:1 PDMS substrates, including 9×10^2, 7×10^4, and 1×10^6 cells/cm^2. As shown in Table 2.1, for all three cell densities of initial attachment, more biofilm growth was observed on 40:1 PDMS surfaces than on 5:1 PDMS surfaces. For example, when there were 9×10^2 cells/cm^2 on both 40:1 PDMS and 5:1 PDMS substrates after initial attachment, there were 12.9 times more cells on the 40:1 PDMS substrates after 5 h of growth ($p < 0.001$, *t* test). This result indicates that surface stiffness also affects biofilm growth and biofilm cells grow faster on soft surfaces (40:1 PDMS compared to 5:1 PDMS) under our experimental condition. To corroborate this result, the biofilm cells after 5 h growth following 2 h attachment with 4×10^7 cells/mL at the inoculum were stained with acridine orange which gives green and red fluorescence when it binds to DNA and RNA, respectively. As shown in Figure 2.4A, the amount of RNA in the attached cells decreased as the surface stiffness increased from 0.1 MPa to 2.6 MPa, while the amount of DNA remained relatively constant. This finding suggests that the cells on soft surfaces (40:1 PDMS, 0.1 MPa) had higher transcriptional activity than those on the stiff surfaces (5:1 PDMS, 2.6 MPa). Similarly, Saha et al.[9] also observed faster growth of *E. coli* MG1655 on 30 kPa surfaces of hydrophilic layer by layer polyelectrolyte compared to 150 kPa surfaces of the same material.

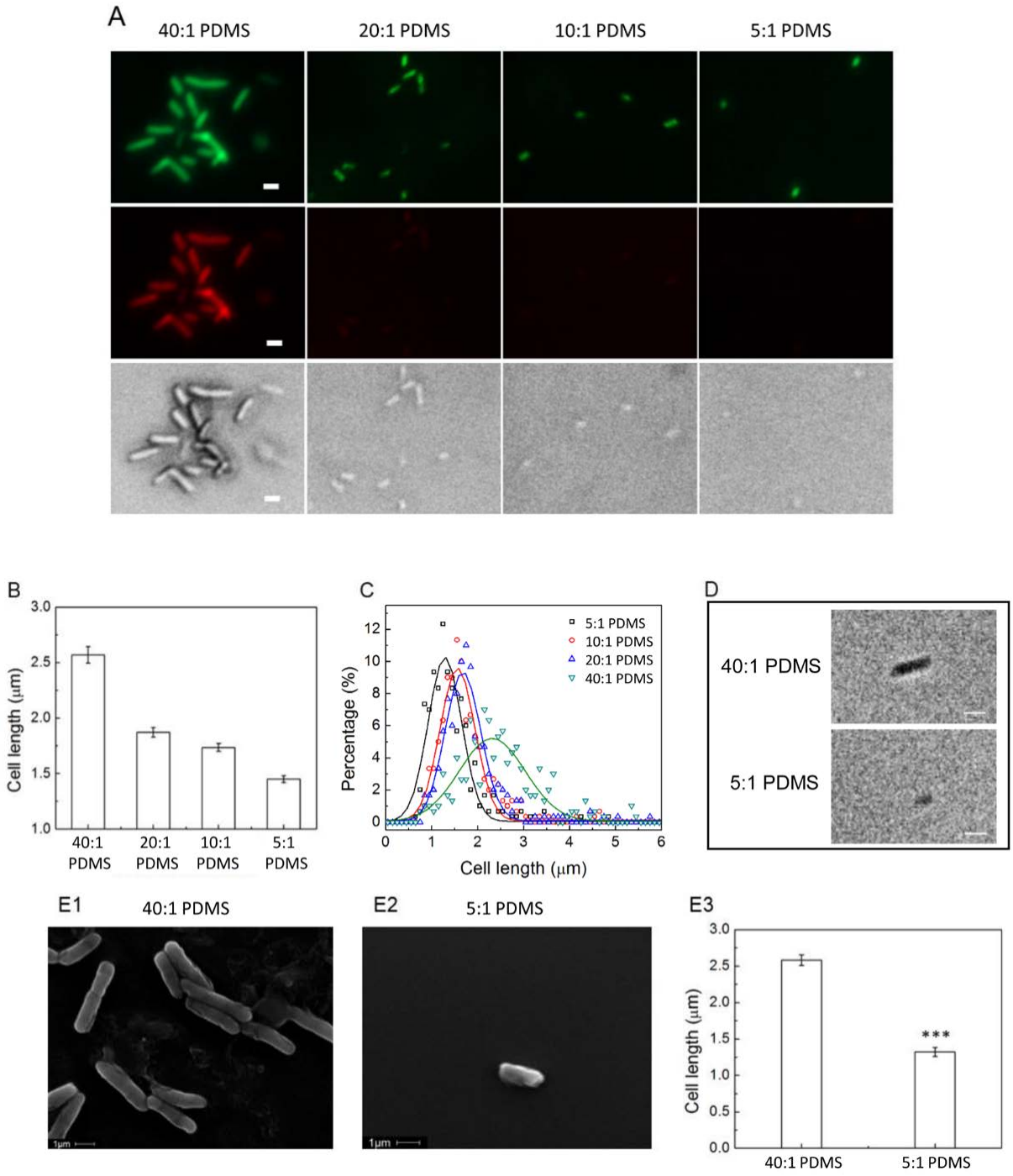

Figure 2.4 Effects of PDMS stiffness on the activity and size of attached *E. coli* RP437 cells. Following inoculation with 4×10^7 cells/mL, *E. coli* RP437 was allowed to attach for 2 h in PBS and then incubated in LB medium for 5 h for biofilm growth. (A) Representative images

of *E. coli* RP437 cells on PDMS surfaces. Cells were stained with acridine orange. Top: green fluorescence images indicating the amount of DNA in attached cells. Middle: red fluorescence images indicating the amount of RNA in attached cells. Bottom: DIC images (Bar = 2 μm). (B) Average lengths of *E. coli* RP437 cells attached on PDMS surfaces with different moduli. The cell length was found to be inversely correlated with surface stiffness ($r = -0.44$, $p < 0.001$, Pearson correlation analysis). (C) Distribution of the length of attached *E. coli* RP437 cells on PDMS surfaces with varying stiffness. (D) Bright field images of detached *E. coli* RP437 biofilm cells (Bar = 2 μm). (E1&2) Representative SEM images of *E. coli* RP437 cells attached to 40:1 PDMS (E1) and 5:1 PDMS (E2) (Bar = 1 μm). (E3) Average length of attached cells calculated from SEM images. ***$p < 0.001$, versus 40:1 PDMS (*t* test).

2.4.4 Effects of surface stiffness on the size of attached *E. coli* cells

Interestingly, our imaging results also revealed that the size of attached *E. coli* cells varied with surface stiffness after the 5-h growth. As shown in Figures 3C&4, the length of attached *E. coli* cells in 5-h biofilms appeared to decrease as the stiffness of substrate increased from 0.1 MPa (40:1 PDMS) to 2.6 MPa (5:1 PDMS). For example, the average length of *E. coli* cells on 40:1 PDMS and 5:1 PDMS substrates after 5-h biofilm growth (inoculated with 4×10^7 cells/mL) was found to be 2.6 ± 0.07 μm and 1.4 ± 0.03 μm, respectively (Figure 2.4B). Thus, the length of *E. coli* biofilm cells on 40:1 PDMS substrates after 5-h growth was nearly twice that of cells on 5:1 PDMS substrates ($p < 0.001$, one-way ANOVA adjusted by Tukey test). No such difference was observed right after the 2-h adhesion (Figure 2.2B), with cell size around 1.1 μm for all surfaces (stationary phase planktonic cells used for inoculation; $p = 0.28$, one-way ANOVA; eighty cells were examined for each condition). Besides the average length

of attached cells, the distribution of cell length was also different between stiff and soft substrates tested in this study. Figure 2.4C shows the distribution calculated from the Live/Dead images. The results suggest that the distribution of bacterial cell length is narrower on stiff substrate (5:1 PDMS) than that on soft substrate (40:1 PDMS). The finding that cells on soft substrate are longer is consistent with the above results that the growth of biofilm cells is slower on 5:1 PDMS surfaces than on 40:1 PDMS surfaces. Interestingly, increase in stiffness of PDMS with Young's modulus in the range of 0.04-3 MPa has also been shown to improve early differentiation of embryonic stem cells;[24,37] thus, PDMS with optimized stiffness in this range may promote the growth of host cells and simultaneously inhibit microbial biofilm growth.

It is worth noting that the fluorescence images only show the projection of bacterial cells on the surface. To understand if the cells on soft surfaces were indeed longer or if the ones on stiff surfaces were "standing", we detached the biofilm cells to further examine with microscopy. To achieve this, the substrates with cells after 5-h growth were gently sonicated for 1 min and vortexed for 30 s. This condition was found not to change the viability of *E. coli* cells based on CFU test (data not shown). By incubating these PDMS surfaces on LB agar plates, it was confirmed that more than 95% biofilm cells were detached. The detached cells were collected using a 96 well filter plate, re-suspended in PBS, and visualized using microscopy. As shown in Figure 2.4D, the length of these harvested *E. coli* cells was found to be consistent with those measured directly from biofilm images; e.g., the length of *E. coli* cells isolated from 40:1 PDMS substrates was also twice of that from 5:1 PDMS substrates. This result indicates that

the *E. coli* cells on 5:1 PDMS substrates were not standing but were actually shorter than those attached on softer substrates.

To further confirm these results, the PDMS surfaces with attached *E. coli* cells were imaged using SEM to directly visualize the 3D shape of attached cells. As shown in Figure 2.4E1&2, the SEM images further confirmed that the *E. coli* cells on soft (40:1 PDMS) surfaces were longer than those on stiff (5:1 PDMS) surfaces, and that the cells on stiff surfaces were attached horizontally, rather than vertically. The lengths of *E. coli* cells calculated from SEM images (Figure 2.4E3) matched well with the lengths measured from fluorescence images (Figure 2.4B).

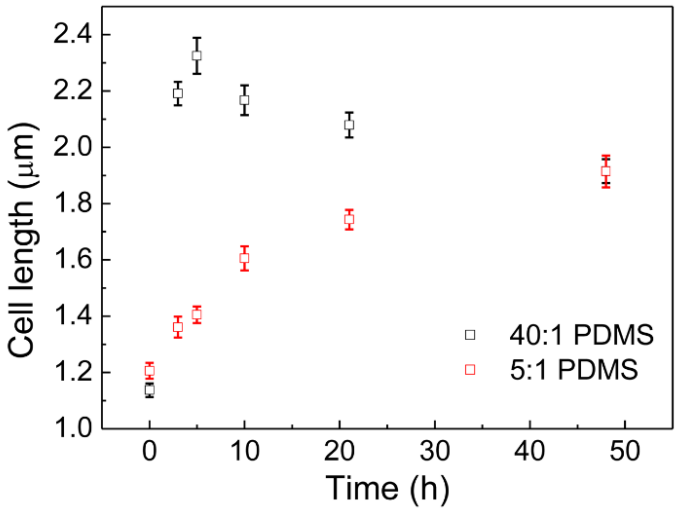

Figure 2.5 Length of *E. coli* RP437 cells on 40:1 PDMS and 5:1 PDMS surfaces. Biofilm cultures were inoculated with 4×10^7 cells/mL and incubated for 2 h for attachment. Then the PDMS surfaces were transferred to LB medium (at t = 0 h) for biofilm growth. The lengths of biofilm cells were found to be significantly different between 40:1 PDMS and 5:1 PDMS

surfaces during 24 h of growth ($p < 0.001$, *t* test, for all time points up to 24 h except for t = 0 h).

Since biofilm formation is a dynamic process and cell size is related to cell growth, we hypothesized that the cell size may also change over time. To test this hypothesis, we followed the size of attached cells for over two days. As shown in Figure 2.5, the average length of attached *E. coli* RP437 cells was found to be different between soft (40:1 PDMS) and stiff (5:1 PDMS) substrates during the first day of biofilm formation. On 40:1 PDMS substrates, the average cell length increased from 1.1 μm (the size of seeding cells from stationary phase cultures) to the maximum (2.4 μm) in the first 6 h of biofilm growth and then decreased slightly (possibly due to high cell density and associated stress). In comparison, on 5:1 PDMS substrates, the average length gradually increased over the first day, but was constantly smaller than that on 40:1 PDMS substrates. At 50 h after inoculation, the cell length was about 1.9 μm on both surfaces (Figure 2.5), indicating that the late stage of growth was approached. The difference in cell length, especially the rapid increase in the first 6 h of growth on 40:1 PDMS, suggests that the cells prefer softer surfaces for biofilm formation under our experimental condition. This is consistent with acridine orange images shown in Figure 2.4A.

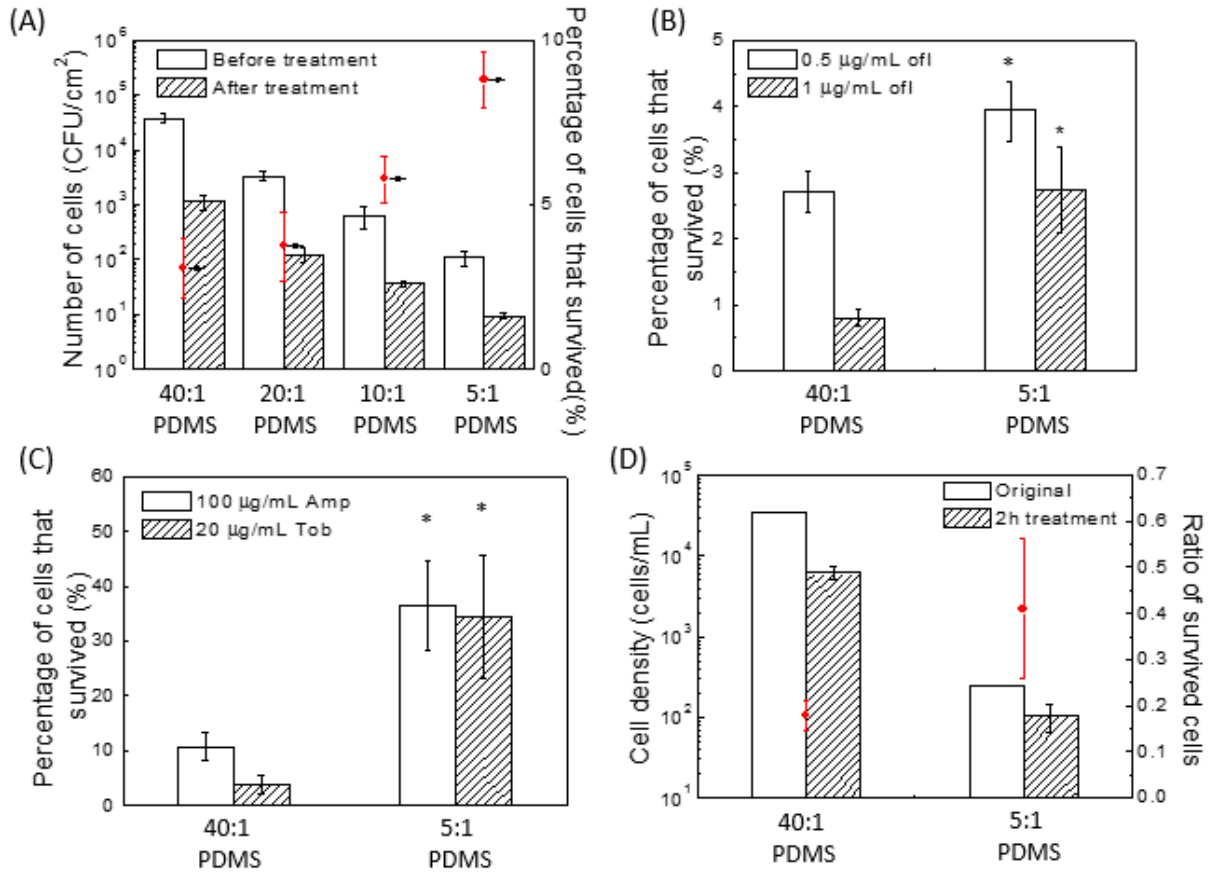

Figure 2.6 Effects of PDMS stiffness on the susceptibility of *E. coli* RP437 to antibiotics. (A) Number of cells before and after treatment with 5 µg/mL ofloxacin (Ofl). The bars represent the number of cells based on CFU. The red dots represent the percentage of cells that survived the treatment, which increased with surface stiffness ($r = 0.58$, $p < 0.001$, Pearson correlation analysis). (B) Susceptibility of detached biofilm cells to 0.5 and 1 µg/mL ofloxacin. Biofilm cells on 40:1 PDMS and 5:1 PDMS surfaces were detached by sonication before being treated with ofloxacin. (C) Relative number of biofilm cells that survived the treatment with 100 µg/mL ampicillin (Amp) or 20 µg/mL tobramycin (Tob). (D) Effects of PDMS stiffness on the susceptibility of *E. coli* RP437 to 1.5 mg/mL lysozyme. *$p < 0.05$, versus 40:1 PDMS (*t* test).

2.4.5 Effect of surface stiffness on antibiotic susceptibility of attached *E. coli* cells

The finding that the size of attached *E. coli* cells changed with surface stiffness is intriguing. Small cells of bacteria have been found under stress conditions and are more tolerant to harmful environmental factors. For example, persister cells (metabolically inactive bacterial cells) are smaller than normal cells and are highly tolerant to antibiotics.[42-44] Thus, we hypothesized that the small cells on stiff (5:1 PDMS) surfaces may be more tolerant to antibiotics compared to those on soft (40:1 PDMS) surfaces. To test this hypothesis, the PDMS surfaces with attached *E. coli* cells (after 5 h of biofilm growth) were treated with or without 5 μg/mL ofloxacin for 3.5 h; and the number of viable *E. coli* cells was determined by counting CFU. As shown in Figure 2.6A, 3.1 ± 0.9% bacteria on 40:1 PDMS substrate survived after the ofloxacin treatment; and the number increased to 8.8 ± 0.9% on 5:1 PDMS substrate ($p < 0.001$, one-way ANOVA adjusted by Tukey test). This result indicates that the *E. coli* RP437 cells on 40:1 PDMS were more susceptible to ofloxacin than those on 5:1 PDMS substrates under our experimental condition. To corroborate these results and determine if the difference is indeed due to the change in susceptibility of cells rather than the protection of biofilm structure, the *E. coli* cells were detached from biofilms and tested for their susceptibility to ofloxacin. As shown in Figure 2.6B, 0.8 ± 0.1% of *E. coli* cells isolated from 40:1 PDMS substrates survived after 1-h treatment with 1 μg/mL ofloxacin; and 2.7 ± 0.6% from 5:1 PDMS substrates survived, corresponding to a 3-fold increase ($p = 0.014$, *t* test). Similar results were also observed for 0.5 μg/mL ofloxacin, with 2.7 ± 0.3% of cells isolated from 40:1 PDMS substrates surviving after 1-h treatment and 3.9 ± 0.4% from 5:1 PDMS substrates surviving ($p = 0.041$, *t* test). These numbers are smaller than those from direct treatment of biofilms presumably due to the loss of protection of some biofilm matrix. Nevertheless, the results with

detached cells provide direct evidence that the cells on 5:1 PDMS surfaces indeed have higher antibiotic tolerance than those on 40:1 PDMS surfaces. To understand if this is a general phenomenon or ofloxacin specific, the substrates with attached *E. coli* RP437 cells were also treated with 100 μg/mL ampicillin or 20 μg/mL tobramycin for 3.5 h. As shown in Figure 2.6C, the cells on 40:1 PDMS substrate were found to be more susceptible to both antibiotics compared to those on 5:1 PDMS surfaces. Ofloxacin, ampicillin, and tobramycin are fluoroquinolone, β-lactam, and aminoglycoside antibiotics, respectively. Thus, the effect of substrate stiffness on susceptibility is not specific to a certain class of antibiotics. In addition, as shown in Figure 2.6D, the attached *E. coli* cells on soft surface are more susceptible to lysozyme than those on stiff surface as well. Because the stiffness of PDMS used in this study is in the range of the stiffness of commercial contact lenses, it may help us to design better contact lenses for preventing eye infection. This finding is interesting and deserves further study.

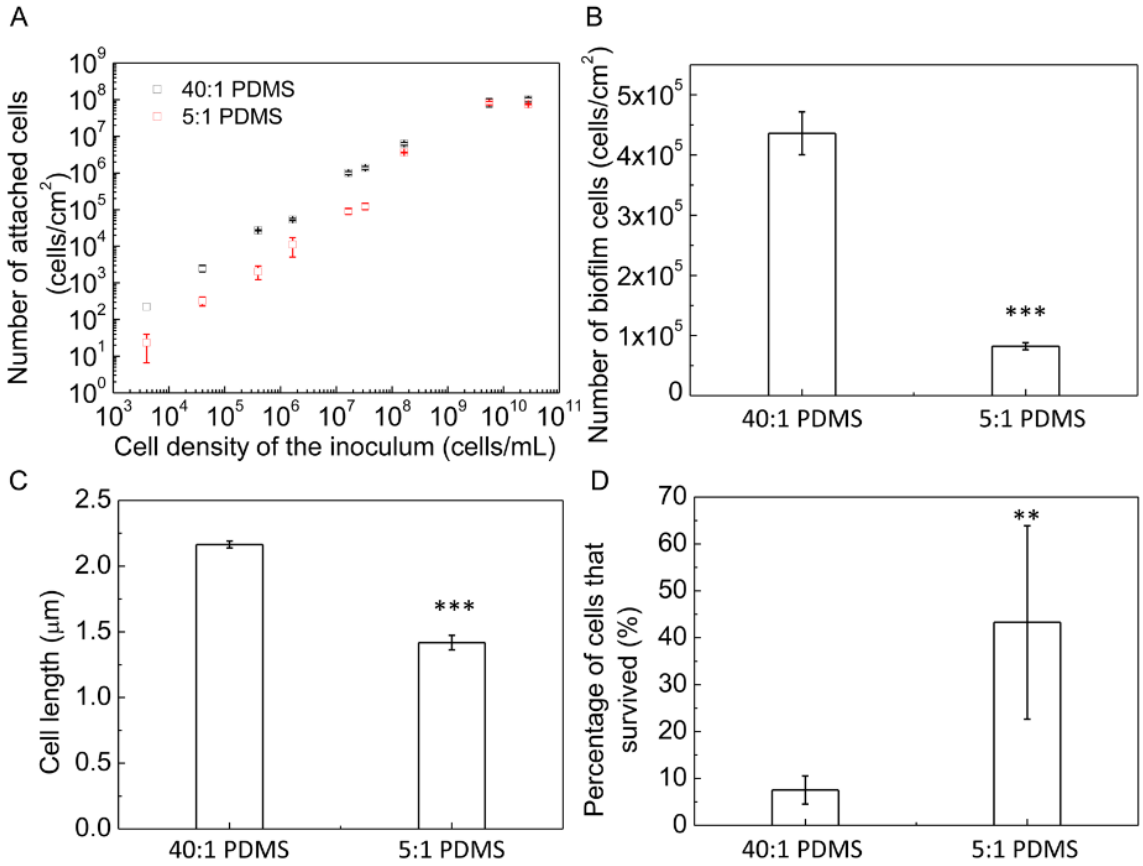

Figure 2.7 Effects of surface stiffness on biofilm formation, cell length, and antibiotic susceptibility of *P. aeruginosa* PAO1 cells. (A) Effects of inoculum cell density and PDMS stiffness on attachment. (B) Number of attached *P. aeruginosa* PAO1 cells on 40:1 PDMS and 5:1 PDMS surfaces. *P. aeruginosa* PAO1 cells were incubated in LB medium for 5 h with 5×10^4 cells/cm^2 cells on each surface after initial attachment. (C) Length of *P. aeruginosa* PAO1 cells attached on 40:1 PDMS and 5:1 PDMS surfaces. (D) Susceptibility of attached *P. aeruginosa* PAO1 cells to 20 μg/mL tobramycin. $^{**}p < 0.01$, $^{***}p < 0.001$, versus 40:1 PDMS (*t* test).

2.4.6 Similar effects were observed for *P. aeruginosa* cells.

To understand if the observed effects of stiffness are limited to *E. coli*, we also investigated the biofilm formation and antibiotic susceptibility of *P. aeruginosa* PAO1 cells; and similar results were also observed for *P. aeruginosa* PAO1 (Figure 2.7). The number of attached *P. aeruginosa* PAO1 cells increased with cell concentration in the inoculum (Figure 2.7A). Although *P. aeruginosa* PAO1 cells are more capable of attachment to PDMS than *E. coli* RP437, the effects of substrate stiffness were found to be similar for both strains under our experimental conditions. When the cell density at inoculation was lower than 10^9 cells/mL, there were always more cells on soft (40:1 PDMS) substrates than on stiff (5:1 PDMS) ones after 2 h attachment of either *E. coli* RP437 or *P. aeruginosa* PAO1. The reason for a threshold cell density at inoculation (10^9 cells/mL) that overcomes the effect of stiffness is unknown and deserves further study. In addition to attachment, the effects of surface stiffness on biofilm growth were also similar between *E. coli* RP437 and *P. aeruginosa* PAO1. For example, as shown in Figure 2.7B, the number of attached *P. aeruginosa* PAO1 cells was $(4.4 \pm 0.5) \times 10^5$ cells/cm^2 on the soft surface (40:1 PDMS) and $(8.2 \pm 0.5) \times 10^4$ cells/cm^2 on the stiff surface (5:1 PDMS) ($p < 0.001$, *t* test), respectively, after 5-h growth with 5×10^4 cells/cm^2 at initial attachment. The average lengths of attached *P. aeruginosa* PAO1 cells were also different, e.g., 2.2 ± 0.03 μm and 1.4 ± 0.06 μm on 40:1 PDMS and 5:1 PDMS surfaces, respectively (Figure 2.7C). Thus, the length of attached cells on 40:1 PDMS substrates was about 1.6 times that of cells on 5:1 PDMS substrates at 5 h after inoculation ($p < 0.001$, *t* test). Similar to the *E. coli* results, *P. aeruginosa* PAO1 cells on soft substrates (40:1 PDMS) were found to be 5 times more susceptible to 20 μg/mL tobramycin than those on stiff substrates (5:1 PDMS) ($p = 0.005$, *t* test; Figure 2.7D). Thus, the effects of surface stiffness are not limited to *E. coli*.

2.4.7 Phagocytosis of the attached cells on soft and stiff surfaces.

Phagocytosis is one of the most important innate immune responses. Here we also tested the phagocytosis of the attached *E. coli* RP437 on stiff surfaces and soft surfaces. As shown in Figure 2.8 (A), differentiated macrophage U-937 killed more isolated biofilm cells on stiff surfaces than those on soft surfaces ($p<0.005$, *t* test). For example, the differentiated U-937 could eliminated (58 ± 1.9) % isolated biofilm cells on stiff surfaces, and (92 ± 3.1) % isolated biofilm cells on soft surfaces. In addition to the phagocytosis of differentiated macrophages U-937, the non-differentiated macrophages also showed the faster internalization on biofilm cells on stiff surfaces than those on soft surfaces ($p<0.05$, *t* test). Figure 2.8 (B) indicated the (97 ± 0.9) % killing on stiff surfaces and (90 ± 1.7) % killing on soft surfaces. These results suggest that the macrophage prefer to internalize the biofilm cells on stiff surface than those on soft surfaces.

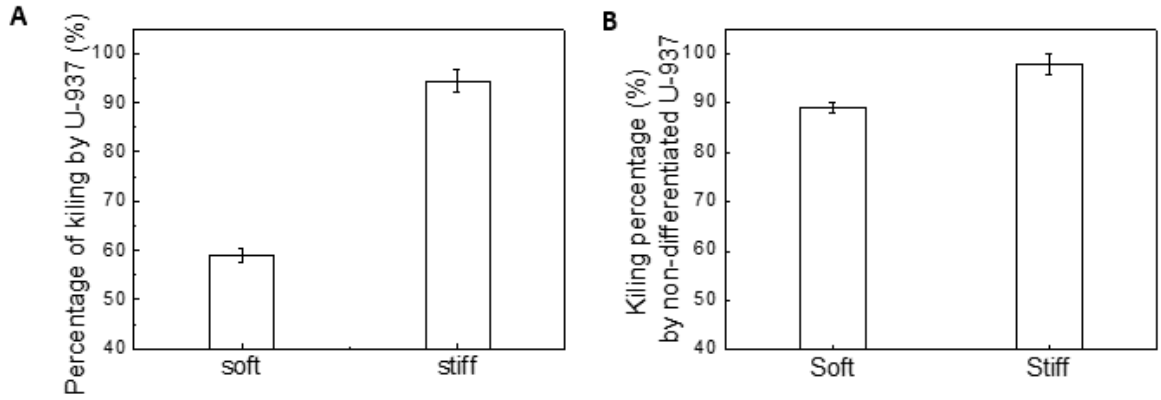

Figure 2.8 The percentage of *E. coli* RP437 eliminated by macrophage U-937 in one hour with the ratio of bacteria : macrophage around 100 : 1 in RPMI medium supplemented with 10% BSA. (A) Phagocytosis of differentiated macrophages on isolated biofilm cells on different surfaces. (B) Phagocytosis of non-differentiated macrophages on biofilm cells.

2.5 Discussion

Compared to other surface properties, such as surface chemistry, topography and charge, the effects of stiffness on bacterial adhesion are less understood. In a previous study reported by Lichter et al.[10], it was found that attachment of *Staphylococcus epidermidis* increases with surface stiffness in the range of 1-100 MPa of Young's modulus. Also, Saha et al.[9] reported a slight increase in *E. coli* MG1655 attachment on PEM surfaces when the stiffness increased from 30 to 150 kPa. These results are seemingly different from the results in the present study. However, it is worth noting that the previous results[9,10] are based on hydrophilic surfaces, while the PDMS surfaces used in this study are hydrophobic. The bacterial strains, charges of surfaces, and ranges of modulus are also different between this and previous studies. Because many surface properties collectively affect bacterial adhesion and biofilm formation, the results from different conditions may not be directly comparable. This emphasizes the importance to decouple these factors in order to understand each specific parameter.

In this study, we varied the surface stiffness by changing the base to curing agent ratio. Jiang et al.[46] measured the composition of soft and stiff PDMS surfaces including the ones with the same base : curing agent ratios used in the present study with XPS; and showed that the surface chemical composition is essentially the same among those surfaces (based on C, O, and Si). To confirm that the difference in adhesion on the surfaces was not caused by toxicity of any leftover base or curing agent, we conducted an additional experiment to compare the 5-h planktonic growth of *E. coli* RP437 at 37°C in LB medium supplemented with different concentrations of base and curing agents (0, 0.1%, 1%, and 2% tested for both). The results showed that the growth yield was not affected by either the base or curing agent ($p > 0.1$ for

both, one-way ANOVA), confirming that the observed results were not caused by killing. Another factor that deserves attention is the effect of crosslinking on surface roughness, which is known to affect bacterial adhesion.[20] Eroshenoko et al.[25] reported that the roughness of 20:1 PDMS, 10:1 PDMS, and 5:1 PDMS are very similar, e.g., 1 nm, 0.8 nm, and 0.8 nm, respectively. In comparison, Wala et al.[47] reported a slightly different result that the roughness of 20:1 PDMS (soft) and 5:1 PDMS (stiff) are 2.6 nm and 1 nm, respectively. Increase in roughness of glass surfaces in this range (from 1.6 nm to 2.8 nm) was found to cause minor inhibition of bacterial adhesion (by up to 2 fold).[48] Thus, if the effects observed in our study were caused by changes in surface roughness, we would expect slightly more cell adhesion on 5:1 PDMS than on 20:1 PDMS. However, the 20:1 PDMS surfaces were found to have 40 times more attached *E. coli* RP437 cells compared to 5:1 PDMS (Figure 2.2A). This finding strongly supports that the effects observed in this study were caused by changes in surface stiffness, rather than roughness. Also, PDMS is essentially not charged, which can avoid the interaction of strong electrostatic force. Thus, effects of surface chemistry, roughness, and electrostatic force are negligible. This allows us to investigate the effects of stiffness more specifically.

It has been shown that bacteria take only minutes to attach to abiotic surfaces, while the host immune cells take several hours to respond.[49-52] Thus, the finding that surface stiffness can affect bacterial adhesion, growth, and antibiotic susceptibility for 24 h is intriguing. Further understanding of the mechanism will help design better biomaterials. For example, the levels of stiffness involved in this study are in the range of those used for contact lenses. Reusable

contact lenses are typically washed after daily use. Thus, tuning the surface stiffness may help reduce eye infections associated with contact lenses.

It was shown that the bacterial cells on stiff surface was internalized by macrophages more easily than those on soft surfaces. Thus, although the bacteria attached on stiff surface is more tolerance to antibiotics, it can be easily internalized by macrophage. In addition, the number of attached bacterial cells is much lower on stiff surfaces than soft surfaces. Therefore, the stiff PDMS will be recommended in the medical application.

However, the viability assay used did not reveal what is the key factor causing the difference in phagocytosis among the AR of the attached cells, the density of attached cells, the activity of macrophages on different surfaces, and the difference in the composition of surface proteins secreted by attached cells. A few of studies have revealed that how macrophages response to different shapes of polymers and how surface stiffness influence the activity of macrophages. For example, Champion et al.[45-47] showed that the poly(lactide-co-glycolie) (PLGA) particles with low aspect ratios (AR) are more easily internalized by macrophages. And Discher et al.[23,48] showed that macrophages on stiff surfaces (100 kPa) are more spreading than those on soft surfaces (1 kPa). However, what is the roles of each factors in the phagocytosis is still not clear. This is part of our on-going project.

In summary, using PDMS and representative Gram-negative bacteria (*E. coli* and *P. aeruginosa*) as a model system, we found that surface stiffness affects not only the adhesion of bacterial cells, but also the growth, morphology, and antibiotic susceptibility of attached

cells. It is interesting to observe that the cell size and surface stiffness are inversely correlated after 5-h growth. This finding suggests that an increase in surface stiffness in the tested range may present a stress to attached cells, which can lead to slow growth, enhanced antibiotic tolerance, and reduced biofilm surface coverage. The stress may be caused by direct interaction between cells and PDMS surface and cell-cell interaction, since increasing the cell density in inoculation was found to alleviate the effects of stiffness. The effects of surface stiffness on biofilm cells at the molecular and genetic levels are unknown. It will be interesting to study the effects on bacterial cell structure (such as cell wall stiffness and membrane composition) and gene expression (especially the genes and pathways involved in growth, cell division, motility, chemotaxis, and stress response). It will also be interesting to test if surface stiffness affects the strength of bacterial adhesion and tolerance of attached cells to shear force. Using cell tracking and flow cells may provide useful information. This is part of our ongoing work.

2.6 Conclusions

By varying the degree of crosslinking of PDMS, we investigated the effects of substrate stiffness on the early stage biofilm formation of *E. coli* and *P. aeruginosa* including attachment, growth, cell length, and the susceptibility of attached cells to antibiotics. Decrease in surface stiffness was found to promote both the attachment and growth of *E. coli* and *P. aeruginosa* cells. More interestingly, the cells on 40:1 PDMS substrates after 5 h of biofilm growth were found significantly longer than those on 5:1 PDMS substrates; and the distribution of cell size was narrower on stiff substrates. The cells on stiff substrates also exhibited decreased susceptibility to antibiotics compared to the cells on soft substrates. And phagocytosis is faster on stiff surfaces than on soft surfaces. Collectively, these results indicate

that the stiffness of a substrate could affect the physiology of attached bacterial cells and possibly the progression of biomaterial associated bacterial infections.

2.7 Reference

(1) Hall-Stoodley, L.; Costerton, J. W.; Stoodley, P. Bacterial biofilms: from the natural environment to infectious diseases. *Nature Reviews Microbiology* **2004,** *2*, 95-108.

(2) Klevens, R. M.; Morrison, M. A.; Nadle, J.; Petit, S.; Gershman, K.; Ray, S.; Harrison, L. H.; Lynfield, R.; Dumyati, G.; Townes, J. M. Invasive methicillin-resistant Staphylococcus aureus infections in the United States. *JAMA: the journal of the American Medical Association* **2007,** *298*, 1763-1771.

(3) Klevens, R. M.; Edwards, J. R.; Richards, C. L.; Horan, T. C.; Gaynes, R. P.; Pollock, D. A.; Cardo, D. M. Estimating health care-associated infections and deaths in US hospitals, 2002. *Public health reports* **2007,** *122*, 160.

(4) Häussler, S.; Parsek, M. R. Biofilms 2009: new perspectives at the heart of surface-associated microbial communities. *Journal of bacteriology* **2010,** *192*, 2941-2949.

(5) Renner, L. D.; Weibel, D. B. Physicochemical regulation of biofilm formation. *MRS bulletin* **2011,** *36*, 347-355.

(6) Cheng, G.; Zhang, Z.; Chen, S.; Bryers, J. D.; Jiang, S. Inhibition of bacterial adhesion and biofilm formation on zwitterionic surfaces. *Biomaterials* **2007,** *28*, 4192-4199.

(7) Nejadnik, M. R.; van der Mei, H. C.; Norde, W.; Busscher, H. J. Bacterial adhesion and growth on a polymer brush-coating. *Biomaterials* **2008,** *29*, 4117-4121.

(8) Hou, S.; Burton, E. A.; Wu, R. L.; Luk, Y.-Y.; Ren, D. Prolonged control of patterned biofilm formation by bio-inert surface chemistry. *Chemical Communications* **2009**, 1207-1209.

(9) Saha, N.; Monge, C.; Dulong, V.; Picart, C.; Glinel, K. Influence of Polyelectrolyte Film Stiffness on Bacterial Growth. *Biomacromolecules* **2013**.

(10) Lichter, J. A.; Thompson, M. T.; Delgadillo, M.; Nishikawa, T.; Rubner, M. F.; Van Vliet, K. J. Substrata mechanical stiffness can regulate adhesion of viable bacteria. *Biomacromolecules* **2008,** *9*, 1571-1578.

(11) Bakker, D. P.; Huijs, F. M.; de Vries, J.; Klijnstra, J. W.; Busscher, H. J.; van der Mei, H. C. Bacterial deposition to fluoridated and non-fluoridated polyurethane coatings with different elastic modulus and surface tension in a parallel plate and a stagnation point flow chamber. *Colloids and Surfaces B: Biointerfaces* **2003,** *32*, 179-190.

(12) Packham, D. E. Surface energy, surface topography and adhesion. *International journal of adhesion and adhesives* **2003,** *23*, 437-448.

(13) Oliveira, R.; Azeredo, J.; Teixeira, P.; Fonseca, A. The role of hydrophobicity in bacterial adhesion. **2001**.

(14) Singh, A. V.; Vyas, V.; Patil, R.; Sharma, V.; Scopelliti, P. E.; Bongiorno, G.; Podestà, A.; Lenardi, C.; Gade, W. N.; Milani, P. Quantitative characterization of the influence of the nanoscale morphology of nanostructured surfaces on bacterial adhesion and biofilm formation. *PloS one* **2011,** *6*, e25029.

(15) Díaz, C.; Cortizo, M. C.; Schilardi, P. L.; Saravia, S. G. G. d.; Mele, M. A. F. L. d. Influence of the nano-micro structure of the surface on bacterial adhesion. *Materials Research* **2007,** *10*, 11-14.

(16) Scheuerman, T. R.; Camper, A. K.; Hamilton, M. A. Effects of substratum topography on bacterial adhesion. *Journal of colloid and interface science* **1998,** *208*, 23-33.

(17) Perni, S.; Prokopovich, P. Micropatterning with conical features can control bacterial adhesion on silicone. *Soft Matter* **2013,** *9*, 1844-1851.

(18) Crawford, R. J.; Webb, H. K.; Truong, V. K.; Hasan, J.; Ivanova, E. P. Surface topographical factors influencing bacterial attachment. *Advances in Colloid and Interface Science* **2012**.

(19) Hou, S.; Gu, H.; Smith, C.; Ren, D. Microtopographic patterns affect Escherichia coli biofilm formation on poly (dimethylsiloxane) surfaces. *Langmuir* **2011,** *27*, 2686-2691.

(20) An, Y. H.; Friedman, R. J. Concise review of mechanisms of bacterial adhesion to biomaterial surfaces. *Journal of biomedical materials research* **1998,** *43*, 338-348.

(21) Palchesko, R. N.; Zhang, L.; Sun, Y.; Feinberg, A. W. Development of Polydimethylsiloxane Substrates with Tunable Elastic Modulus to Study Cell Mechanobiology in Muscle and Nerve. *PloS one* **2012,** *7*, e51499.

(22) Discher, D. E.; Mooney, D. J.; Zandstra, P. W. Growth factors, matrices, and forces combine and control stem cells. *Science* **2009,** *324*, 1673-1677.

(23) Discher, D. E.; Janmey, P.; Wang, Y.-l. Tissue cells feel and respond to the stiffness of their substrate. *Science* **2005,** *310*, 1139-1143.

(24) Eroshenko, N.; Ramachandran, R.; Yadavalli, V. K.; Rao, R. R. Effect of substrate stiffness on early human embryonic stem cell differentiation. *Journal of biological engineering* **2013,** *7*, 7.

(25) Pozos Vázquez, C. m.; Boudou, T.; Dulong, V.; Nicolas, C.; Picart, C.; Glinel, K. Variation of polyelectrolyte film stiffness by photo-cross-linking: a new way to control cell adhesion. *Langmuir* **2009,** *25*, 3556-3563.

(26) Chen, C.-C.; Hsieh, P. C.-H.; Wang, G.-M.; Chen, W.-C.; Yeh, M.-L. The influence of surface morphology and rigidity of the substrata on cell motility. *Materials Letters* **2009,** *63*, 1872-1875.

(27) Engler, A. J.; Sen, S.; Sweeney, H. L.; Discher, D. E. Matrix elasticity directs stem cell lineage specification. *Cell* **2006,** *126*, 677-689.

(28) Kim, S. H.; Moon, J.-H.; Kim, J. H.; Jeong, S. M.; Lee, S.-H. Flexible, stretchable and implantable PDMS encapsulated cable for implantable medical device. *Biomedical Engineering Letters* **2011,** *1*, 199-203.

(29) Crnich, C. J.; Halfmann, J. A.; Crone, W. C.; Maki, D. G. The effects of prolonged ethanol exposure on the mechanical properties of polyurethane and silicone catheters used for intravascular access. *Infection control and hospital epidemiology* **2005,** *26*, 708-714.

(30) Habal, M. B. The biologic basis for the clinical application of the silicones: a correlate to their biocompatibility. *Archives of Surgery* **1984,** *119*, 843.

(31) Sabri, F.; Marchetta, J. G.; Sinden-Redding, M.; Habenicht, J. J.; Chung, T. P.; Melton, C. N.; Hatch, C. J.; Lirette, R. L. Effect of Surface Plasma Treatments on the Adhesion of Mars JSC 1 Simulant Dust to RTV 655, RTV 615, and Sylgard 184. *PloS one* **2012,** *7*, e45719.

(32) Gu, H.; Hou, S.; Yongyat, C.; De Tore, S.; Ren, D. Patterned Biofilm Formation Reveals a Mechanism for Structural Heterogeneity in Bacterial Biofilms. *Langmuir* **2013,** *29*, 11145-11153.

(33) Horst, C. R.; Brodland, B.; Jones, L. W.; Brodland, G. W. Measuring the Modulus of Silicone Hydrogel Contact Lenses. *Optometry & Vision Science* **2012,** *89,* 1468-1476.

(34) Parkinson, J. S.; Houts, S. E. Isolation and behavior of Escherichia coli deletion mutants lacking chemotaxis functions. *Journal of bacteriology* **1982,** *151*, 106-113.

(35) Han, Y.; Hou, S.; Simon, K. A.; Ren, D.; Luk, Y.-Y. Identifying the important structural elements of brominated furanones for inhibiting biofilm formation by Escherichia coli. *Bioorganic & medicinal chemistry letters* **2008,** *18*, 1006-1010.

(36) Maniatis, T.; Fritsch, E. F.; Sambrook, J., *Molecular cloning: a laboratory manual*. Cold Spring Harbor Laboratory Cold Spring Harbor, NY: 1982; Vol. 545.

(37) Evans, N. D.; Minelli, C.; Gentleman, E.; LaPointe, V.; Patankar, S. N.; Kallivretaki, M.; Chen, X.; Roberts, C. J.; Stevens, M. M. Substrate stiffness affects early differentiation events in embryonic stem cells. *Eur Cell Mater* **2009,** *18,* 13-14.

(38) Wang, Z. Polydimethylsiloxane Mechanical Properties Measured by Macroscopic Compression and Nanoindentation Techniques. University of South Florida, 2011.

(39) Fuard, D.; Tzvetkova-Chevolleau, T.; Decossas, S.; Tracqui, P.; Schiavone, P. Optimization of poly-di-methyl-siloxane (PDMS) substrates for studying cellular adhesion and motility. *Microelectronic Engineering* **2008,** *85*, 1289-1293.

(40) Chen, C.-Y.; Nace, G. W.; Irwin, P. L. A 6× 6 drop plate method for simultaneous colony counting and MPN enumeration of Campylobacter jejuni, Listeria monocytogenes, and Escherichia coli. *Journal of Microbiological Methods* **2003,** *55*, 475-479.

(41) Heydorn, A.; Nielsen, A. T.; Hentzer, M.; Sternberg, C.; Givskov, M.; Ersbøll, B. K.; Molin, S. Quantification of biofilm structures by the novel computer program COMSTAT. *Microbiology* **2000,** *146*, 2395-2407.

(42) LaFleur, M. D.; Qi, Q.; Lewis, K. Patients with long-term oral carriage harbor high-persister mutants of Candida albicans. *Antimicrobial agents and chemotherapy* **2010,** *54*, 39-44.

(43) Dawson, C. C.; Intapa, C.; Jabra-Rizk, M. A. "Persisters": Survival at the Cellular Level. *PLoS pathogens* **2011,** *7*, e1002121.

(44) Lewis, K. Persister cells, dormancy and infectious disease. *Nature Reviews Microbiology* **2006,** *5*, 48-56.

(45) Yoo, J.-W.; Mitragotri, S. Polymer particles that switch shape in response to a stimulus. *Proceedings of the National Academy of Sciences* **2010,** *107*, 11205-11210.

(46) Champion, J. A.; Mitragotri, S. Role of target geometry in phagocytosis. *Proceedings of the National Academy of Sciences of the United States of America* **2006,** *103*, 4930-4934.

(47) Champion, J. A.; Mitragotri, S. Shape induced inhibition of phagocytosis of polymer particles. *Pharmaceutical research* **2009,** *26*, 244-249.

(48) Patel, N. R.; Bole, M.; Chen, C.; Hardin, C. C.; Kho, A. T.; Mih, J.; Deng, L.; Butler, J.; Tschumperlin, D.; Fredberg, J. J. Cell elasticity determines macrophage function. *PloS one* **2012,** *7*, e41024.

Chapter 3

Motility reveals *motB* is involved in response to material stiffness during *Escherichia coli* biofilm formation

The ACT*IV*E package used in this Chapter for tracking the bacterial motility was modified by Megan Brasch and Dr. James Henderson.

3.1 Abstract

Escherichia coli RP437 and its isogenic mutants of motility (*motB*), flagella (*fliC*) and type I fimbriae (*fimA*) were used to investigate bacterial response to material stiffness during the initial attachment on cross-linked poly(dimethylsiloxane) (PDMS) surfaces with different Young's moduli (0.1 and 2.6 MPa), which were prepared by controlling the degree of crosslinking. The results of cell counting and tracking revealed that the *motB* mutant of *E. coli* RP437 has defects in response to the stiffness of PDMS, which was rescued by complementation of the *motB* gene. The cell tracking results indicated that the *E. coli* cells on stiff surfaces were more motile than those on soft surfaces, and mutation of *motB* led to larger differences in terms of the types and velocity of motility on stiff surfaces than wild type *E. coli* RP437 strains.

3.2 Introduction

Over 90% of bacteria on earth live in biofilms with cells attached on surfaces and surrounded by extracellular polysaccharides and self-produced DNA, RNA and proteins.[1] Due to the high-level tolerance to antimicrobial and host immune factors, the biofilms colonized implanted medical devices and host tissues can cause persistent infections, which result in nearly 100,000 deaths and 28-45 billion dollars of losses each year in the U.S. alone.[2-5] Additionally, the biofilms formed on water pipe and ship hulls hydro-dynamically increase the energy cost and cause a heavy burden on our economy.[1,6] Therefore, understanding the mechanism of biofilm formation and physiology of biofilm cells is critical for solving these problems. There are multiple steps in the transition of bacterial cells from planktonic growth to biofilm formation, including initial attachment, cell growth, biofilm maturation, and dispersion. Among these steps, initial attachment (including reversible and irreversible attachment) plays an important role in biofilm formation and is known to be influenced by many properties of the substratum surface such as surface chemistry,[7-10] stiffness,[11-13] hydrophobicity,[14,15] roughness,[16,17] topography,[18-21] and charge.[7,22] In a recent study,[23] we reported that decrease in stiffness of cross-linked poly(dimethylsiloxane) promotes the bacterial adhesion and growth, and the attached bacterial cells on soft surfaces are longer and more sensitive to antibiotics. [2021,243] However, how bacteria response to surface stiffness during the initial attachment is still unknown. It has been reported previously that bacteria can sense surface by flagella, fimbriae or other surface appendages.[25-31] For example, some bacteria use flagella to detect the contact with a surface, and start biofilm formation with polysaccharide synthesis.[32] However, how bacteria sense and response to surface stiffness has not been studied. Here, we investigated the effects of surface stiffness on the initial attachment and the motility of attached *E. coli* RP437 using imaging and cell tracking.

3.3 Materials and Methods

3.3.1 Bacterial strains and Growth media.

Escherichia coli RP437, [335] one of the model strains for studying motility and biofilm formation, and its isogenic mutants, *motB*, *fliC*, and *fimA*, were used to investigated the roles of motility, flagella, and type I fimbriae in bacterial response to surface stiffness. To follow cells with imaging, the plasmid pRSH103 was transduced into each strains to label the cells with constitutively expressed red fluorescence. The strains used in this study were summarized in Table 3.1. *E. coli* RP437 and its mutants were routinely grown at 37ºC with shaking at 200 rpm in Lysogeny Broth (henceforth LB medium) containing 10 g/L tryptone, 5 g/L yeast extract, and 10 g/L NaCl in DI water. [21,34] *E. coli* RP437/pRSH103, *E. coli* RP3087/pRSH103, *E. coli* RP437 Δ*fim*A/pRSH103, and *E. coli* RP437 Δ*fli*C/pRSH103 were routinely grown at 37ºC with shaking at 200 rpm in LB medium supplemented with 30 µg/mL tetracycline.

3.3.2 Preparation of PDMS surfaces.

PDMS surfaces were prepared using SYLGARD184 Silicone Elastomer Kit (Dow Corning Corporation, Midland, MI). The stiffness was adjusted by varying the mass ratio of base to curing agent (5:1 and 40:1 tested) following a protocol described previously.[35-37] For each given ratio, elastomer base and curing agent were thoroughly mixed and degased under vacuum for 30 min. Then, the mixture was poured into a petri-dish, cured at 60ºC for 24 h, and incubated at room temperature for another 24 h to fully polymerize. The PDMS surface was then peeled off the petri-dish and cut into 1.0 cm by 0.6 cm pieces (1.5 mm thick), which were sterilized by soaking in 200 proof ethanol for 20 min and dried with sterile air. All of the sterilized PDMS substrates were stored at room temperature until use. The Young's moduli of

PDMS 5:1 and 40:1 are 2.6 MPa (stiff) and 0.1 MPa (soft), respectively, as we reported previously.[23]

3.3.3 Bacterial adhesion on PDMS.

Bacterial cells from overnight cultures were harvested by centrifugation at 8,000 rpm for 3 min at 4ºC, washed with phosphate buffered saline (PBS) (pH 7.3) three times, and then used to inoculate PBS to desired cell density. The cell density of inoculum was controlled by measuring optical density at 600 nm (OD_{600}). This cell suspension (30 mL) was transferred to a petri-dish containing sterilized PDMS surfaces (facing up, shown in supplementary Figure 3.1a; or facing down, shown in supplementary Figure 3.1b). Meanwhile, the cell suspension was dropped on a LB plate after a series of 10× dilution (10 μL in each drop) for confirming the cell density of the inoculum. [38] After incubation at 37ºC for 2 h without shaking, the PDMS surfaces were gently washed by dipping in PBS three times (changed to clean PBS for each step). The viability of cells was determined using the drop plate assay as described previously.[38] Briefly, the attached cells were harvested by gentle sonication for 1 min and vortexing for 30 s. Then the cell suspension was dropped on a LB plate after a series of 10× dilution (10 μL in each drop) for measuring the density of attached cells on surfaces. The plates were incubated at 37°C overnight to count colony forming units (CFU). All conditions were tested with at least 3 replicates.

3.3.4 Cell tracking and data analysis.

Bacterial cells from overnight cultures were harvested by centrifugation at 8,000 rpm for 3 min at 4ºC, washed with phosphate buffered saline (PBS) (pH 7.3), and then used to inoculate PBS

to desired cell density. This cell suspension was transferred to a petri-dish containing sterilized PDMS surfaces. The initial attachment of the fluorescent bacterial cells were visualized using an Axio Observer Z1 fluorescence microscope (Carl Zeiss Inc., Berlin, Germany). Images were taken every 5 s and the results were analyzed using the cell tracking package ACT*IV*E.[39] The cells were identified and contoured by adjusting the parameters in ACT*IV*E. And then the cells were categorized into three types, "still" (The cells whose mass center did not move more than a quarter of the body length in 5 s), "rotating" (the cells whose mass center moved more than a quarter but less than one body length in 5 s), and "moving" (the cells whose mass center moved more than one body length in 5s). The average of moving speed was calculated for each cell. And the distribution of speeds were analyzed and fit by Boltzmann distribution.

3.4 Results

3.4.1 *motB* of *E. coli* is important to the response to PDMS stiffness during attachment.

Our recent study has shown that bacteria prefer to attach on soft PDMS surfaces than stiff PDMS surfaces (0.1 -2.6 mPa Young's Modulus) .[23] However, how bacteria sense and reponse to surface stiffness is still unknown. To understand the mechanism of mechanosensing by bacteria, *E. coli* RP437, which is a model wild-type strain for biofilm research, and its mutants of *motB, fimA,* and *fliC* genes were compared (Table 1). Each inoculum was washed three times with PBS and the adhesion (for 2 h) was carried out in PBS in the absence of any carbon source so that adhesion can be studied in the absence of cell growth. The cell density of inoculum was controlled to be 3×10^7 cells/mL – 6×10^7 cells/mL. After 2 h attachment, there were $(1.1 \pm 0.4) \times 10^6$ cells/cm^2 of *E. coli* RP437 on soft surfaces and $(5.3 \pm 2.4) \times 10^3$ cells/cm^2 of *E. coli* RP437 on stiff surfaces (Figure 3.1). When the stiffness increased from 0.1 MPa to

2.6 MPa, the number of attached *E. coli* RP437 cells decreased more than 2 logs, consistent with our earlier report.[23] In comparison, the number of attached *E. coli* RP437 Δ*fli*C was (1.6 ± 0.2) × 10^5 cells/cm^2 on soft surfaces and (2.3 ± 0.7) × 10^3 cells/cm^2 on stiff surfaces, corresponding to a 2 log decrease in adhesion; and the attachment of *E. coli* RP437 Δ*fimA* decreased from (2.0 ± 0.3) × 10^5 cells/cm^2 on soft surfaces to (4.4 ± 0.5) × 10^2 cells/cm^2 on stiff surfaces, corresponding to more than 2 logs of decrease in adhesion. Both mutants have relatively lower number of attached cells than the wild-type strain on the same surfaces. These findings are consistent with the previous results that both flagella and type I fimbriae are important in the initial attachment.[32,40] For example, bacteria could use flagella to touch a surface and type I fimbriae to inreversely attach on it. However, both *fimA* and *fliC* mutants still exhibited substantial comparable differences in attachment between soft and stiff surfaces. Thus, these two genes are not essential for sensing stiffness. Interestingly, *E. coli* RP437 *motB* mutant showed reduced difference in attachment between soft and stiff surfaces, while the wilde-type *E. coli* RP437 and *motB* mutant had similar numbers of cells attached on soft PDMS, the *motB* mutant had around 10 times more cells on the sitff surface than the wilde type strain. This led to 1 log decrease in the difference between soft and stiff surfces, suggesting that *motB* may play a role in mechanosensing.

Table 3.1. List of *E. coli* strains and plasmids used in this study.

E. coli strains or plasmids	Genotype	Characteristics	Source/ Reference
RP437	Wild type Strain [thr-1(Am) leuB6 his-4 metF159(Am) eda-50 rpsL1356 thi-1ara-14mtl-1 xyl-5 tonA31 tsx-78 lacY1 F-]	Wild type strain for biofilm study	[33]
RP3087	RP437 Δ(*motB*)580	Motility mutant (point mutation in *motB*)	[43]
Δ*fli*C		Flagella mutant (deletion mutation of *fliC*)	This study
Δ*fim*A		Type I fimbriae mutant (deletion mutation of *fimA*)	This study
pRSH103	Plasmid, Tet^r, constitutive *rfp*	Red fluorescence	[21]
pRHG03	Plasmid, *motB* complementation	*motB* complementation	This study

To comfirm if this change was indeed caused by *motB* mutation, *E. coli* RP3087/pRGH03 (*motB* complementation strain) was also studied under the same condition (Table 1). As shown in Figure 3.1, the defects of *motB* mutant was fully recovered by *motB* complementation, and the numbers of attached cells on both soft and stiff surfaces were similar to the wild-type strains ($p>0.05$, *t* test). These results confirmed that the decrease in the number of attached cells between soft and stiff PDMS surfaces was indeed caused by *motB* mutation.

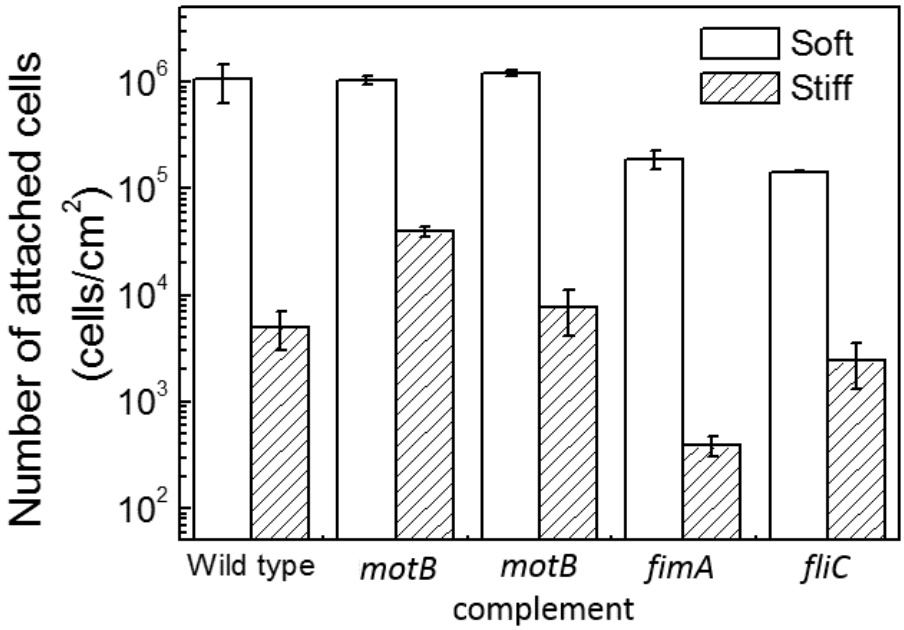

Figure 3.1. The number of attached *E. coli* RP437 wild type, Δ(*mot*B)580, Δ*fim*A, Δ*fli*C, and *motB* complement strains on facing up stiff (2.6 MPa) and soft (0.1 MPa) PDMS after 2 hours attachment in PBS with initial inoculum density between $3 \times 10^7 – 6 \times 10^7$ cells/mL.

It is worth noting that the mutation of *motB* did not fully abolish the ability of *E. coli* to respond to PDMS stiffness. To further understand the role of *motB* in mechanosensing, the number of attached wild-type cells and *motB* mutant cells on soft and stiff surface with different inoculum cell densities were compared. As shown in Figure 3.2, when the inoculum cell density was varied from 2×10^4 cells/mL to 2×10^8 cells/mL, the number of *motB* mutant cells on soft surfaces was similar to that of the wild-type cells. Howver, the number of attached *motB* mutant cells on stiff surfaces was significantly higher than the number of attached *E. coli* RP437 wild-type cells on stiff surfaces for all the tested conditions ($p<0.05$, one-way ANOVA), which led to a dramatically decreased difference in the number of attached cells between soft and on stiff

surfaces in the range of inoculum cell density tested. Moreover, the number of attached *motB* complemented cells was siminlar to that of the wild-type strain on both soft and stiff surfaces. Thus, the defects of *motB* mutant were fully recovered by genetic complementation of the *motB* gene. These results support that *motB* may be involved in the response of *E. coli* to surface stiffness during biofilm formation.

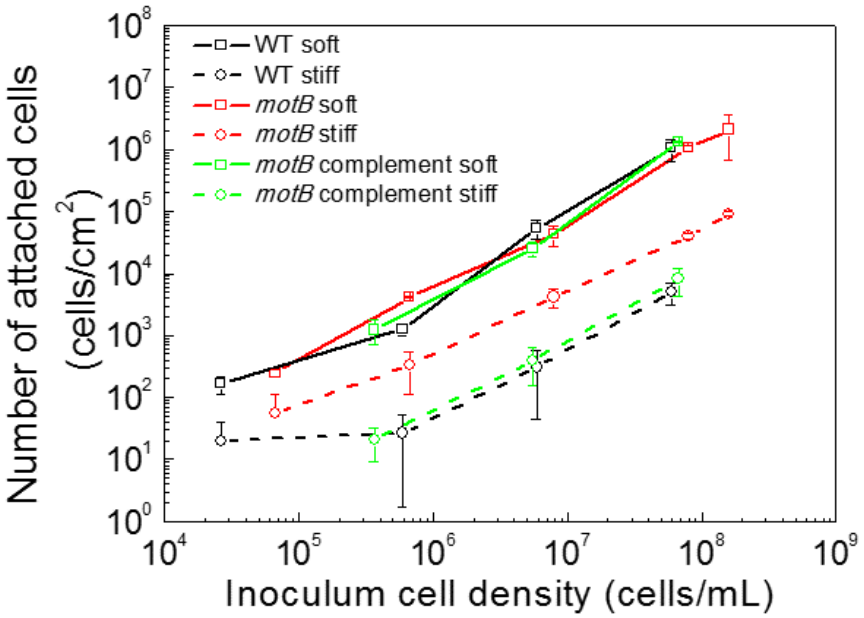

Figure 3.2 Effects of cell density of inoculum on the attachment of *E. coli* RP437 wild type, *motB* and *motB* complementation.

3.4.2 Adhesion to inverted surfaces

It was interesting to observe that the mutation of *motB* caused defects in the response of *E. coli* to PDMS stiffness. The experiments above were based on attachment to face-up surfaces. To specifically study attachment in the absence of gravity driven settlement, we repeated the

adhesion experiments using face-down surfaces with the inocululm density between 2×10^7 cells/mL and 4×10^7 cells/mL.

As shown in Figure 3.3, the numbers of attached cells of all tested strains are at least one log lower than those on face-up surfaces, suggesting that gravity does facilitate cell settlement and adhesion. Nevertheless, *E. coli* still showed preference in adhesion on soft PDMS surfaces than stiff PDMS surfaces. For example, the number of attached *E. coli* RP437 cells on soft PDMS surfaces was $(5.2 \pm 1.8) \times 10^3$ cells/cm^2, which is 1.5 log higher than that on stiff surface [$(2.2 \pm 0.6) \times 10^2$ cells/cm^2]. As expected, the *E. coli* RP437 *motB* mutant also caused the defects in the response of *E. coli* to PDMS stiffness, since the difference in the numbers of attached cells was reduced to 0.8 log for the *motB* mutant. This defects was fully recovered in the complemented strain, as observed for adhesion on face-up surfaces.

To understand if the defects in response to surface stiffness of *E. coli* RP437 *motB* mutant was caused by single physical factors or also involve cellular functions, *E. coli* RP437 was treated with 20 μg/mL chloramphenicol, a bacteriostatic antibiotics that inhibits protein synthesis, before adhesion. As shown in Figure 3.3, the chloramphenicol treatment abolished the difference in adhesion between soft and stiff surfaces. This finding indicats that cellular funtions may be involved in the response to material stiffness during *E. coli* attachment to PDMS.

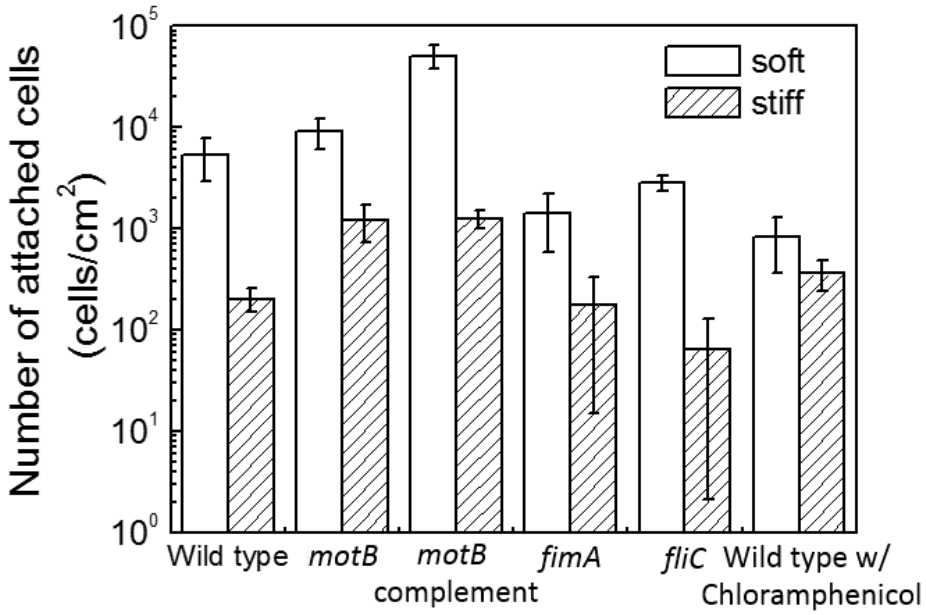

Figure 3.3 The number of attached *E. coli* RP437 wild type, Δ(*mot*B)580, *motB* complementation, Δ*fim*A, Δ*fli*C, and wild type treated by 20 μg/mL chloramphenicol on facing-down stiff (2.6 MPa) and soft (0.1 MPa) PDMS after 2 hours attachment in PBS with initial inoculum density between $2 \times 10^7 – 4 \times 10^7$ cells/mL.

3.4.3 Tracking bacterial motility by automated contour-based tracking package for *in vitro* environment (ACT*IV*E).

Bacterial adhesion on a surface is a complex dynamic process involving initial physical interaction, reversible attachment, cell movement, and irreversible attachment. To further understand how material stiffness affects this process and role of *motB* gene, *E. coli* RP437 and its mutants were labeled with constitutive red fluorescence protein expressed from the plasmid pRSH103. The overnight cultures of each strain were washed with PBS and then diluted to around 3×10^7 cells/mL in PBS to study the attachment on soft and stiff PDMS

surfaces. The attachment on PDMS in PBS was recorded at room temperature by imaging every 5 s for 18 min using fluorescence microscopy.

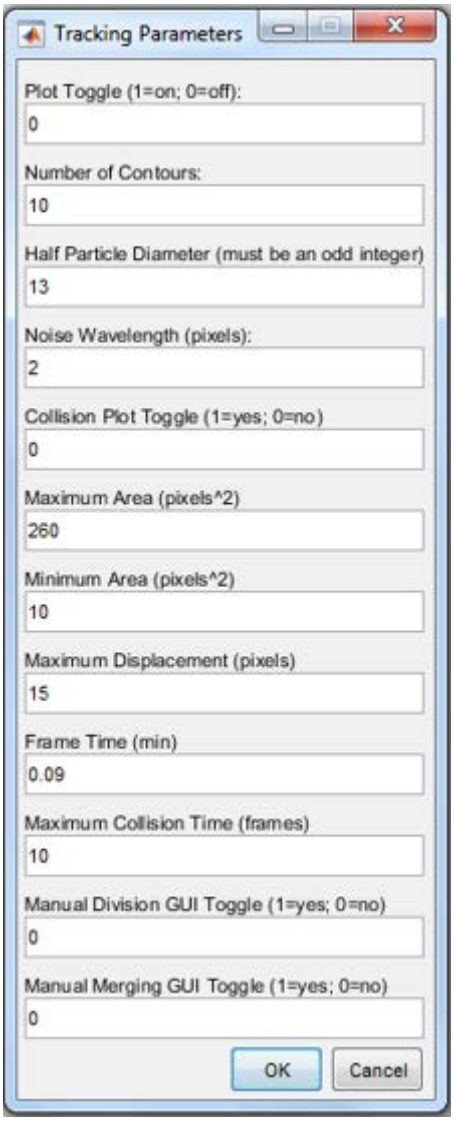

Figure 3.4. Parameters for tracking bacterial motility on surfaces using ACT*IV*E.

The data were analyzed using a MATLAB based automated contour-based tracking package for *in vitro* environment (ACT*IV*E).[39] This package has been shown to have a great performance in tracking the motility of mouse fibroblasts in a complex *in vitro* model.[39] This

is the first time to using this package for microbial research. Because the size of bacterial cells (around 2 µm) is much smaller than the size of fibroblasts (12 µm), the ACT*IV*E package was validated first using *E. coli* RP437/pGLO expressing strong green fluorescence upon induction with arabinose. The initial attachment was recorded for 10 min and representative images of the cells attached on a glass surface are shown in Figure 3.5A. By adjusting the parameter of the ACT*IV*E package (Figure 3.4), all bacterial cells were successfully identified (Figure 3.5B), and the cell contours were automatically detected with good accuracy (Figure 3.5C). ACT*IV*E was also validated for tracking bacterial cells over time as shown in Figure 3.5D.

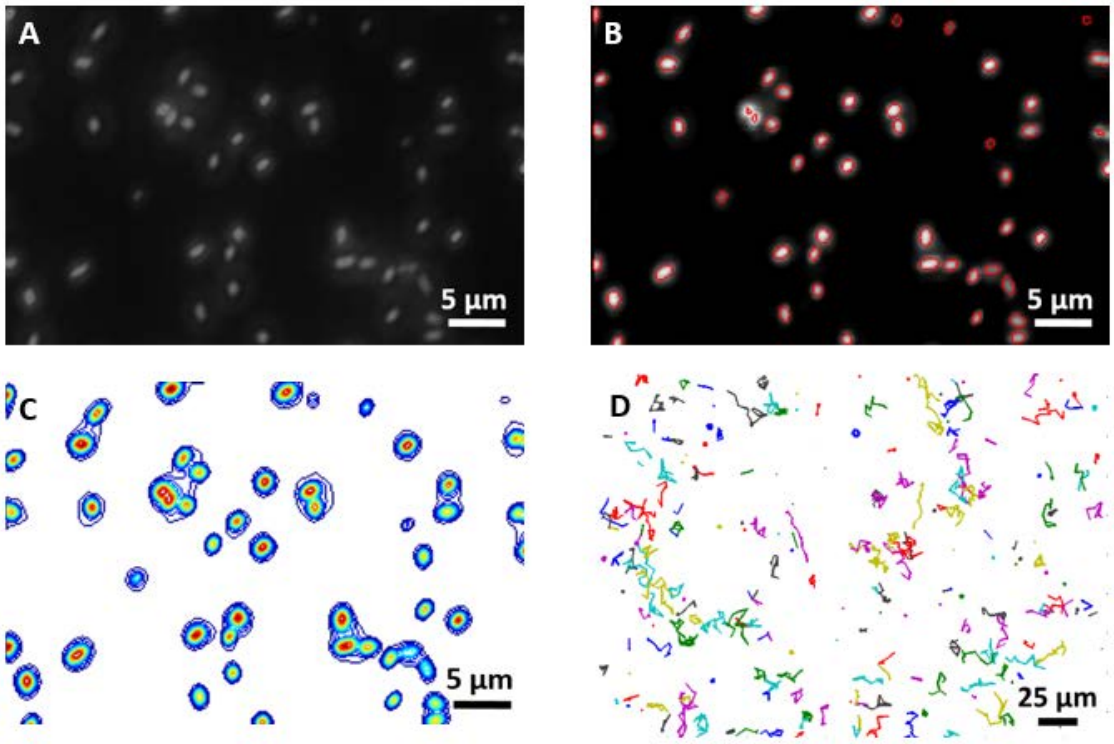

Figure 3.5. Scheme depicting example (A) Image of *E. coli* RP437/pGLO. (B) *E. coli* RP437 was identified by ACT*IV*E. (C) Contour profiles are established based on the fluorescence density fluctuations. (D) Plot of cell tracks with different color.

3.4.4 Effects of surface stiffness on cell motility on soft and stiff PDMS surfaces.

After validation, ACT*IV*E was used to compare *E. coli* RP437 and its mutants for adhesion on PDMS surfaces with different levels of stiffness. Rapidly moving planktonic cells were excluded from analysis by focusing on the cells that did not move with more than one body length in 5 s initially. The detected cells were categorized into three groups (Fig. 3.5), “still cells” that did not move, “rotating cells” that moved in a circular motion (either full, partial or back and forth) with the mass center moved less than one body length, and “moving cells” that had the mass center moved for more than one body length.. The cell types were automatically categorized by ACT*IV*E frame by frame (5 s per frame), and the results from a representative movie are shown in Figure 3.6A. The average numbers of “still cells”, “rotating cells” and “moving cells” are summarized in Figure 3.6B. In addition, by averaging the results in three movies (with at least 320 frames in each), the average fractions of “still cells”, “rotating cells” and “moving cells” with standard deviations are shown in Figure 3.6C.

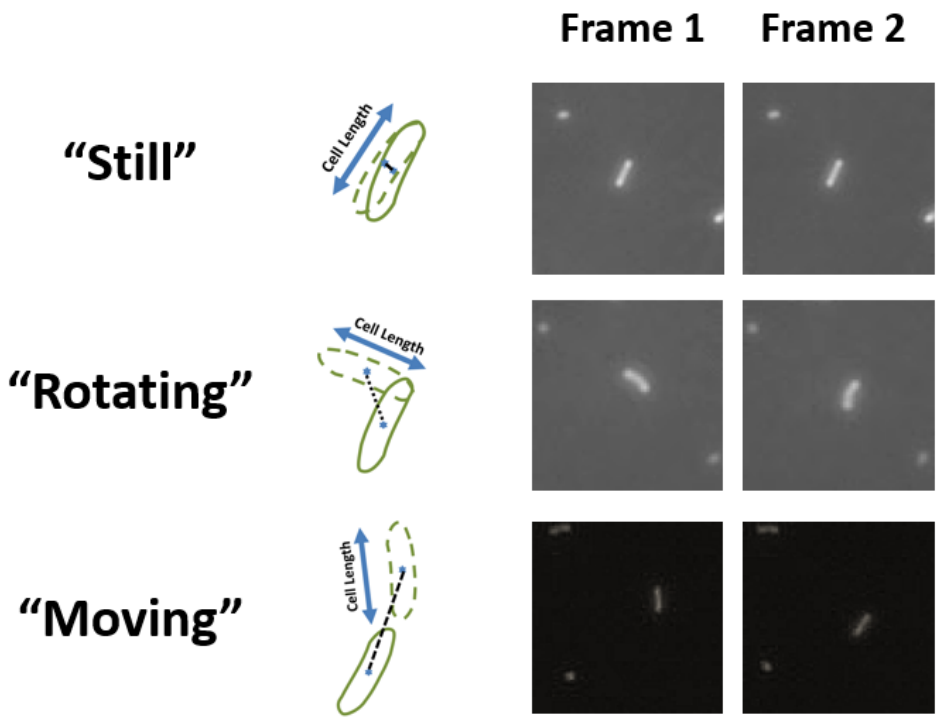

Figure 3.6. Three types of movement of bacterial cells on surfaces categorized by ACT*IV*E. "Still" represents the cells with a displacement of mass center less than a quarter of cell length in 5 s. "Rotating" represents the cells moved in a circular motion but with a displacement of mass less than the cell length in 5 s. "Moving" represents the cells with a displacement of mass center of the cell more than a quarter the cell length in 5 s.

Consistent with the CFU and imaging data,[23] *E. coli* RP437 was found to prefer soft surfaces for attachment on PDMS. As shown in Figure 3.7B, most of the *E. coli* RP437 wild-type cells were "still" on soft surfaces, while the fractions of "rotating cells" and "moving cells" dramatically increased on stiff surfaces. For example, on soft PDMS surfaces, 62% of the attached *E. coli* RP437 cells were not actively moving ("still"), and the rotating and moving cells represented only 27% and 11% of the population, respectively. On stiff surfaces, however, the fraction of still cells of *E. coli* RP437 was only 40% of the whole population, while the

fraction of rotating cells increased to 39%, and that of moving cells increased to 21%. These results are in agreement with our previous observation that *E. coli* prefers soft PDMS surfaces for adhesion.

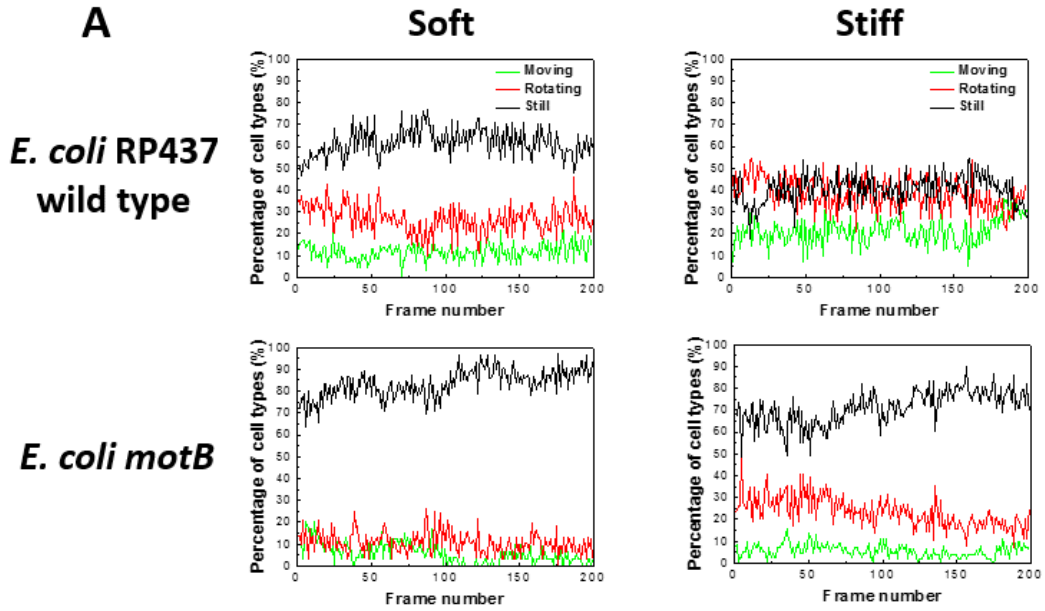

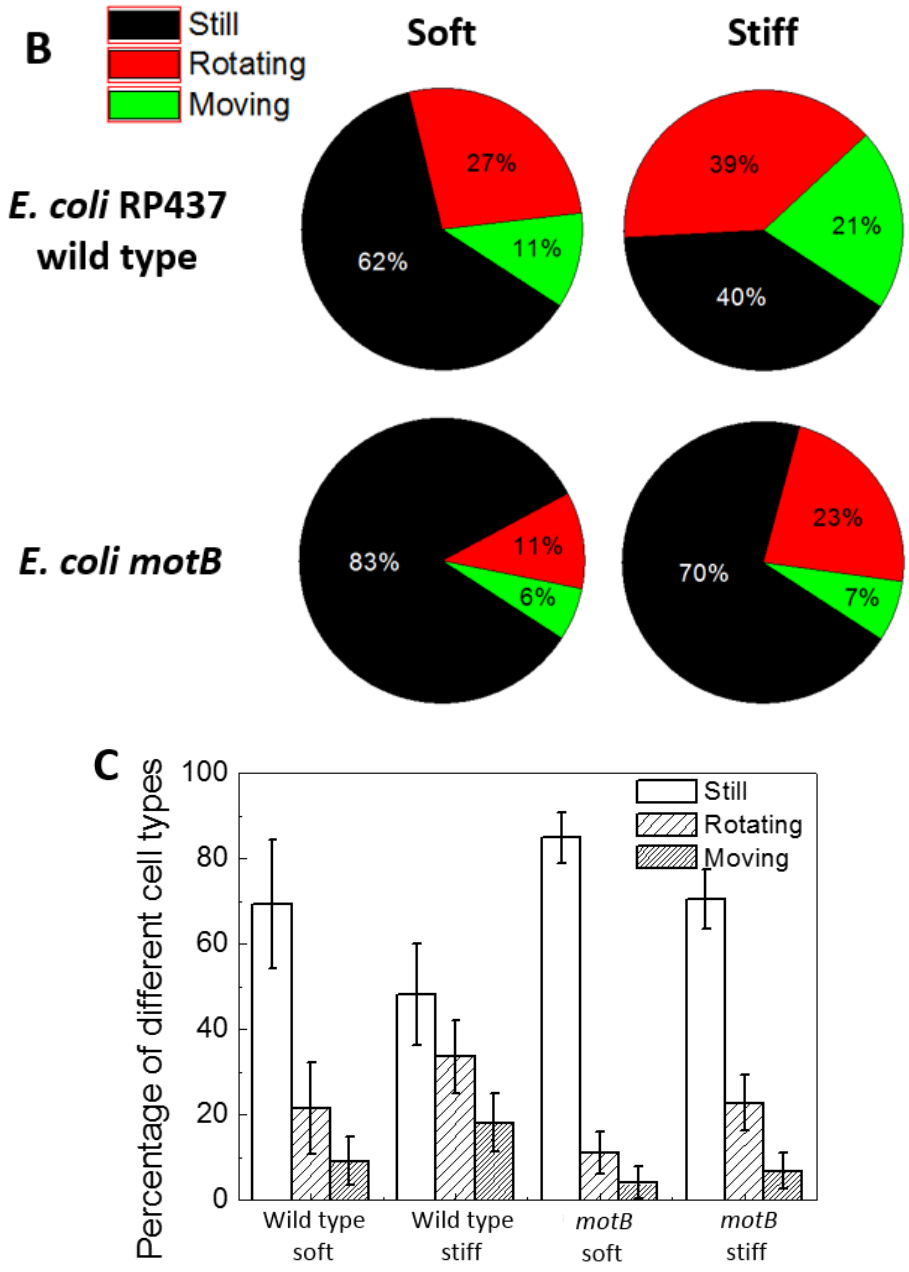

Figure 3.8. Percentage of "still", "rotating" and "moving" cells in the attached *E. coli* RP437 wild type and *motB* strains. (A) The percentage of "still", "rotating" and "moving" cells in each frame. (B) Average percentage of "still", "rotating" and "moving" cells in the representative movie. (C) Average percentage of "still", "rotating" and "moving" cells. The

results were calculated by averaging the date from at least 320 frames in 3 movies. Error bars represent standard deviations.

By comparing the numbers of “still”, “rotating” and “moving” cells on soft PDMS with those on stiff PDMS, it was found that *E. coli* RP437 *motB* mutant also prefers soft surface; e.g., 83% of the attached cells were still cells on soft surfaces. This is much higher than the still cells on stiff surfaces (70%). And more cells on stiff surfaces were rotating (23%) than on soft surfaces (11%). These results indicate surfaces stiffness could still influence the adhesion of *E. coli* RP437 *motB* mutant, which consistent with the results in Figure 3.1.

In addition to cell location, the speed of movement was also analyzed for each cell using ACT*IV*E. The representative results are shown in Figure 3.8A, in which each dot represents the velocity of a cell at one time point, and black lines show the average velocities of all cells at a given time point. The average velocity calculated from all cells over all time points is shown on the top of each plot. By analyzing at least 200 cells in 3 movies, the average velocities of *E. coli* RP437 and its *motB* mutant on soft and stiff PDMS surfaces are summarized in Figure 3.8B. Based on the average velocity of each cells, the distribution of the velocities was also calculated and is shown in Figure 3.7C in which the fitting curves based on Boltzmann distribution represent the trends of each distribution.

The differences were also observed for the velocity of *E. coli* RP437 and its *motB* mutant. As shown in Figure 3.8A, the average velocities on stiff surfaces for *E. coli* RP437 (6.2 μm/min) and its *motB* mutant (3.2 μm/min) were higher than those on soft surfaces, e.g., 3.4 μm/min

(*E. coli* RP437) and 2.0 μm/min (*motB* mutant), respectively. Moreover, the distributions of the velocity on stiff surfaces dropped much faster for both *E. coli* RP437 and its *motB* mutant than those on soft surfaces, suggesting that there are more cells having low velocity on soft surfaces for both strains than on soft surfaces. Collectively, these results indicated that the *E. coli* RP437 cells were more motile on stiff surface than soft surface.

3.4.5 The role of *motB* gene on bacterial motility on soft and stiff PDMS surfaces.

It has been shown that material stiffness affects the adhesion and motility of *E. coli* RP437, and mutation of *E. coli* RP437 *motB* gene reduced the difference in adhesion between on soft and stiff PDMS surfaces. To further investigate the role of *motB* gene in the bacterial motility on both surfaces, the fraction of the "still", "rotating", and "moving" cells between *E. coli* RP437 and its *motB* mutant on soft and stiff PDMS surfaces were compared. As shown in Figure 3.8B, the percentage of "still" cells was much higher for *E. coli* RP437 *motB* mutant than *E. coli* RP437 wild-type strains on either stiff or soft surfaces. In particular, the percentage of *E. coli* RP437 *motB* mutant on stiff surfaces (70%) is 75% higher than the percentage of its wild-type strain (40%). Accordingly, the percentages of "rotating" and "moving" cells were lower for *E. coli* RP437 *motB* mutant than *E. coli* RP437 wild-type strains on stiff and soft surfaces (Figure 3.8B). For example, the percentage of "rotating" *E. coli* RP437 *motB* mutant on soft surfaces was 11%, which is much lower than those of *E. coli* RP437 wild-type strain (27%). Especially, the percentages of "moving" *E. coli* RP437 *motB* mutants on soft and stiff surfaces were only 6% and 7%, respectively. These are much lower than the percentage of "moving" *E. coli* RP437 wild type on soft surfaces (11%) and stiff surfaces (21%). The results

suggest that *E. coli* RP437 *motB* mutants prefer “still” to “rotating” and “moving”, compared to the its wild-type strains.

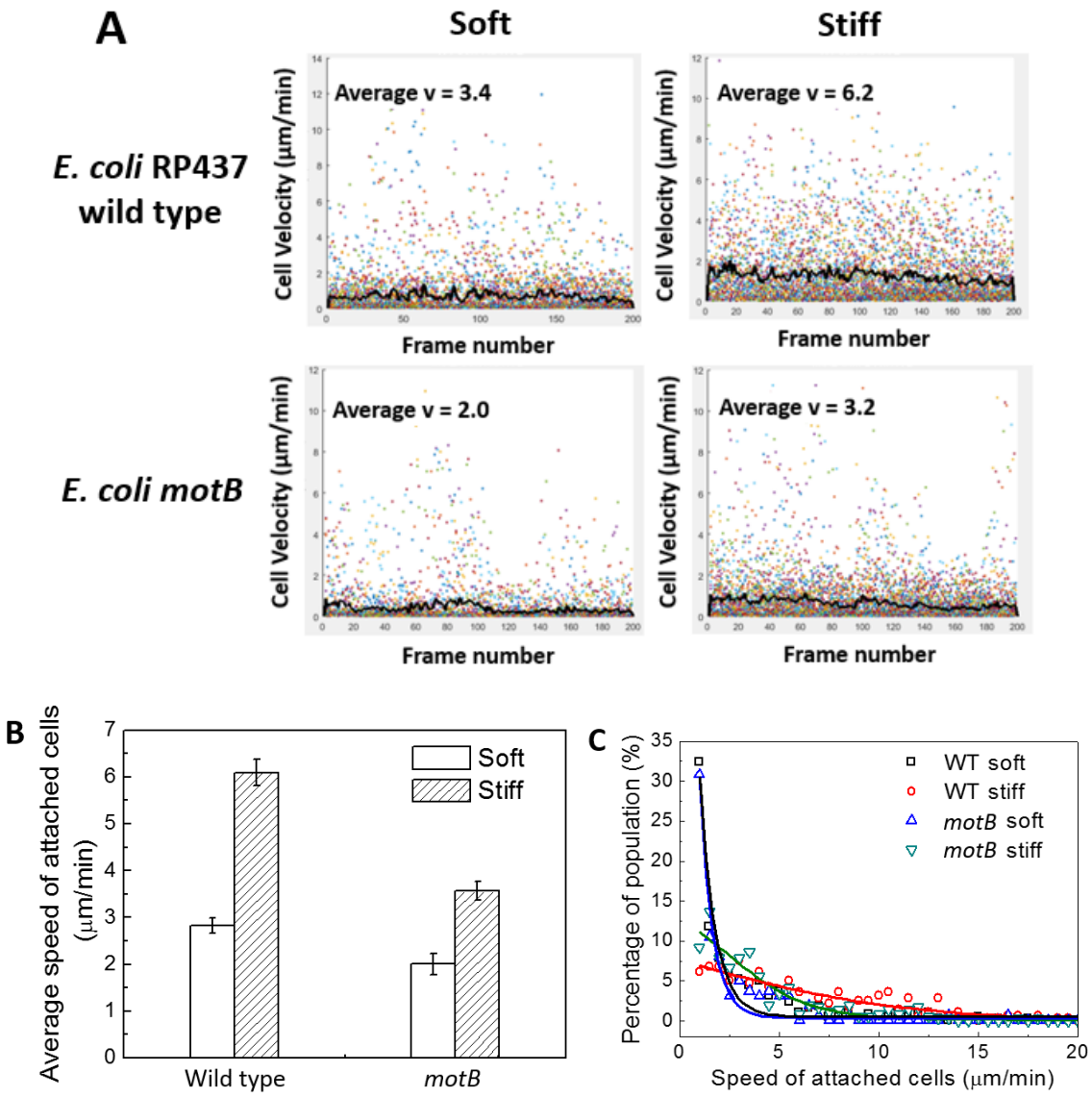

Figure 3.9. Movement speed of the wild-type *E. coli* RP437 and its *motB* mutation soft and stiff PDMS surfaces. (A) The speed of every moving cell in each frame. Each dot represent a cell, and black line shows the average velocity of all cells at each time point. Y axis shows the one fifth of the velocity of attached cells. (B) Overall average speed of cell movement. The

results were averaged from at least 200 cells in 3 movies (17 min long for each). Error bars show the standard errors. (C) Distributions of movement speeds of *E. coli* RP437 and its *motB* mutation on soft and stiff PDMS. Each movie includes at least 200 cells. There movies were analyzed.

As shown in Figure 3.9A, the average velocity of *E. coli* RP437 *motB* mutant cells on was also lower than the wild-type RP437 on both soft (2.0 vs. 3.4 μm/min) and stiff surfaces (3.2 vs. 6.2 μm/min) In addition, the decrease of movement speed of *motB* mutant cells on stiff surfaces is around 50% compared to the wild-type cells, which is much bigger than this on soft surface (around 30 %). The distribution of cell movement speeds is shown in Figure 3.7C. The percentage of motile cells decreased as the velocity increased for all conditions, and the distribution of the velocity on soft surfaces were narrower than that on stiff surfaces for both strains. To describe the distribution of the velocity, the dispersity of the velocity is defined using the formula below,

$$Dispersity\ (D) = \sum Pv^2$$

P is the percentage of the cells with the velocity v. The dispersity indicates how wide the distribution. The dispersity was found to be *E. coli* RP437 *motB* mutant on soft surfaces (0.54) < *E. coli* RP437 wild-type strain on soft surfaces (0.76) < *E. coli* RP437 *motB* mutant on stiff surfaces (1.12) < *E. coli* RP437 wild-type strain on stiff surfaces (2.51). This result suggests that the *E. coli* RP437 wild-type strains on stiff surface is the most motile and *E. coli* RP437 *motB* mutant on soft surfaces is the least motile. These results are consistent with the findings described in Fig. 3.1 and suggest that the motility is important to adhesion on PDMS.

3.5 Discussion

In this study, we compared *E. coli* RP437, and *motB, fliC, fimA* mutants for adhesion on PDMS surfaces with varying stiffness. Specifically 40:1 (soft) and 5:1 (sitff) PDMS surfaces were used. The results show that *motB* mutation negatively impacted the capability of *E. coli* cells to differentiate soft and stiff surfaces, which was recovered by complementing the *motB* gene. The defect of the adhsion primaryly occur on stiff surfaces, on which there are 10 times more attached *E. coli* RP437 *motB* mutant cells than *E. coli* RP437 wild-type strains. Cell tracking during the initial attachment showed that more of the *motB* mutant cells are still than its wild-tpye strains. And *E. coli* RP437 *motB* mutant rotate and moving much less than the type to its wild-type strains. Compared the average velocity of *E. coli* RP437 wild type and its *motB* mutant on soft and stiff surfaces, the difference for *E. coli* RP437 *motB* mutant on both surfaces is much smaller than this for *E. coli* RP437 wild-type strains. This is consistent with the finding that the difference in the number of attached *E. coli* RP437 *motB* mutant on both surfaces is smaller than that of the wild-type strain. Also, the distribution of the velocity indicates that the *E. coli* RP437 *motB* mutant is much less motile than *E. coli* RP437 wild-type strains.

Based on the results in chapter 2 study, we speculate that Material stiffness may affect bacterial biofilm formation by influencing adhesion and cell motility. During initial attachment, *E. coli* may using extracellular appendages (e.g. flagella) to sense the stiffness. If the stiffness is appropriate, the cells will attach (less motile) and start biofilm growth sooner. In comparison, if the stiffness is not desired, the cells may move more before settling, as observed on stiff surfaces. It is also possible that some cells may leave the surface and return to planktonic stage

if the surface is not in favor for attachment. Further study of 3D cell tracking will be helpful to answer this questions.

It is not surprising to find that the *motB* gene is important to the observed difference in bioflm formaiton between soft and stiff PDMS surfaces. MotB is an important component of bacterial flagella. Mutation of *motB* could render the cells to be non-motile and thus less capable of surface attachment. However, the motB mutant still exhibited difference in adhesion (although markedly reduced) between soft and stiff surfaces. This suggests that other factors are also involved in mechanosensing. To identify these factors, it will be important to study more mutants and create double mutants of important genes. This is part of our ongoing work.

3.6 Conclusion

The *motB* mutant of *E. coli* RP437 exhibited defects in response to the stiffness of PDMS, which was fully recovered by the *motB* complementation, in a wide range of inoculum cell density. The cell tracking results during initial attachment suggest that the *E. coli* cells on stiff surfaces were more motile than those on soft surfaces. The mutation of *motB* could led to lower mobility on both surfaces. However, the decrease in the mobility of the *motB* mutant compared to the wild-type strain was more dramatic on stiff surfaces is larger than that on soft surfaces. This is consistent with the CFU results and indicate other factors may also be involved in mechanosensing of material stiffness by *E. coli*.

3.7 References

(1) Hall-Stoodley, L.; Costerton, J. W.; Stoodley, P. Bacterial biofilms: from the natural environment to infectious diseases. *Nature Reviews Microbiology* **2004,** *2*, 95-108.

(2) Klevens, R. M.; Morrison, M. A.; Nadle, J.; Petit, S.; Gershman, K.; Ray, S.; Harrison, L. H.; Lynfield, R.; Dumyati, G.; Townes, J. M. Invasive methicillin-resistant Staphylococcus aureus infections in the United States. *JAMA: the journal of the American Medical Association* **2007,** *298*, 1763-1771.

(3) Klevens, R. M.; Edwards, J. R.; Richards, C. L.; Horan, T. C.; Gaynes, R. P.; Pollock, D. A.; Cardo, D. M. Estimating health care-associated infections and deaths in US hospitals, 2002. *Public health reports* **2007,** *122*, 160.

(4) Häussler, S.; Parsek, M. R. Biofilms 2009: new perspectives at the heart of surface-associated microbial communities. *Journal of bacteriology* **2010,** *192*, 2941-2949.

(5) Costerton, J.; Stewart, P. S.; Greenberg, E. Bacterial biofilms: a common cause of persistent infections. *Science* **1999,** *284*, 1318-1322.

(6) Costerton, J. W.; Lewandowski, Z.; Caldwell, D. E.; Korber, D. R.; Lappin-Scott, H. M. Microbial biofilms. *Annual Reviews in Microbiology* **1995,** *49*, 711-745.

(7) Renner, L. D.; Weibel, D. B. Physicochemical regulation of biofilm formation. *MRS bulletin* **2011,** *36*, 347-355.

(8) Cheng, G.; Zhang, Z.; Chen, S.; Bryers, J. D.; Jiang, S. Inhibition of bacterial adhesion and biofilm formation on zwitterionic surfaces. *Biomaterials* **2007,** *28*, 4192-4199.

(9) Nejadnik, M. R.; van der Mei, H. C.; Norde, W.; Busscher, H. J. Bacterial adhesion and growth on a polymer brush-coating. *Biomaterials* **2008,** *29*, 4117-4121.

(10) Hou, S.; Burton, E. A.; Wu, R. L.; Luk, Y.-Y.; Ren, D. Prolonged control of patterned biofilm formation by bio-inert surface chemistry. *Chemical Communications* **2009**, 1207-1209.

(11) Saha, N.; Monge, C.; Dulong, V.; Picart, C.; Glinel, K. Influence of Polyelectrolyte Film Stiffness on Bacterial Growth. *Biomacromolecules* **2013**.

(12) Lichter, J. A.; Thompson, M. T.; Delgadillo, M.; Nishikawa, T.; Rubner, M. F.; Van Vliet, K. J. Substrata mechanical stiffness can regulate adhesion of viable bacteria. *Biomacromolecules* **2008,** *9*, 1571-1578.

(13) Bakker, D. P.; Huijs, F. M.; de Vries, J.; Klijnstra, J. W.; Busscher, H. J.; van der Mei, H. C. Bacterial deposition to fluoridated and non-fluoridated polyurethane coatings with different elastic modulus and surface tension in a parallel plate and a stagnation point flow chamber. *Colloids and Surfaces B: Biointerfaces* **2003,** *32*, 179-190.

(14) Packham, D. E. Surface energy, surface topography and adhesion. *International journal of adhesion and adhesives* **2003,** *23*, 437-448.

(15) Oliveira, R.; Azeredo, J.; Teixeira, P.; Fonseca, A. The role of hydrophobicity in bacterial adhesion. **2001**.

(16) Singh, A. V.; Vyas, V.; Patil, R.; Sharma, V.; Scopelliti, P. E.; Bongiorno, G.; Podestà, A.; Lenardi, C.; Gade, W. N.; Milani, P. Quantitative characterization of the influence of the nanoscale morphology of nanostructured surfaces on bacterial adhesion and biofilm formation. *PloS one* **2011,** *6*, e25029.

(17) Díaz, C.; Cortizo, M. C.; Schilardi, P. L.; Saravia, S. G. G. d.; Mele, M. A. F. L. d. Influence of the nano-micro structure of the surface on bacterial adhesion. *Materials Research* **2007,** *10*, 11-14.

(18) Scheuerman, T. R.; Camper, A. K.; Hamilton, M. A. Effects of substratum topography on bacterial adhesion. *Journal of colloid and interface science* **1998,** *208*, 23-33.

(19) Perni, S.; Prokopovich, P. Micropatterning with conical features can control bacterial adhesion on silicone. *Soft Matter* **2013,** *9*, 1844-1851.

(20) Crawford, R. J.; Webb, H. K.; Truong, V. K.; Hasan, J.; Ivanova, E. P. Surface topographical factors influencing bacterial attachment. *Advances in Colloid and Interface Science* **2012**.

(21) Hou, S.; Gu, H.; Smith, C.; Ren, D. Microtopographic patterns affect Escherichia coli biofilm formation on poly (dimethylsiloxane) surfaces. *Langmuir* **2011,** *27*, 2686-2691.

(22) An, Y. H.; Friedman, R. J. Concise review of mechanisms of bacterial adhesion to biomaterial surfaces. *Journal of biomedical materials research* **1998,** *43*, 338-348.

(23) Song, F.; Ren, D. Stiffness of cross-linked poly (dimethylsiloxane) affects bacterial adhesion and antibiotic susceptibility of attached cells. *Langmuir* **2014,** *30*, 10354-10362.

(24) Gu, H.; Hou, S.; Yongyat, C.; De Tore, S.; Ren, D. Patterned biofilm formation reveals a mechanism for structural heterogeneity in bacterial biofilms. *Langmuir* **2013,** *29*, 11145-11153.

(25) Palchesko, R. N.; Zhang, L.; Sun, Y.; Feinberg, A. W. Development of Polydimethylsiloxane Substrates with Tunable Elastic Modulus to Study Cell Mechanobiology in Muscle and Nerve. *PloS one* **2012,** *7*, e51499.

(26) Discher, D. E.; Mooney, D. J.; Zandstra, P. W. Growth factors, matrices, and forces combine and control stem cells. *Science* **2009,** *324*, 1673-1677.

(27) Discher, D. E.; Janmey, P.; Wang, Y.-l. Tissue cells feel and respond to the stiffness of their substrate. *Science* **2005,** *310*, 1139-1143.

(28) Eroshenko, N.; Ramachandran, R.; Yadavalli, V. K.; Rao, R. R. Effect of substrate stiffness on early human embryonic stem cell differentiation. *Journal of biological engineering* **2013,** *7*, 7.

(29) Pozos Vázquez, C. m.; Boudou, T.; Dulong, V.; Nicolas, C.; Picart, C.; Glinel, K. Variation of polyelectrolyte film stiffness by photo-cross-linking: a new way to control cell adhesion. *Langmuir* **2009,** *25*, 3556-3563.

(30) Chen, C.-C.; Hsieh, P. C.-H.; Wang, G.-M.; Chen, W.-C.; Yeh, M.-L. The influence of surface morphology and rigidity of the substrata on cell motility. *Materials Letters* **2009,** *63*, 1872-1875.

(31) Engler, A. J.; Sen, S.; Sweeney, H. L.; Discher, D. E. Matrix elasticity directs stem cell lineage specification. *Cell* **2006,** *126*, 677-689.

(32) Petrova, O. E.; Sauer, K. Sticky situations: key components that control bacterial surface attachment. *Journal of bacteriology* **2012,** *194*, 2413-25.

(33) Parkinson, J. S.; Houts, S. E. Isolation and behavior of Escherichia coli deletion mutants lacking chemotaxis functions. *Journal of bacteriology* **1982,** *151*, 106-113.

(34) Maniatis, T.; Fritsch, E. F.; Sambrook, J., *Molecular cloning: a laboratory manual*. Cold Spring Harbor Laboratory Cold Spring Harbor, NY: 1982; Vol. 545.

(35) Evans, N. D.; Minelli, C.; Gentleman, E.; LaPointe, V.; Patankar, S. N.; Kallivretaki, M.; Chen, X.; Roberts, C. J.; Stevens, M. M. Substrate stiffness affects early differentiation events in embryonic stem cells. *Eur Cell Mater* **2009,** *18*, 13-14.

(36) Wang, Z. Polydimethylsiloxane Mechanical Properties Measured by Macroscopic Compression and Nanoindentation Techniques. University of South Florida, 2011.

(37) Fuard, D.; Tzvetkova-Chevolleau, T.; Decossas, S.; Tracqui, P.; Schiavone, P. Optimization of poly-di-methyl-siloxane (PDMS) substrates for studying cellular adhesion and motility. *Microelectronic Engineering* **2008,** *85*, 1289-1293.

(38) Chen, C.-Y.; Nace, G. W.; Irwin, P. L. A 6× 6 drop plate method for simultaneous colony counting and MPN enumeration of Campylobacter jejuni, Listeria monocytogenes, and Escherichia coli. *Journal of Microbiological Methods* **2003,** *55*, 475-479.

(39) Baker, R. M.; Brasch, M. E.; Manning, M. L.; Henderson, J. H. Automated, contour-based tracking and analysis of cell behaviour over long time scales in environments of varying complexity and cell density. *Journal of The Royal Society Interface* **2014,** *11*, 20140386.

(40) Busscher, H. J.; van der Mei, H. C. How do bacteria know they are on a surface and regulate their response to an adhering state? *PLoS Pathogens* **2012,** *8*, e1002440.

(41) McDougald, D.; Rice, S. A.; Barraud, N.; Steinberg, P. D.; Kjelleberg, S. Should we stay or should we go: mechanisms and ecological consequences for biofilm dispersal. *Nature Reviews Microbiology* **2011,** *10*, 39-50.

(42) Monds, R. D.; O'Toole, G. A. The developmental model of microbial biofilms: ten years of a paradigm up for review. *Trends in microbiology* **2009,** *17*, 73-87.

(43) Blair, D. F.; Kim, D.; Berg, H. Mutant MotB proteins in Escherichia coli. *Journal of bacteriology* **1991,** *173*, 4049-4055.

Chapter 4

oprF is involved in sensing of material stiffness by *Pseudomonas aeruginosa*

4.1 Abstract

In this study, *P. aeruginosa* PAO1 and several isogenic mutants were compared for their adhesion on soft (40:1 PDMS) and stiff (5:1 PDMS) surfaces. Mutation of the *oprF* caused major defects in sensing surface PDMS stiffness by *P. aeruginosa*; e.g., it abolished the differences in adhesion and growth, morphology and antibiotic susceptibility of attached cells between soft and stiff PDMS surfaces. These defects were rescued by genetic complementation of *oprF*. Another gene *fleQ* was also shown to partially abolish the ability of sensing surface stiffness. Because both *oprF* and *fleQ* could cause the increase of c-di-GMP in cells, high level of c-di-GMP is considered to harm the response to surface stiffness. Consistently, *P. aeruginosa* PAO1 cells attached on soft PDMS surfaces were found to have higher level of intracellular c-di-GMP than those on stiff PDMS surfaces. To our best knowledge, this is the first report of *P. aeruginosa* genes involved in response to material stiffness during biofilm formation.

4.2 Introduction

Biofilms are communities of bacteria attached on surfaces and embedded in a self-produced matrix comprised of polysaccharides, DNA, and proteins. Biofilms of pathogenic bacteria cause serious chronic infections due to highly tolerance to antibiotics and host immune systems compared to their planktonic compartments.[1-4] As an opportunistic pathogen, *Pseudomonas aeruginosa* is a primary causative agent of chronic lung infections in cystic fibrosis patients and is blamed for many other infections such as those associated with chronic wounds and indwelling medical devices.[5] Many surface properties influence biofilm formation, such as surface chemistry,[7-10] stiffness,[11-21] hydrophobicity,[22,234] roughness,[24,256] topography,[26-2920] and charge.[7,301] In our previous research, we reported that soft surfaces of cross-linked poly(dimethylsiloxane) (PDMS) could promote the bacterial adhesion and growth, and the attached bacterial cells on soft surfaces are longer and less tolerant to antibiotics.[21]

A few pioneering studies have explored how bacteria sense the contact with a surface and transit from planktonic growth to biofilm formation.[30-32] In particular, a number of genes, including *pilA, wspA, wspR, wspF, fleQ,* are used by *P. aeruginosa* for surface sensing. It is believed that motile bacteria can touch a surface with flagella to overcome the repellent force between cell body and surfaces, and then use fimbriae to further secure the binding.[33-35] In this process, both flagella and pili are involved in surface sensing,[31,33,36] and the chemotaxis pathway and Cpx pathway were hypothesized to be the signal transduction pathway.[37,38] In addition, another surface sensing pathway named Wsp has been identified for the surface sensing by *P. aeruginosa*.[39] In this system, an inner membrane protein WspA was shown to be

a sensor, and the signal is transduced through WspB, WspC, WspE and WspR to cyclic-di-GMP which is an important initiator of bacterial motility and biofilm formation.[40,41]

Although the general sensing of surface contact has been studied, little is known about how bacteria sense the stiffness of a surface. In this study, we investigated the roles of several *P. aeruginosa* genes in response of this bacterium to PDMS stiffness during biofilm formation.

4.3 Materials and Methods.

4.3.1 Bacterial strains and Growth medium

The wild-type *P. aeruginosa* PAO1 [42] and its isogenic mutants used in this study were listed in Table 4.1. All strains were routinely grown at 37^{o}C in Lysogeny Broth (henceforth LB medium) containing 10 g/L tryptone, 5 g/L yeast extract, and 10 g/L NaCl in deionized (DI) water.[29,43]

4.3.2 Preparation of PDMS surfaces

PDMS surfaces were prepared using SYLGARD184 Silicone Elastomer Kit (Dow Corning Corporation, Midland, MI, USA). The stiffness was adjusted by varying the mass ratio of base to curing agent following a protocol described previously.[44-46] The base : curing agent ratios (wt/wt) of 5:1 and 40: 1 were tested. For each given ratio, elastomer base and curing agent were thoroughly mixed and degased under vacuum for 30 min. Then, the mixture was poured into a petri-dish, cured at 60^{o}C for 24 h, and incubated at room temperature for another 24 h to fully polymerize. The PDMS surface was then peeled off the petri-dish and cut into 1.0 cm by 0.6 cm pieces (1.5 mm thick), which were sterilized by soaking in 200 proof ethanol for 20

min and dried with sterile air. All of the sterilized PDMS substrates were stored at room temperature until use. The Young's moduli of PDMS surfaces were measured using dynamic mechanical analysis (DMA) (Q800, TA instrument, DE, USA) as described in our previous study.[39]

4.3.3 *P. aeruginosa* adhesion on PDMS

P. aeruginosa cells from overnight cultures were harvested by centrifugation at 8,000 rpm for 3 min at 4°C, washed with phosphate buffered saline (PBS) (pH 7.3) three times, and diluted by PBS to desired cell density. This cell suspension (30 mL) was transferred to a petri-dish containing sterilized face-down PDMS surfaces. After incubation at 37°C for 2 h without shaking, the PDMS surfaces were gently washed by dipping in PBS three times (changed to clean PBS for each step). The viability of cells was determined using the drop plate assay as described previously.[47] Briefly, the attached cells were harvested by gentle sonication for 1 min and vortexing for 30 s, which was validated to effectively detach more than 92% of the attached cells. Then the cell suspension was dropped on a LB plate after a series of 10× dilution (10 μL in each drop). The plate was included at 37°C overnight to count colony forming units (CFU).

Meanwhile, some PDMS surfaces were examined using an Axio Imager M1 fluorescence microscope (Carl Zeiss Inc., Berlin, Germany) to directly visualize the cells attached on PDMS surfaces. Aridine orange (500 μg/mL) was used to stain attached *P. aeruginosa* cells. At least five images were randomly taken from each sample, and the surface coverage by attached cells was calculated using COMSTAT.[48] The data of surface coverage and CFU were analyzed with

t test, Pearson correlation analysis, and one-way ANOVA followed by Tukey test as appropriate using SAS 9.2 software (SAS Institute, Cary, NC, USA).

4.3.4 Biofilm growth

After attachment, the surfaces were washed three times with PBS to remove the planktonic cells. The washed surfaces with attached cells were transferred to a new petri-dish containing 30 mL LB medium, and incubated at 37^{o}C without shaking for 5 h. After incubation, the PDMS surfaces were gently washed and analyzed as described above. Surface coverage was determined using COMSTAT. The length of attached cells was measured directly from microscope images. At least 300 cells were analyzed for each condition. To understand if surface stiffness affects the growth of attached cells, the biofilm cells after 5 h of growth were stained with 500 µg/mL acridine orange (Sigma-Aldrich, St. Louis, MO, USA) in PBS for 2 min, and imaged with fluorescence microscopy. The same cells were also imaged using DIC (differential interference contrast) as control.

4.3.5 Antibiotic susceptibility of attached cells

The washed surfaces after 5-h growth were transferred to a 12 well plate containing 2 mL PBS in each well supplemented with 20 µg/mL tobramycin, and incubated at 37^{o}C without shaking for 3.5 h. The control surfaces were incubated in the same condition without antibiotic. After incubation, the number of viable cells was determined by counting CFU as described above.

4.3.6 Genetic complementation of the *oprF* mutant.

The *oprF* mutant of *P. aeruginosa* PAO1 was complemented with plasmid pMH391, which was obtained from Prof. Soren Molin at Technical University of Denmark. The *oprF* gene and its native promoters were amplified from the wild-type of *P. aeruginosa* PAO1 with primers 5' CGCGGATCCTTGGGTAAATATTGTCTCTCT 3' (forward primer with BamHI site) and 5' CTAGTCTAGAAGGCTCAGCCGATTACTTGGC 3' (reverse primer with XbaI site). The 1204 bp PCR product was inserted into the pMH391 vector between the BamHI and XbaI restriction sites to create pMH391-*oprF*. The new plasmid pMH391-*oprF* was transformed into the *oprF* mutant of *P. aeruginosa* PAO1 by electroporation and selection with 50 µg/mL gentamicin.

4.3.7 Measurement of green fluorescence in the c-di-GMP reporter strain using fluorescence microscopy and flow cytometer.

P. aeruginosa PAO1/pCdrA::*gfp*^{s} cultured overnight in LB supplemented with 60 µg/mL gentamicin were harvested by centrifugation at 6,000 g for 3 min at 4°C, washed with phosphate buffered saline (PBS) (pH 7.3) and then used to inoculate PBS to desired cell density. This cell suspension (30 mL) was transferred to a petri-dish containing sterilized face-up PDMS surfaces. After incubation at 37ºC for 2 h without shaking, the PDMS surfaces were gently washed by dipping in PBS. Then the surfaces were imaged with fluorescence microscopy. Also, some samples were sconicated and vortexed to detach the cells as described above, and analyzed using a flow cytometer with the *gfp* detector (BD Accuri C6, BD, USA). The data of cell density were corroborated by counting CFU as described above.

4.4 Results

4.4.1 Effects of *oprF* mutation on mechnosensing by *P. aeruginosa*

Material stiffness has been shown to affect the adhesion of *E. coli* and *P. aeruginosa*, and the growth, morphology and antibiotic susceptibility of attached cells in our previous research.[21] However, how do bacterial cells sense and response to surface stiffness is still unknown, although several genes have been shown to be involved in general sensing of surface contact and the initiation of initial adhesion, such as those related flagella, fimbriae, and the Wsp pathway.[31,33,39] To understand how bacteria sense surface stiffness, the adhesion assay was used for screening several isogenic mutants showing in Figure 4.1a. The results are shown in Figure 4.1a. After 2 h adhesion, there were $(2.1 \pm 0.7) \times 10^5$ cells/cm^2 PAO1 cells attached on soft surfaces and $(1.8 \pm 0.1) \times 10^4$ cells/cm^2 attached on stiff surfaces. When the stiffness increased from 0.1 MPa to 2.6 MPa, the number of attached PAO1 cells decreased by 16 % (~ 1 log). In comparison, there were similar numbers of *oprF* mutant cells on these surfaces, e.g., $(8.9 \pm 0.03) \times 10^5$ cells/cm^2 on soft surface and $(7.8 \pm 0.7) \times 10^5$ cells/cm^2 on stiff surfaces, suggesting that *oprF* is possibly involved in the sensing the stiffness of substratum material. Except for *oprF*, mutation of other genes did not cause a significant defect sensing material stiffness. All mutants exhibited ~ 1 log difference in the number of attached cells between stiff and soft surfaces, as observed for the wild type PAO1. Thus, these mutants were excluded and we focused on *oprF* for further study.

Table 4.1. List of *P. aeruginosa* strains and plasmids used in this study.

***P. aeruginosa* strains or plasmids**	**Relevant genotype and/or characteristics**	**Source**
P. aeruginosa strains		
PAO1 wild type		[66]
PAO1 *oprF*	*oprF* transposon mutant	[66]
PAO1 *motB*	*motB* transposon mutant	[66]
PAO1 *fliC*	*fliC* transposon mutant	[66]
PAO1 *pilA*	*pilA* transposon mutant	[66]
PAO1 *pelB*	*pelB* transposon mutant	[66]
PAO1 *pslD*	*pslD* transposon mutant	[66]
PAO1 *algC*	*algC* transposon mutant	[66]
PAO1 *oprE*	*oprE* transposon mutant	[66]
PAO1 *sadB*	*sadB* transposon mutant	[66]
PAO1 *sadC*	*sadC* transposon mutant	[66]
PAO1 *wspE*	*wspE* transposon mutant	[66]
PAO1 *wspR*	*wspR* transposon mutant	[66]
PAO1 *bifA*	*bifA* transposon mutant	[66]
PAO1 *rpoS*	*rpoS* transposon mutant	[66]
PAO1 *rpoN*	*rpoN* transposon mutant	[66]
PAO1 *rhlA*	*rhlA* transposon mutant	[66]
PAO1 σ_{70}	σ_{70} transposon mutant	[66]
PAO1 *sigX*	*sigX* transposon mutant	[66]
PAO1 *fdxA*	*fdxA* transposon mutant	[66]
PAO1 *lecB*	*lecB* transposon mutant	[66]
PAO1 *mreC*	*mreC* transposon mutant	[66]

PAO1 *exoT*	*exoT* transposon mutant	[66]
PAO1 *fleQ*	*fleQ* transposon mutant	[66]
PAO1/pMH391		This study
PAO1 *oprF*/pMH391		This study
PAO1 *oprF*/pMH391-*oprF*	*oprF* complement strain	This study
PAO1/pCdrA::*gfp*^{s}	c-di-GMP reporter	[67]
PAO1/pCdrA::*gfp*(ASV)^{s}	c-di-GMP reporter	[67]
Plasmids		
pMH391	Plasmid, Amp^{r}, Gm^{r}	[68]
pMH391-oprF	oprF complement plasmid, Gm^{r}	This study
pCdrA::*gfp*^{s}	pUCP22Not-PcdrA-RBS-CDS-RNaseIII-gfp(Mut3)-T_0-T_1, Amp^{r}, Gm^{r}	[67]
pCdrA::*gfp*(ASV)^{s}	pUCP22Not-PcdrA-RBS-CDS-RNaseIII-gfp(ASV)-T_0-T_1, Amp^{r}, Gm^{r}	[67]

Because surface stiffness also affects the growth, morphology and antibiotic susceptibility of attached *P. aeruginosa* PAO1 cells,[21], we speculated that the mutation of *oprF* gene can also cause the difference in growth, cell size and antibiotic susceptibility of *P. aeruginosa* cells between soft and stiff surfaces. To test this, the stiff and soft PDMS surfaces were incubated in PBS with 2×10^7 cells/mL for 2 h to allow the cells to attach, and then transferred to LB medium to allow the cells to grow for 5 h. The surfaces were washed three times with PBS to remove planktonic cells before transfer. As shown in Figure 4.2, after 5 h growth, the surface coverage of PAO1 *oprF* mutant were similar between soft surfaces and stiff surfaces (p>0.05, t test.).

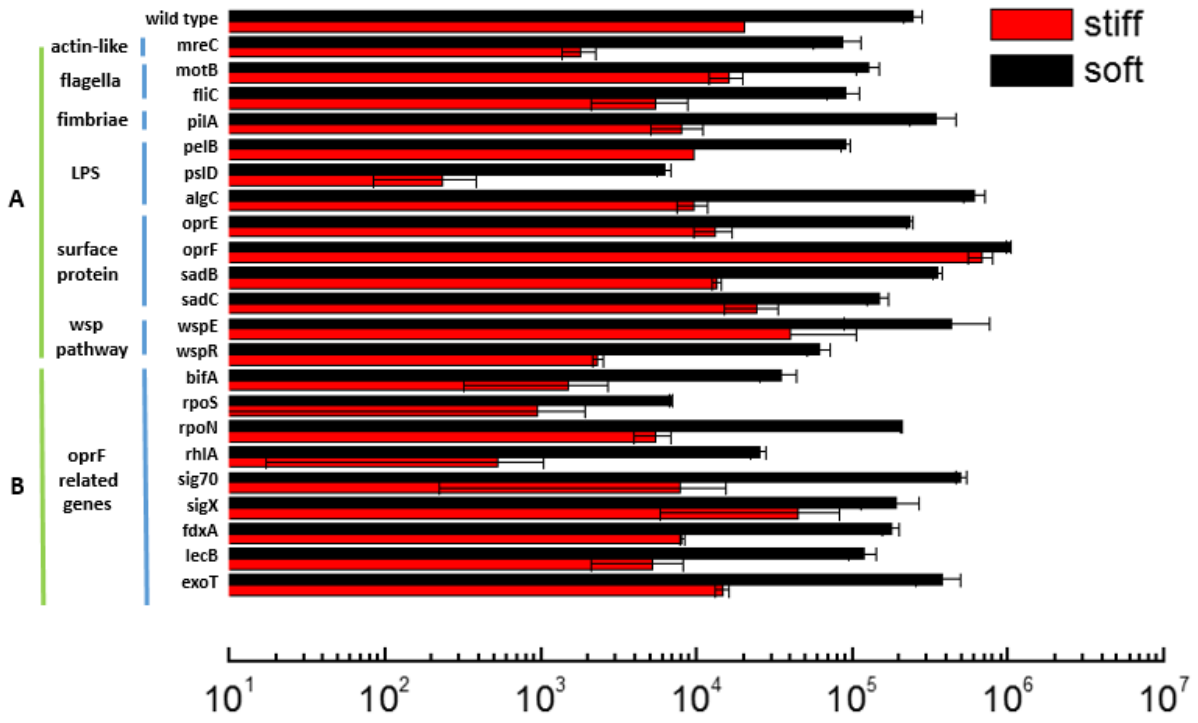

Figure 4.1 Adhesion of the wild-type PAO1 and its isogenic mutants on soft (40:1) and stiff (5:1) PDMS surfaces. (A) The mutants related to sensing surface contact. (B) The mutants of genes that have interaction with *oprF*.

Mutation of *oprF* also abolished the difference in cell length between on soft and stiff PDMS surfaces exhibited by the wild-type strain. As we reported previously, the average length of attached wild-type PAO1 cells on soft PDMS surfaces was 1.6 times that of cells on stiff PDMS surfaces. The average length of *oprF* mutant cells was 1.76 ± 0.42 μm and 1.70 ± 0.31 μm on soft and stiff surface, respectively (p >0.5, t test; Figure 4.3).

Consistent with the changes in cell adhesion, growth, and cell size, *oprF* mutation also abolished the difference in antibiotic susceptibility of attached cells. We found previously that the wild type PAO1 cells on soft PDMS after 5 h growth (the cells were allowed to attach for

2 h in PBS first before switching to LB medium for biofilm growth for 5 h) are 5 times more susceptible to 20 µg/mL tobramycin in 3.5 h treatment than those on stiff substrates. However, the *oprF* mutant exhibited similar susceptibility to 20 µg/mL tobramycin ($p>0.05$, t test) (Figure 4.4).

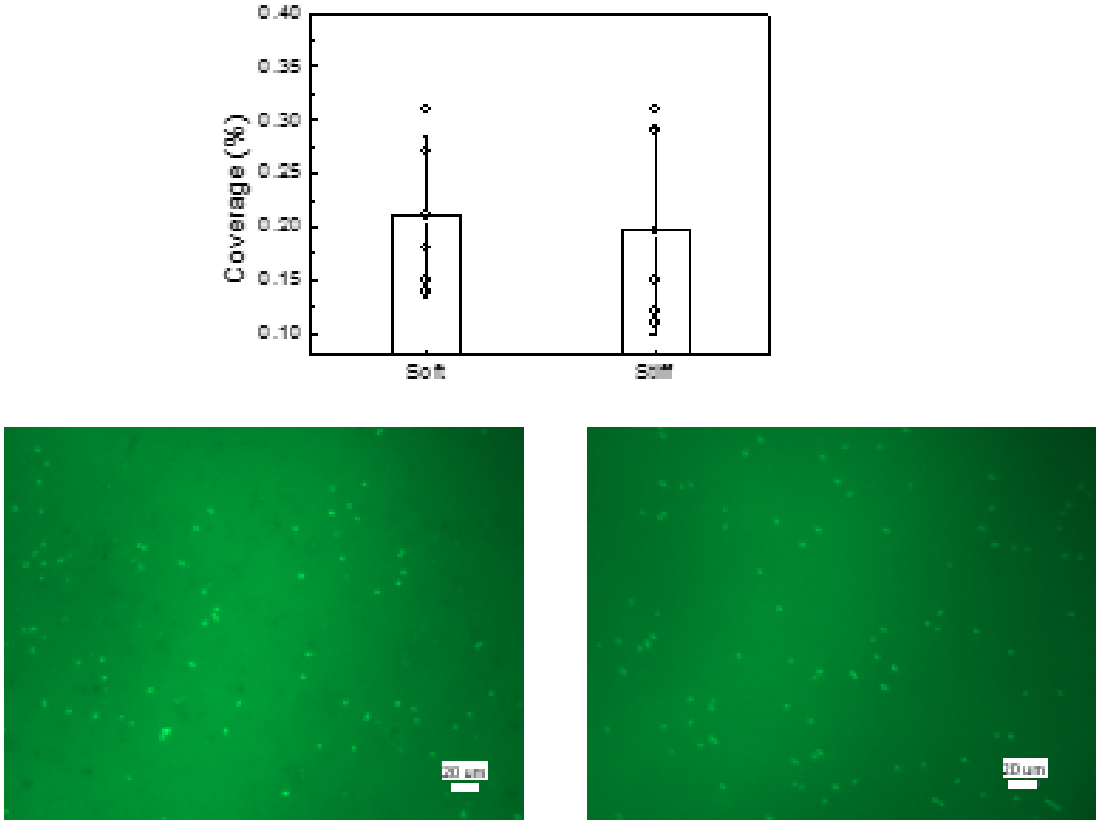

Figure 4.2 Effects of PDMS stiffness on the growth of *P. aeruginosa* PAO1 *oprF* mutant cells. (A) Surface coverage of attached cells calculated using COMSTAT. (B) Representative images of attached cells strained with acridine orange. (Bar = 20 µm)

Collectively, these results indicated that *oprF* mutant lost the capability to respond to surface stiffness during adhesion and thus the differences in growth, morphology and antibiotic

susceptibility of attached cells between stiff and soft surfaces, suggesting *oprF* may be involved in mechanosensing.

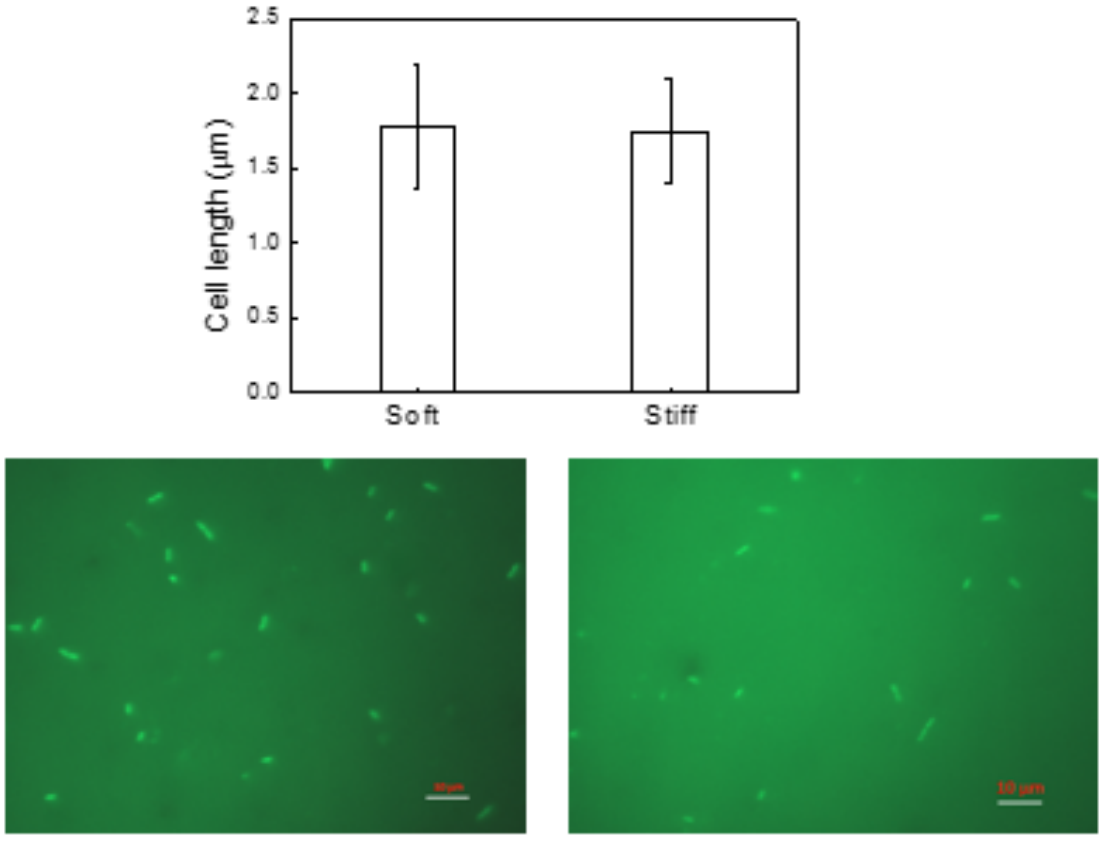

Figure 4.3 Effects of PDMS stiffness on the size of *oprF* mutant cells. (A) Average length of attached cells on soft (40:1 PDMS) and stiff (5:1 PDMS) surfaces. (B) Representative images of attached cells strained with acridine orange. (Bar = 10 μm).

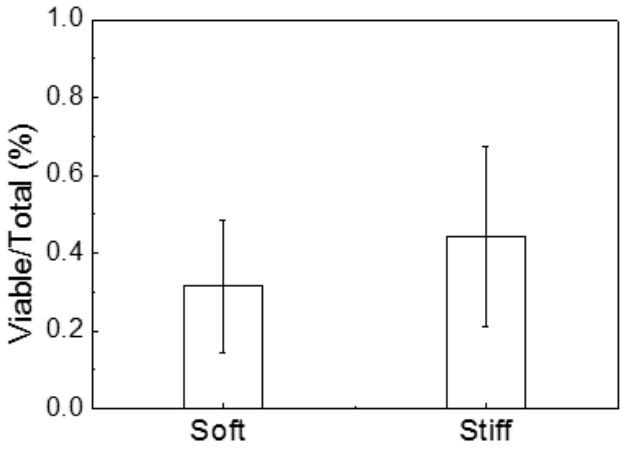

Figure 4.4 Effects of PDMS stiffness on the susceptibility of *oprF* mutant cells *to* 20 µg/mL tobramycin. The figure showed the relative number of 5-h biofilm cells that survived the treatment of 20 µg/mL tobramycin.

4.4.2 The defects in *oprF* mutant were rescued by genetic complementation.

To verify if the changed observed in *oprF* mutant were not caused by any polar effect, pMH391-*oprF* (Supplementary Figure 4.5) was constructed to complement the *oprF* mutation. The complemented strain was studied following the same protocols used for the wild-type PAO1 and its *oprF* mutant. To specifically study the effects of *oprF*, the original vector pMH391 (without *oprF*) was also electroporated into the wild-type PAO1 and its *oprF* mutant. Insertion of this plasmid caused decrease in attachment for all samples compared to plasmid-free cells, presumably due to the metabolic burden caused by this high copy number plasmid. Nevertheless, complementation fully recovered the phenotypic changes observed for the *oprF* mutation (Fig. 4.6). For example, the difference in the number of attached cells between soft and stiff PDMS surfaces 1, 0 and 0.8 logs for the wild-type PAO1 (carrying original pMH391

without *oprF*), *oprF* mutant (carrying original pMH391 without *oprF*), and the complemented strain, respectively (Figure 4.6).

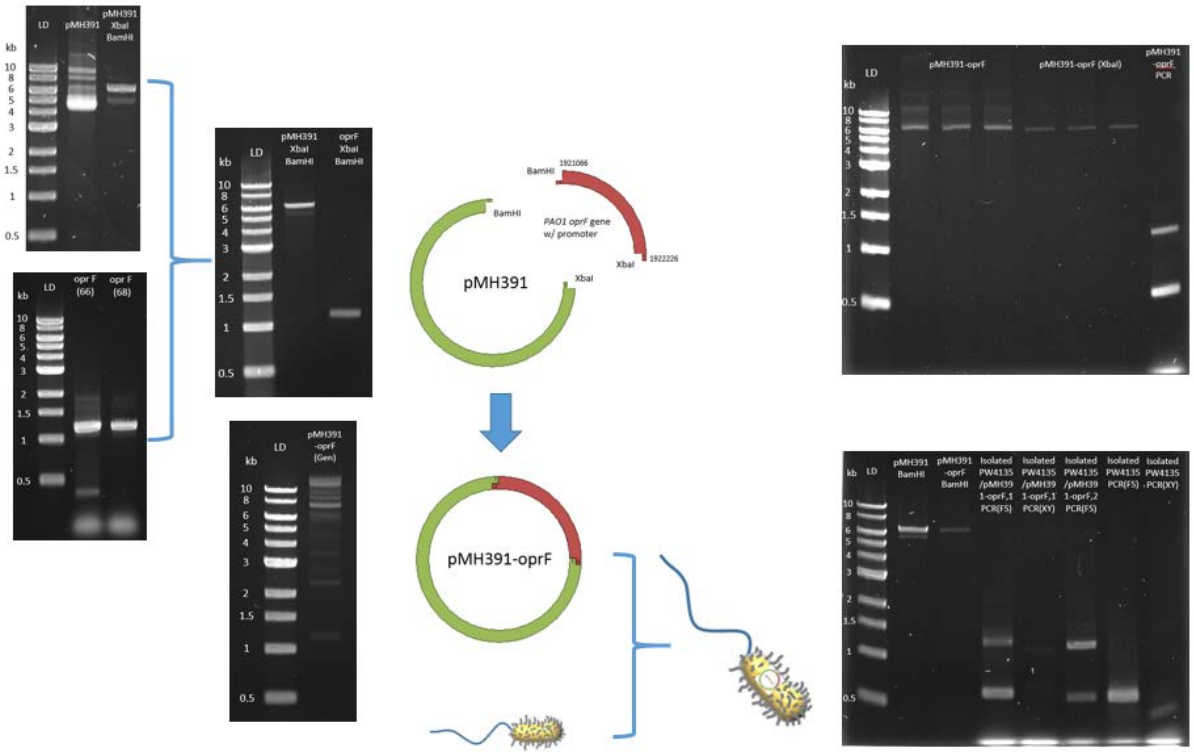

Figure 4.5 Construction and of the complementation of *the oprF mutant.*

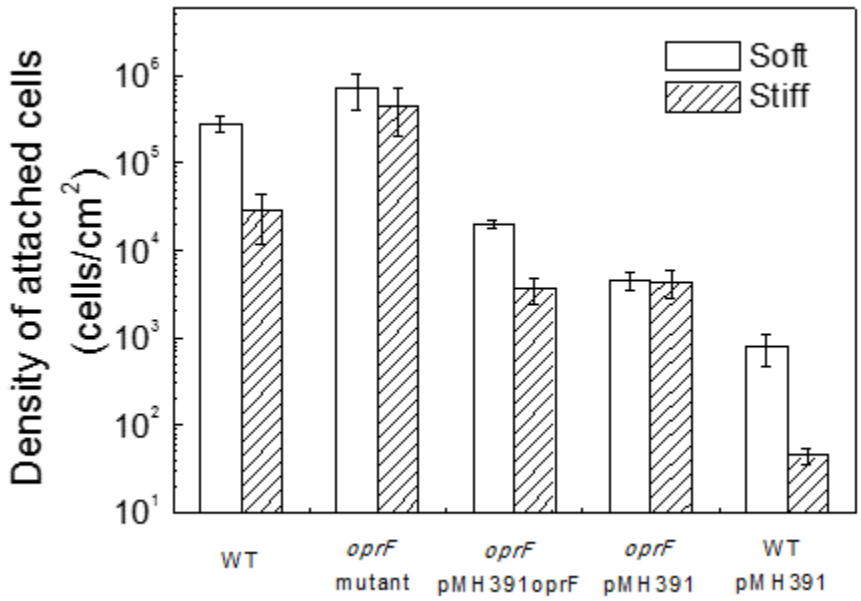

Figure 4.6 Effects of PDMS stiffness on the attachment of the wild type, *oprF* mutant and the complemented strain sensing. The number of attached cells on soft (40:1) and stiff (5:1) PDMS surfaces after 2-h adhesion.

Complementation of the *oprF* gene also led to similar results of biofilm cell growth and cell morphology observed for the wild-type PAO1[21]. As shown in Figure 4.6B, there were more attached cells on soft PDMS surfaces than stiff PDMS surfaces, and the cell length was larger on soft PDMS surfaces. The average length of attached cells was around 2 μm and 1.3 μm on soft and stiff surfaces, respectively. These results are suggest the defects in mechanosensing by the *oprF* mutant were fully recovered by the complementation of *oprF* mutant.

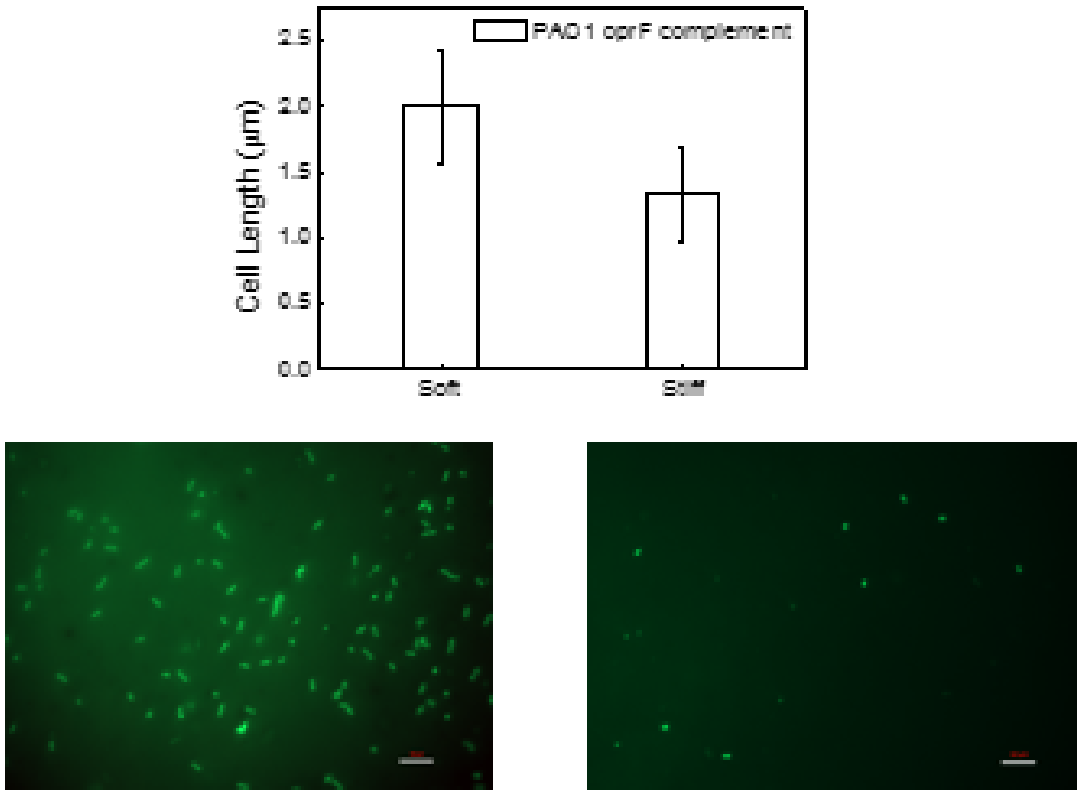

Figure 4.7 Effects of PDMS stiffness on the size of the complementation of *oprF* mutant cells. (A) Average length of attached cells on soft (40:1 PDMS) and stiff (5:1 PDMS) surfaces. (B) Representative acridine orange staining images of attached cells. (Bar = 10 μm)

4.4.3 The role of other *oprF* related genes in the mechanosensing

oprF encodes the major outer membrane surface porin protein OprF of *P. aeruginosa* for exchange of various solutes[50] OprF also functions for adhesion to animal cells,[51] and is responsible for the secretion of several toxins such as *ExoT* and *ExoS*[52] required for virulence.[53] Moreover, *oprF* is related to cell envelop stress, for example, it has three promoters which are P_{algU}, $P_{\sigma 70}$, and P_{sigX}.[54] In addition, it was reported that the absence of *oprF* could abolish

swarming and biofilm formation of *P. aeruginosa*, and caused the increase in the expression of c-di-GMP.[55,56]

To understand how *oprF* is involved in mechanosensing, we further tested 2 h adhesion of PAO1 mutants of the genes related to *oprF* including. As shown in Figure 4.1B. The *sigX* mutant showed a slight decrease in the difference of the number of attached cells between soft and on stiff PDMS surfaces. For example, there was $(1.9 \pm 0.7) \times 10^5$ cells/ cm^2 on stiff PDMS surfaces after 2 h adhesion, and $(4.7 \pm 2.9) \times 10^5$ cells/ cm^2 on soft PDMS surfaces. The difference is around half log which is smaller than the 1 log difference of the wild-type PAO1. It is probably because P_{sigX} is the most critical promoter out of all the three promoters of *oprF* gene.[54] Since xxx controls the expression of oprF, we speculate that the absence of *sigX* could cause decrease the expression level of *oprF*, which then affect mechanosensing. Except for the *sigX* mutant, all the other mutants tested including *rpoN*, *lecB*, *fdxA, rhlA, bifA, rpoS, σ_{70}*, *exoT*, did not show a significant effect.

Mammalian cells sense material stiffness using integrin and then transfer the signal to the nuclear envelop using myosin, actin and nesprin.[57-59] Actin is the key connection in the mechanotransduction of surface stiffness sensing by eukaryotic cells.[59] Several homologs of eukaryotic microfilaments (actin) have been identified in prokaryotic cells such as *mreB*, *mreC* et al..[60] MreB and MreC are located on the opposite sides of the inner membrane of bacteria. We speculate that MreB&C may directly connect with the outer membrane protein OprF and transduce the mechanical signal into the cell. To verify if bacteria use a similar mechanotransduction pathway as eukaryotic cells, the 2 h adhesion of the *mreC* mutant was

exanimated using the same adhesion assay. The results show that mutation of *mreC* does not have the same effects as observed for the *oprF* mutant. For example, there was (8.1 ± 2.1) × 10^4 cells/ cm^2 on soft PDMS surfaces after 2 h adhesion, and (1.8 ± 0.4) × 10^3 cells/ cm^2 on stiff PDMS surfaces. The number of attached cells on soft surfaces is much more than those on stiff surfaces, like the wild-type strain, suggesting that the homolog of microfilaments may not be involved in the bacterial sensing of surface stiffness.

4.4.4 The level of cyclic-di-GMP may influence the surface stiffness sensing

Cyclic-di-GMP has been reported to be a key factor in the transition between the motile planktonic state and the biofilm state.[61,62] It was reported that the absence of *oprF* can increase the level of c-di-GMP.[56] Since *oprF* is important to mechnosensing, we were curious if it works by changing the level of c-di-GMP. To test this, we compared the adhesion on soft and stiff PDMS of a *fleQ* mutant. FleQ is a precursor of flagella synthesis and can bind to c-di-GMP and form FleQ-c-di-GMP. This interaction decreases the intracellular level of c-di-GMP.[63-65] Thus, the PAO1 *fleQ* mutant could cause the increase of the level of c-di-GMP. As shown in Figure 4.8, the number of attached *fleQ* mutant cells on soft PDMS surfaces was much close to the number of attached cells on stiff PDMS surfaces (p=0.04, t test). For example, the number of attached cells on soft and stiff PDMS surfaces was *(6.1 ± 5.2)* × 10^3 cells/ cm^2 and (1.4 ± 2.3) × 10^3 cells/ cm^2, respectively. This finding plus the results of *oprF* mutant, suggest that c-di-GMP may be involved in bacterial mechnosensing.

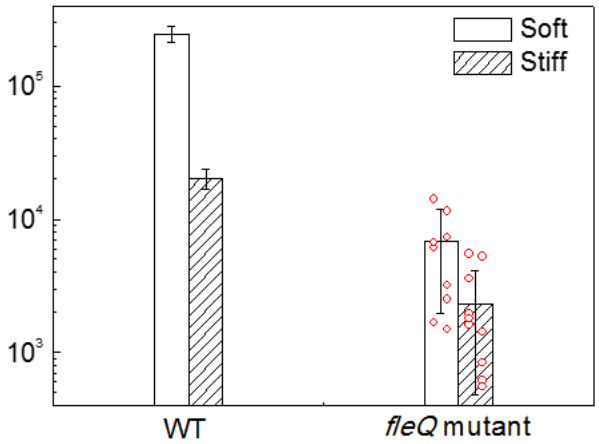

Figure 4.8 Effects of PDMS stiffness on the adhesion of the wild-type strain and its *fleQ* mutant. The number of attached cells on soft (40:1) and stiff (5:1) PDMS surfaces after 2-h adhesion are shown. (Red dots showed the data for each experiment.)

To further understand if the level of c-di-GMP of the attached cells changes with substratum stiffness, a PAO1 c-di-GMP reporter strain PAO1/pCdrA::*gfp*^{s} was used in this research. This strain has a *gfp* gene under the control of promoter of cdrA; thus, it allows real time monitoring of c-di-GMP synthesis. After 2 h attachment (the adhesion assay as described above.), the PAO1/pCdrA::*gfp*^{s} cells attached on soft and stiff PDMS surfaces were collected by sonication and analyzed by a flow cytometer. The average intensity of the green fluorescence in PAO1/pCdrA::*gfp*^{s} cells on soft surfaces was found higher than that on stiff surfaces. The distribution of the green fluorescence in PAO1/pCdrA::*gfp*^{s} cells on soft surfaces was also wider than that on stiff surfaces (Figure 4.9A). These results were corroborated by microscopic images, which showed that PAO1/pCdrA::*gfp*(ASV)^{s} on soft and stiff PDMS surfaces have stronger green fluorescence than those on stiff surfaces (Figure 4.9B). Because the intensity of the green fluorescence in these strains is directly related to the intracellular level of c-di-GMP,

the c-di-GMP level appeared higher in *P. aeruginosa* PAO1 on soft surfaces than those on stiff surfaces. This is consistent with increased biofilm formation on soft surfaces.

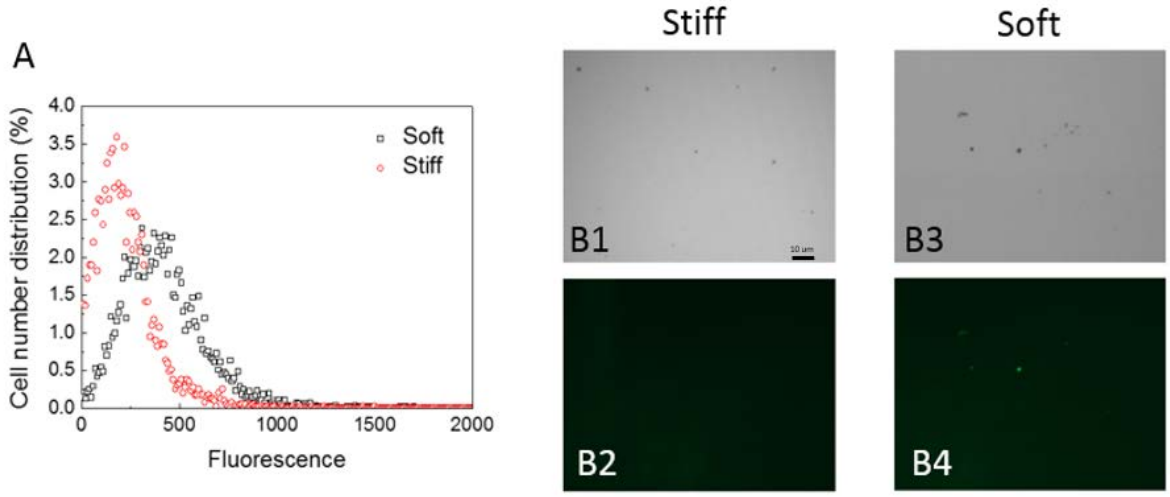

Figure 4.9 The level of c-di-GMP of the attached PAO1/pCdrA::*gfp*^{s} cells on soft (40:1) and stiff (5:1) PDMS surfaces after 2-h adhesion. (A) The distribution of the fluorescence signals measured by flow cytometer. (B) Representative images of PAO1/pCdrA::gfp(ASV)^{s} cells attached on soft (40:1) and stiff (5:1) PDMS surfaces after 2-h adhesion (Bar = 10 μm).

4.5 Discussion

Some pioneering work has revealed how bacteria sense the contact with a surface. However, how the mechanical properties of the surface affect surface sensing is largely unknown. Here we demonstrated that mutation of the *oprF* gene in *P. aeruginosa* PAO1 abolished its response to surface stiffness during adhesion and biofilm formation. How OprF functions in such mechanosensing is still unknown. As an important membrane protein, OprF may have direct contact with the surfaces and transfer the signal to other components to trigger the genes related

to motility, adhesion, and biofilm formation. The increase in the level of c-di-GMP supports this hypothesis that increase in c-di-GMP level is known to reduce bacterial motility, and promote biofilm formation.[62] The increase in the level of c-di-GMP on soft surfaces observed here is consistent with our earlier report that PAO1 forms more biofilms on soft PDMS than stiff PDMS.[21]

Some important questions remain to be answered. For example, is OprF the true sensor or just involved in the signal transduction? How is the signal transferred to change the level of c-di-GMP? How is the stiffness sensing related to that of general contact with a surface? These questions require additional studies and is part of our ongoing work. Because the c-di-GMP level and *oprF* are correlated with the expression of *cdrA* and the surface stress genes, the role of *cdrA* and surface stress genes in mechanosensing is also interesting to investigate.

4.6 Conclusions

In this study, we demonstrated that mutation of *oprF in P. aeruginosa* PAO1 abolished its response to material stiffness during adhesion and biofilm formation on PDMS surfaces, which was rescued by complementing the *oprF* gene. Using a fluorescent reporter of the *cdrA* gene, we obtained evidence that of the level of c-di-GMP is higher in cells attached on soft PDMS than those on stiff PDMS. Consistently, mutation of *fleQ*, which causes overproduction of c-di-GMP, abolished the difference in biofilm formation between soft and stiff surfaces exhibited by the wild-type PAO1. These results provided information evidence that bacteria can actively sensing the mechanical properties of a surface and adjust cell physiology to switch between planktonic growth and biofilm formation.

4.7 References

(1) Harrison, J. J.; Ceri, H.; Turner, R. J. Multimental resistance and tolerant in microbial biofilms. *Nature Reviews* **2007,** *5*.

(2) Hall-Stoodley, L.; Costerton, J. W.; Stoodley, P. Bacterial biofilms: from the natural environment to infectious diseases. *Nature Reviews Microbiology* **2004,** *2*, 95-108.

(3) Häussler, S.; Parsek, M. R. Biofilms 2009: new perspectives at the heart of surface-associated microbial communities. *Journal of bacteriology* **2010,** *192*, 2941-2949.

(4) Stewart, P. S. Mechanisms of antibiotic resistance in bacterial biofilms. *Int. J. Med. Microbiol.* **2002,** *292*, 107-13.

(5) Shirtliff, M.; Leid, J., *The Role of Biofilms in Device-Related infections*. Springer: 2009.

(6) Control, C. f. D.; Prevention, *Antibiotic resistance threats in the United States, 2013*. Centres for Disease Control and Prevention, US Department of Health and Human Services: 2013.

(7) Renner, L. D.; Weibel, D. B. Physicochemical regulation of biofilm formation. *MRS bulletin* **2011,** *36*, 347-355.

(8) Cheng, G.; Zhang, Z.; Chen, S.; Bryers, J. D.; Jiang, S. Inhibition of bacterial adhesion and biofilm formation on zwitterionic surfaces. *Biomaterials* **2007,** *28*, 4192-4199.

(9) Nejadnik, M. R.; van der Mei, H. C.; Norde, W.; Busscher, H. J. Bacterial adhesion and growth on a polymer brush-coating. *Biomaterials* **2008,** *29*, 4117-4121.

(10) Hou, S.; Burton, E. A.; Wu, R. L.; Luk, Y.-Y.; Ren, D. Prolonged control of patterned biofilm formation by bio-inert surface chemistry. *Chemical Communications* **2009**, 1207-1209.

(11) Bakker, D. P.; Huijs, F. M.; de Vries, J.; Klijnstra, J. W.; Busscher, H. J.; van der Mei, H. C. Bacterial deposition to fluoridated and non-fluoridated polyurethane coatings with different elastic modulus and surface tension in a parallel plate and a stagnation point flow chamber. *Colloids and Surfaces B: Biointerfaces* **2003,** *32*, 179-190.

(12) Cottenye, N.; Anselme, K.; Ploux, L.; Vebert-Nardin, C. Vesicular Structures Self-Assembled from Oligonucleotide-Polymer Hybrids: Mechanical Prevention of Bacterial Colonization Upon their Surface Tethering Through Hybridization. *Advanced Functional Materials* **2012,** *22*, 4891-4898.

(13) Cowles, K. N.; Gitai, Z. Surface association and the MreB cytoskeleton regulate pilus production, localization and function in Pseudomonas aeruginosa. *Molecular microbiology* **2010,** *76*, 1411-1426.

(14) Delgadillo, M. Study of the effect of mechanical stiffness substrata, assembled with polyelectrolyte multilayer thin films, on biofilm forming staphylococcus epidermidis' initial adhesion mechanism. Massachusetts Institute of Technology, 2008.

(15) Epstein, A.; Hochbaum, A.; Kim, P.; Aizenberg, J. Control of bacterial biofilm growth on surfaces by nanostructural mechanics and geometry. *Nanotechnology* **2011,** *22*, 494007.

(16) Guégan, C.; Garderes, J.; Le Pennec, G.; Gaillard, F.; Fay, F.; Linossier, I.; Herry, J.-M.; Fontaine, M.-N. B.; Réhel, K. V. Alteration of bacterial adhesion induced by the substrate stiffness. *Colloids and Surfaces B: Biointerfaces* **2014,** *114*, 193-200.

(17) Kolewe, K. W.; Peyton, S. R.; Schiffman, J. D. Fewer Bacteria Adhere to Softer Hydrogels. *ACS applied materials & interfaces* **2015,** *7*, 19562-19569.

(18) Lichter, J. A.; Thompson, M. T.; Delgadillo, M.; Nishikawa, T.; Rubner, M. F.; Van Vliet, K. J. Substrata mechanical stiffness can regulate adhesion of viable bacteria. *Biomacromolecules* **2008,** *9*, 1571-1578.

(19) Park, E.-J.; Cho, M.-O.; Lee, D.; Kim, J. K. Growth responses of Escherichia coli and Myxococcus xanthus on agar gel substrates with different levels of stiffness. *African Journal of Biotechnology* **2012,** *11*, 15477-15483.

(20) Saha, N.; Monge, C.; Dulong, V.; Picart, C.; Glinel, K. Influence of Polyelectrolyte Film Stiffness on Bacterial Growth. *Biomacromolecules* **2013**.

(21) Song, F.; Ren, D. Stiffness of cross-linked poly (dimethylsiloxane) affects bacterial adhesion and antibiotic susceptibility of attached cells. *Langmuir* **2014,** *30*, 10354-10362.

(22) Packham, D. E. Surface energy, surface topography and adhesion. *International journal of adhesion and adhesives* **2003,** *23*, 437-448.

(23) Oliveira, R.; Azeredo, J.; Teixeira, P.; Fonseca, A. The role of hydrophobicity in bacterial adhesion. **2001**.

(24) Singh, A. V.; Vyas, V.; Patil, R.; Sharma, V.; Scopelliti, P. E.; Bongiorno, G.; Podestà, A.; Lenardi, C.; Gade, W. N.; Milani, P. Quantitative characterization of the influence of the nanoscale morphology of nanostructured surfaces on bacterial adhesion and biofilm formation. *PloS one* **2011,** *6*, e25029.

(25) Díaz, C.; Cortizo, M. C.; Schilardi, P. L.; Saravia, S. G. G. d.; Mele, M. A. F. L. d. Influence of the nano-micro structure of the surface on bacterial adhesion. *Materials Research* **2007,** *10*, 11-14.

(26) Scheuerman, T. R.; Camper, A. K.; Hamilton, M. A. Effects of substratum topography on bacterial adhesion. *Journal of colloid and interface science* **1998,** *208*, 23-33.

(27) Perni, S.; Prokopovich, P. Micropatterning with conical features can control bacterial adhesion on silicone. *Soft Matter* **2013,** *9*, 1844-1851.

(28) Crawford, R. J.; Webb, H. K.; Truong, V. K.; Hasan, J.; Ivanova, E. P. Surface topographical factors influencing bacterial attachment. *Advances in Colloid and Interface Science* **2012**.

(29) Hou, S.; Gu, H.; Smith, C.; Ren, D. Microtopographic patterns affect Escherichia coli biofilm formation on poly (dimethylsiloxane) surfaces. *Langmuir* **2011,** *27*, 2686-2691.

(30) An, Y. H.; Friedman, R. J. Concise review of mechanisms of bacterial adhesion to biomaterial surfaces. *Journal of biomedical materials research* **1998,** *43*, 338-348.

(31) Aprikian, P.; Interlandi, G.; Kidd, B. A.; Le Trong, I.; Tchesnokova, V.; Yakovenko, O.; Whitfield, M. J.; Bullitt, E.; Stenkamp, R. E.; Thomas, W. E. The bacterial fimbrial tip acts as a mechanical force sensor. *PLoS biology* **2011,** *9*, e1000617.

(32) Tuson, H. H.; Weibel, D. B. Bacteria–surface interactions. *Soft Matter* **2013**.

(33) Petrova, O. E.; Sauer, K. Sticky situations: key components that control bacterial surface attachment. *Journal of bacteriology* **2012,** *194*, 2413-25.

(34) Ploux, L.; Ponche, A.; Anselme, K. Bacteria/material interfaces: role of the material and cell wall properties. *Journal of Adhesion Science and Technology* **2010,** *24*, 2165-2201.

(35) Bos, R.; van der Mei, H. C.; Busscher, H. J. Physico-chemistry of initial microbial adhesive interactions its

mechanisms and methods for study. *FEMS Microbiology Reviews* **1999,** *23*, 179-230.

(36) Bhomkar, P.; Materi, W.; Semenchenko, V.; Wishart, D. S. Transcriptional response of E. coli upon FimH-mediated fimbrial adhesion. *Gene Regulation and Systems Biology* **2010,** *4*, 1.

(37) He, K.; Bauer, C. E. Chemosensory signaling systems that control bacterial survival. *Trends in microbiology* **2014,** *22*, 389-398.

(38) Otto, K.; Silhavy, T. J. Surface sensing and adhesion of Escherichia coli controlled by the Cpx-signaling pathway. *Proceedings of the National Academy of Sciences of the United States of America* **2002,** *99*, 2287-92.

(39) Hickman, J. W.; Tifrea, D. F.; Harwood, C. S. A chemosensory system that regulates biofilm formation through modulation of cyclic diguanylate levels. *Proceedings of the National Academy of Sciences of the United States of America* **2005,** *102*, 14422-14427.

(40) O'Connor, J. R.; Kuwada, N. J.; Huangyutitham, V.; Wiggins, P. A.; Harwood, C. S. Surface sensing and lateral subcellular localization of WspA, the receptor in a chemosensory-like system leading to c-di-GMP production. *Molecular microbiology* **2012,** *86*, 720-729.

(41) Huangyutitham, V.; Güvener, Z. T.; Harwood, C. S. Subcellular clustering of the phosphorylated WspR response regulator protein stimulates its diguanylate cyclase activity. *MBio* **2013,** *4*, e00242-13.

(42) Han, Y.; Hou, S.; Simon, K. A.; Ren, D.; Luk, Y.-Y. Identifying the important structural elements of brominated furanones for inhibiting biofilm formation by Escherichia coli. *Bioorganic & medicinal chemistry letters* **2008,** *18*, 1006-1010.

(43) Maniatis, T.; Fritsch, E. F.; Sambrook, J., *Molecular cloning: a laboratory manual*. Cold Spring Harbor Laboratory Cold Spring Harbor, NY: 1982; Vol. 545.

(44) Evans, N. D.; Minelli, C.; Gentleman, E.; LaPointe, V.; Patankar, S. N.; Kallivretaki, M.; Chen, X.; Roberts, C. J.; Stevens, M. M. Substrate stiffness affects early differentiation events in embryonic stem cells. *Eur Cell Mater* **2009,** *18*, 13-14.

(45) Wang, Z. Polydimethylsiloxane Mechanical Properties Measured by Macroscopic Compression and Nanoindentation Techniques. University of South Florida, 2011.

(46) Fuard, D.; Tzvetkova-Chevolleau, T.; Decossas, S.; Tracqui, P.; Schiavone, P. Optimization of poly-di-methyl-siloxane (PDMS) substrates for studying cellular adhesion and motility. *Microelectronic Engineering* **2008,** *85*, 1289-1293.

(47) Chen, C.-Y.; Nace, G. W.; Irwin, P. L. A 6× 6 drop plate method for simultaneous colony counting and MPN enumeration of Campylobacter jejuni, Listeria monocytogenes, and Escherichia coli. *Journal of Microbiological Methods* **2003,** *55*, 475-479.

(48) Heydorn, A.; Nielsen, A. T.; Hentzer, M.; Sternberg, C.; Givskov, M.; Ersbøll, B. K.; Molin, S. Quantification of biofilm structures by the novel computer program COMSTAT. *Microbiology* **2000,** *146*, 2395-2407.

(49) Togna, A. P.; Shuler, M. L.; Wilson, D. B. Effects of plasmid copy number and runaway plasmid replication on overproduction and excretion of. beta.-lactamase from Escherichia coli. *Biotechnology progress* **1993,** *9*, 31-39.

(50) Sugawara, E.; Nestorovich, E. M.; Bezrukov, S. M.; Nikaido, H. Pseudomonas aeruginosa porin OprF exists in two different conformations. *Journal of Biological Chemistry* **2006,** *281*, 16220-16229.

(51) Azghani, A. O.; Idell, S.; Bains, M.; Hancock, R. E. Pseudomonas aeruginosa outer membrane protein F is an adhesin in bacterial binding to lung epithelial cells in culture. *Microbial pathogenesis* **2002,** *33*, 109-114.

(52) Wu, L.; Estrada, O.; Zaborina, O.; Bains, M.; Shen, L.; Kohler, J. E.; Patel, N.; Musch, M. W.; Chang, E. B.; Fu, Y.-X. Recognition of host immune activation by Pseudomonas aeruginosa. *Science* **2005,** *309*, 774-777.

(53) Fito-Boncompte, L.; Chapalain, A.; Bouffartigues, E.; Chaker, H.; Lesouhaitier, O.; Gicquel, G.; Bazire, A.; Madi, A.; Connil, N.; Véron, W. Full virulence of Pseudomonas aeruginosa requires OprF. *Infection and immunity* **2011,** *79*, 1176-1186.

(54) Bouffartigues, E.; Gicquel, G.; Bazire, A.; Bains, M.; Maillot, O.; Vieillard, J.; Feuilloley, M. G.; Orange, N.; Hancock, R.; Dufour, A. Transcription of the oprF gene of Pseudomonas aeruginosa is dependent mainly on the SigX sigma factor and is sucrose induced. *Journal of bacteriology* **2012,** *194*, 4301-4311.

(55) Bouffartigues, E.; Gicquel, G.; Bazire, A.; Fito-Boncompte, L.; Taupin, L.; Maillot, O.; Groboillot, A.; Poc-Duclairoir, C.; Orange, N.; Feuilloley, M. The major outer membrane protein OprF is required for rhamnolipid production in Pseudomonas aeruginosa. *J Bacteriol Parasitol* **2011,** *2*, 2.

(56) Bouffartigues, E.; Moscoso, J. A.; Duchesne, R.; Rosay, T.; Fito-Boncompte, L.; Gicquel, G.; Maillot, O.; Bénard, M.; Bazire, A.; Brenner-Weiss, G. The absence of the Pseudomonas aeruginosa OprF protein leads to increased biofilm formation through variation in c-di-GMP level. *Frontiers in microbiology* **2015,** *6*.

(57) Wang, N.; Tytell, J. D.; Ingber, D. E. Mechanotransduction at a distance: mechanically coupling the extracellular matrix with the nucleus. *Nature reviews Molecular cell biology* **2009,** *10*, 75-82.

(58) Wells, R. G. The role of matrix stiffness in regulating cell behavior. *Hepatology* **2008,** *47*, 1394-400.

(59) Ladoux, B.; Nicolas, A. Physically based principles of cell adhesion mechanosensitivity in tissues. *Rep. Prog. Phys.* **2012,** *75*, 116601.

(60) Shaevitz, J. W.; Gitai, Z. The structure and function of bacterial actin homologs. *Cold Spring Harbor perspectives in biology* **2010,** *2*, a000364.

(61) Hengge, R. Principles of c-di-GMP signalling in bacteria. *Nature Reviews Microbiology* **2009,** *7*, 263-273.

(62) Chua, S. L.; Sivakumar, K.; Rybtke, M.; Yuan, M.; Andersen, J. B.; Nielsen, T. E.; Givskov, M.; Tolker-Nielsen, T.; Cao, B.; Kjelleberg, S. C-di-GMP regulates Pseudomonas aeruginosa stress response to tellurite during both planktonic and biofilm modes of growth. *Scientific reports* **2015,** *5*.

(63) Guttenplan, S. B.; Kearns, D. B. Regulation of flagellar motility during biofilm formation. *FEMS microbiology reviews* **2013,** *37*, 849-871.

(64) Arora, S. K.; Ritchings, B. W.; Almira, E. C.; Lory, S.; Ramphal, R. A transcriptional activator, FleQ, regulates mucin adhesion and flagellar gene expression in Pseudomonas aeruginosa in a cascade manner. *Journal of bacteriology* **1997,** *179*, 5574-5581.

(65) Hickman, J. W.; Harwood, C. S. Identification of FleQ from Pseudomonas aeruginosa as ac-di-GMP-responsive transcription factor. *Molecular microbiology* **2008,** *69*, 376-389.

(66) Jacobs, M. A.; Alwood, A.; Thaipisuttikul, I.; Spencer, D.; Haugen, E.; Ernst, S.; Will, O.; Kaul, R.; Raymond, C.; Levy, R. Comprehensive transposon mutant library of Pseudomonas aeruginosa. *Proceedings of the National Academy of Sciences* **2003,** *100*, 14339-14344.

(67) Rybtke, M. T.; Borlee, B. R.; Murakami, K.; Irie, Y.; Hentzer, M.; Nielsen, T. E.; Givskov, M.; Parsek, M. R.; Tolker-Nielsen, T. Fluorescence-based reporter for gauging cyclic di-GMP levels in Pseudomonas aeruginosa. *Applied and environmental microbiology* **2012,** *78*, 5060-5069.

(68) Hentzer, M.; Riedel, K.; Rasmussen, T. B.; Heydorn, A.; Andersen, J. B.; Parsek, M. R.; Rice, S. A.; Eberl, L.; Molin, S.; Høiby, N. Inhibition of quorum sensing in Pseudomonas aeruginosa biofilm bacteria by a halogenated furanone compound. *Microbiology* **2002,** *148*, 87-102.

Chapter 5
Conclusions and Recommendations for Future Work

5.1 Conclusions

In this project, we first demonstrated that material stiffness affects bacterial biofilm formation, including adhesion, growth, antimicrobial susceptibility, and motility of biofilm cells. These data indicate that bacteria have capability to sense and respond to material stiffness and adjust physiology accordingly. Consistently, *motB* of *E. coli* and *oprF* in *P. aeruginosa* were found important to the observed phenomenon. Based on the finding, a descriptive model of mechanosensing of material stiffness is proposed.

In Chapter 2, we investigated the effects of substrate stiffness on the early stage biofilm formation of *E. coli* and *P. aeruginosa* including attachment, growth, cell length, and the susceptibility of attached cells to antibiotics with varying stiffness of poly(dimethylsiloxane) (PDMS) from 0.1 MPa to 2.6 MPa, which were prepared by controlling the degree of crosslinking. The decrease in surface stiffness was found to promote both the attachment and growth of *E. coli* and *P. aeruginosa* cells. More interestingly, the cells on 40:1 PDMS substrates after 5 h of biofilm growth are found significantly longer than those on 5:1 PDMS substrates; and the distribution of cell size was narrower on stiff substrates. The cells on stiff substrates also exhibited decreased susceptibility to antibiotics and lysozyme compared to the

cells on soft substrates. In addition, the attached bacterial cells on stiff surfaces was appeared to be internalized faster by human macrophages than those on soft surfaces. It has been reported that polymer particles with low aspect ratio are internalized by macrophages faster than those with high aspect ratio. To my best knowledge, this is the first report of the effects material on phagocytosis of biofilm cells. Collectively, these results suggest that stiffer PDMS are more resistant to biofilm infection than soft PDMS. In particular, because the stiffness of PDMS used in this study is in the range of the stiffness of contact lenses (most of them are silicon based polymers), tuning the surface stiffness may help reduce eye infections associated with contact lenses.

In Chapter 3, a custom tracking algorithm, automated contour-based tracking package for *in vitro* environment (ACT*IV*E), was used to follow the bacterial motility during attachment. ACT*IV*E has been shown to actively track the motility of mouse fibroblasts in complex *in vitro* model.[1] Here, we validated it for tracking bacterial cells over time. Cell motility was described using a set of physics based metrics that revealed the differences in cell movement and velocity between soft (0.1 MPa) and stiff (2.6 MPa) PDMS surfaces. The cell tracking results indicated that the *E. coli* cells on stiff surfaces were more mobile than those on soft surfaces.

To understand the mechanism of mechanosensing by bacteria, *E. coli* RP437 and its isogenic mutants of motility (*motB*), flagella (*fliC*) and type I fimbriae (*fimA*) were used to compare the attachment on PDMS surfaces with different Young's moduli (0.1 and 2.6 MPa) in Chapter 3. The CFU results revealed that the *motB* mutant of *E. coli* RP437 had defects in response to the stiffness of PDMS with the inoculum cell density varying from 2×10^4 cells/mL to 2×10^8

cells/mL, which was rescued by complementation of the *motB* gene. The cell tracking results indicated mutation of *motB* gene led to larger decrease in velocity of cell movement on stiff surfaces than soft surfaces. The tracking results are consistent with the CFU results, suggesting that *motB* is involved in mechanosensing during *E. coli* attachment on PDMS. However, *motB* mutation only partially reduces the difference in adhesion between soft and stiff PDMS, but did not totally abolish it. This suggests other geens are also involved in mechnosensing.

In Chapter 4, *P. aeruginosa* PAO1 and several of its isogenic mutants related to surface appendages (*fliC, filA*), cell capsule (*pelB, pslD, algC*), surface proteins (*oprF, oprE, sadB, sadC*), Wsp pathway (*wspE, wspR*) were compared for their adhesion on soft and stiff surfaces. Mutation of the *oprF* caused major defects in sensing PDMS stiffness by *P. aeruginosa*; e.g., it abolished the differences in adhesion and growth, morphology and antibiotic susceptibility of attached cells between soft and stiff PDMS surfaces. These defects were rescued by genetic complementation of *oprF*. Collectively, these results suggest that *oprF* is involved in the mechanosensing of *P. aeruginosa*.

To further understand how *oprF* influences the sensing of substrate stiffness, several isogenic mutants of *P. aeruginosa* PAO1 related to *oprF* genes were tested for 2 h adhesion. However, none of them showed the defects in adhesion between soft and stiff PDMS surfaces, indicating that these genes are not involved in the bacterial mechanosensing. Because c-di-GMP was reported to be increased by the absence of *oprF* gene, the intracellular c-di-GMP levels in the attached cells on both soft and stiff surfaces were determined using reporter strain constructed with the *cdrA* promoter fused to a *gfp* gene.[2-4] The results showed that *P. aeruginosa* PAO1

cells attached on soft PDMS surfaces have higher levels of intracellular c-di-GMP than those on stiff PDMS surfaces, indicating the signal of substrate stiffness may be transmitted through c-di-GMP. To confirm that the mechanosensing could be influenced by disturbing the level of c-di-GMP, *P. aeruginosa* PAO1 *fleQ* mutant (a strain with high level of c-di-GMP) was tested for 2 h adhesion.[2-4] The results showed that P. aeruginosa PAO1 *fleQ* mutant abolished mechanosensing of PDMS stiffness. This is consistent with the increase in c-di-GMP on soft surfaces.

The findings from this study are summarized in Fig 5.1. We speculate that bacteria use some unknown sensor to detect the stiffness of the substrate, and this signal is transmitted through c-di-GMP. On soft surfaces, the intracellular level of c-di-GMP is increased, which renders the attached cells to biofilm formation. These cells become less mobile and grow faster on the surfaces. Such active cellular metabolism could make the cells on soft surface more susceptible to antibiotics. On stiff surfaces, however, the level of c-di-GMP decreases, which reduces biofilm formation and the growth. The cells on stiff surfaces remain rather motile and detach more frequently. The attached cells with low level of c-di-GMP also grow more slowly and thus are more dormant, leading to lower susceptibility to antibiotics. The *motB* gene in *E. coli* and the *oprF* gene in *P. aeruginosa* were found important to the observed results. How these genes are involved in mechnosensing remains to be understood.

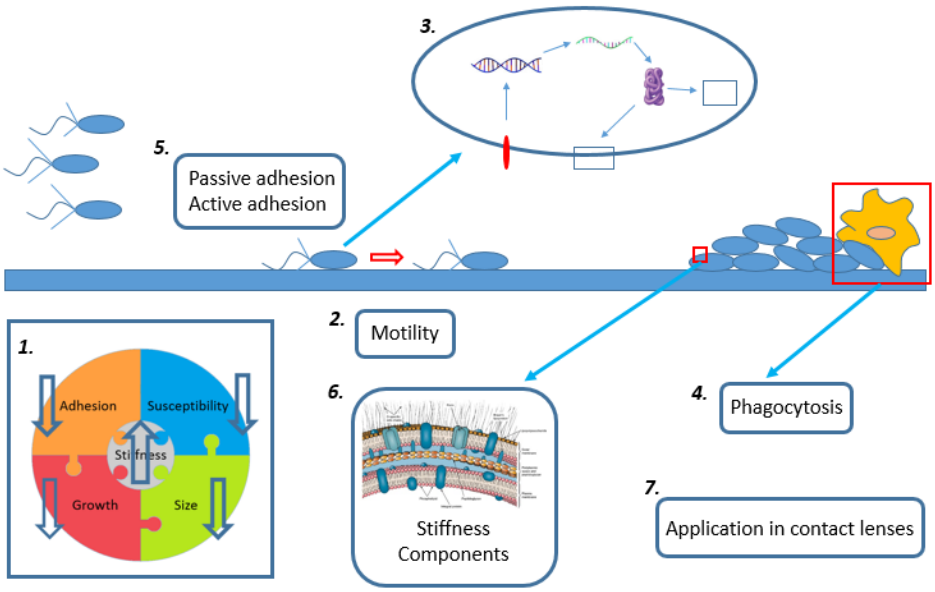

Figure 5.1 The summary of the works in this thesis and the suggested works in future.

5.2 Recommendations for future work

Although biofilm formation has been known to be influenced by many factors of the surface such as surface chemistry,[5-8] hydrophobicity,[9,10] roughness,[11,12] topography,[13-16] and charge,[5,17] there have been few studies on the effects of substrate stiffness.[18,19] Although we found the potent effects of material stiffness on bacterial adhesion and the growth and the antibiotic susceptibility of attached cells, there are still lots of many unanswered questions on the mechanism. The following sections summarized some of the future work.

5.2.1 Bacterial pathways responsible for mechanosensing.

Although *motB* in *E. coli* and *oprF* in *P. aeruginosa* were found to be involved in mechanosensing, how they are involved is still unknown. By screening the genes and the metabolites related to *motB* and *oprF*, c-di-GMP is found important in the pathway of

mechanosensing. However, the actual sensor and how the signal is transducted are not clear. Additional experiments of DNA microarray or RNAseq can be carried to identify the related pathway by comparing the gene expression profiles and the effects of material stiffness.

5.2.2 Bacterial motility on soft and stiff surfaces

In Chapter 3, the motility and velocity of cell movement were found different between soft and stiff PDMS. It has been shown that bacterial slingshot more on soft electrolytes surfaces,[20] and the rotating frequency on glass could be different due to the difference of proton motive force and viscous load.[21] Thus, it will be interesting to investigate if the substrate stiffness influences the bacterial slingshot behavior and rotating frequency. To study this, a high speed camera with at least a frame rate of 10 fps and an advanced processing algorithm are required.

5.2.3 Phagocytosis of the attached bacterial cells on soft and stiff surfaces

Phagocytosis is one of the most important innate immune responses. Champion et al.[22-24] showed that the poly(lactide-co-glycolie) (PLGA) particles with low aspect ratios (AR) are more easily internalized by macrophages. As shown in our results in Chapter 2, surface stiffness of PDMS affected the size and AR of attached bacterial cells; e.g. the size of attached cells on stiff surfaces are shorter, and have lower AR than those on soft surfaces. Interestingly, Discher et al.[25,26] showed that macrophages on stiff surfaces (100 kPa) are more spreading than those on soft surfaces (1 kPa), which suggests that the macrophage on stiff surfaces may be more active than those on soft surfaces. In Chapter 2, we showed that the bacterial cells on stiff surface was internalized by macrophages more easily than those on soft surfaces. However, the viability assay used in Chapter 2 did not reveal if the effects are due to the AR of the

attached cells, the density of attached cells, the activity of macrophages on different surfaces, or any difference in the composition of surface proteins secreted by attached cells. To answer this question, more investigation on the phagocytosis on soft and stiff surfaces is needed. The results will not only answer if the effects of aspect ratio on phagocytosis could be extended to live bacteria from polymer particles, but also contribute to the fundamental knowledge on how surface properties influence phagocytosis.

5.2.4 Application to contact lenses

There are approximately 85 million people worldwide wearing contact lenses.[27] And the contact lenses wear increases the risk of eye infection because of the contact lenses related keratitis. It was reported[27] that 6% of the population are affected by Keratitis, and *P. aeruginosa* is one of the most common pathogens related to the infection.[28,29] Because the range of stiffness of contact lenses is the same as the range of PDMS surface stiffness used in this study (Table 5.1), the results from this study may help design better contact lenses. In Chapter 2, the smaller bacterial cells attached on stiff surface have been found to be less susceptible to lysozyme, which is the major antimicrobial in human tears, compared to the cells on soft surfaces. However, the real eye environment is more complex, which contains not only lysozyme but also antimicrobial peptides and proteins. In addition, the silicon-based contact lenses also comprised of other additives as shown in Table 5.1. To understand the effects of these additives is also important for understanding biofilm formation on contact lenses.

Table 5.1. The properties of commercial contact lenses.[30]

Proprietary name	PureVision	Focus Night & Day	Acuvue Advance
United States adopted name	Balafilcon A	Lotrafilcon A	Galyfilcon A
Manufacturer	Bausch & Lomb	CIBA Vision	Vistakon
Centre thickness (@ -3.00 D) mm	0.09	0.08	0.07
Water Content	36%	24%	47%
Oxygen permeability (x 10-11)	99	140	60
Oxygen transmissibility (x 10-9)	110	175	86
Modulus (psi)*	148	238	65
Surface treatment	Plasma oxidation, producing glassy islands	25 nm plasma coating with high refractive index	No surface treatment. Internal wetting agent (PVP)
FDA Group	III	I	I
Principal monomers	NVP, TPVC, NCVE, PBVC	DMA, TRIS, siloxane macromer	unpublished

1Mpa 2MPa 0.4MPa

DMA *N,N*-dimethylacrylamide; HEMA 2-hydroxyethylmethacrylate; MA methacrylic acid; NVP N-vinyl pyrrolidone; TPVC tris-(trimethylsiloxysilyl) propylvinyl carbamate; NCVE *N*-carboxyvinyl ester; PBVC poly[dimethylsiloxyl] di [silylbutanol] bis[vinyl carbamate]; PVP polyvinyl pyrrolidone
* modulus data provided by Johnson & Johnson

5.2.5 To understand how the cell density influence the effects of substrate stiffness

In Chapter 1, it was found that when the inoculum cell density is higher than 10^9 cells/mL, there is no difference in adhesion between soft and stiff PDMS surfaces. Also, in 24 h biofilm, the difference was abolished. Both results indicate that high cell density or secreted metabolites could possibly influence the effects of surface stiffness. It will be interesting to investigate if the quorum sensing, physical contact, or certain metabolites also contribute to the influence of material stiffness on biofilm formation.

5.2.6 To understand the interaction between surface properties

Materials have many properties such as stiffness, topography, charges, chemistry etc. All the properties should be considered in material design. Although the effects of each surface

property on biofilm formation have been reported, how these factors interact has only been scarcely studied. It will be interesting to study it and how factors interact with each other, which can help reveal antagonist and synergistic effects.

5.3 References

(1) Baker, R. M.; Brasch, M. E.; Manning, M. L.; Henderson, J. H. Automated, contour-based tracking and analysis of cell behaviour over long time scales in environments of varying complexity and cell density. *Journal of The Royal Society Interface* **2014,** *11*, 20140386.

(2) Guttenplan, S. B.; Kearns, D. B. Regulation of flagellar motility during biofilm formation. *FEMS microbiology reviews* **2013,** *37*, 849-871.

(3) Arora, S. K.; Ritchings, B. W.; Almira, E. C.; Lory, S.; Ramphal, R. A transcriptional activator, FleQ, regulates mucin adhesion and flagellar gene expression in Pseudomonas aeruginosa in a cascade manner. *Journal of bacteriology* **1997,** *179*, 5574-5581.

(4) Hickman, J. W.; Harwood, C. S. Identification of FleQ from Pseudomonas aeruginosa as ac-di-GMP-responsive transcription factor. *Molecular microbiology* **2008,** *69*, 376-389.

(5) Renner, L. D.; Weibel, D. B. Physicochemical regulation of biofilm formation. *MRS bulletin* **2011,** *36*, 347-355.

(6) Cheng, G.; Zhang, Z.; Chen, S.; Bryers, J. D.; Jiang, S. Inhibition of bacterial adhesion and biofilm formation on zwitterionic surfaces. *Biomaterials* **2007,** *28*, 4192-4199.

(7) Nejadnik, M. R.; van der Mei, H. C.; Norde, W.; Busscher, H. J. Bacterial adhesion and growth on a polymer brush-coating. *Biomaterials* **2008,** *29*, 4117-4121.

(8) Hou, S.; Burton, E. A.; Wu, R. L.; Luk, Y.-Y.; Ren, D. Prolonged control of patterned biofilm formation by bio-inert surface chemistry. *Chemical Communications* **2009**, 1207-1209.

(9) Packham, D. E. Surface energy, surface topography and adhesion. *International journal of adhesion and adhesives* **2003,** *23*, 437-448.

(10) Oliveira, R.; Azeredo, J.; Teixeira, P.; Fonseca, A. The role of hydrophobicity in bacterial adhesion. **2001**.

(11) Singh, A. V.; Vyas, V.; Patil, R.; Sharma, V.; Scopelliti, P. E.; Bongiorno, G.; Podestà, A.; Lenardi, C.; Gade, W. N.; Milani, P. Quantitative characterization of the influence of the nanoscale morphology of nanostructured surfaces on bacterial adhesion and biofilm formation. *PloS one* **2011,** *6*, e25029.

(12) Díaz, C.; Cortizo, M. C.; Schilardi, P. L.; Saravia, S. G. G. d.; Mele, M. A. F. L. d. Influence of the nano-micro structure of the surface on bacterial adhesion. *Materials Research* **2007,** *10*, 11-14.

(13) Scheuerman, T. R.; Camper, A. K.; Hamilton, M. A. Effects of substratum topography on bacterial adhesion. *Journal of colloid and interface science* **1998,** *208*, 23-33.

(14) Perni, S.; Prokopovich, P. Micropatterning with conical features can control bacterial adhesion on silicone. *Soft Matter* **2013,** *9*, 1844-1851.

(15) Crawford, R. J.; Webb, H. K.; Truong, V. K.; Hasan, J.; Ivanova, E. P. Surface topographical factors influencing bacterial attachment. *Advances in Colloid and Interface Science* **2012**.

(16) Hou, S.; Gu, H.; Smith, C.; Ren, D. Microtopographic patterns affect Escherichia coli biofilm formation on poly (dimethylsiloxane) surfaces. *Langmuir* **2011,** *27*, 2686-2691.

(17) An, Y. H.; Friedman, R. J. Concise review of mechanisms of bacterial adhesion to biomaterial surfaces. *Journal of biomedical materials research* **1998,** *43*, 338-348.

(18) Lichter, J. A.; Thompson, M. T.; Delgadillo, M.; Nishikawa, T.; Rubner, M. F.; Van Vliet, K. J. Substrata mechanical stiffness can regulate adhesion of viable bacteria. *Biomacromolecules* **2008,** *9*, 1571-1578.

(19) Kolewe, K. W.; Peyton, S. R.; Schiffman, J. D. Fewer Bacteria Adhere to Softer Hydrogels. *ACS applied materials & interfaces* **2015,** *7*, 19562-19569.

(20) Zhang, R.; Ni, L.; Jin, Z.; Li, J.; Jin, F. Bacteria slingshot more on soft surfaces. *Nature communications* **2014,** *5*.

(21) Gabel, C. V.; Berg, H. C. The speed of the flagellar rotary motor of Escherichia coli varies linearly with protonmotive force. *Proceedings of the National Academy of Sciences* **2003,** *100*, 8748-8751.

(22) Yoo, J.-W.; Mitragotri, S. Polymer particles that switch shape in response to a stimulus. *Proceedings of the National Academy of Sciences* **2010,** *107*, 11205-11210.

(23) Champion, J. A.; Mitragotri, S. Role of target geometry in phagocytosis. *Proceedings of the National Academy of Sciences of the United States of America* **2006,** *103*, 4930-4934.

(24) Champion, J. A.; Mitragotri, S. Shape induced inhibition of phagocytosis of polymer particles. *Pharmaceutical research* **2009,** *26*, 244-249.

(25) Patel, N. R.; Bole, M.; Chen, C.; Hardin, C. C.; Kho, A. T.; Mih, J.; Deng, L.; Butler, J.; Tschumperlin, D.; Fredberg, J. J. Cell elasticity determines macrophage function. *PloS one* **2012,** *7*, e41024.

(26) Discher, D. E.; Janmey, P.; Wang, Y.-l. Tissue cells feel and respond to the stiffness of their substrate. *Science* **2005,** *310*, 1139-1143.

(27) Willcox, M.; Harmis, N.; Cowell, B.; Williams, T.; Holden, B. Bacterial interactions with contact lenses; effects of lens material, lens wear and microbial physiology. *Biomaterials* **2001,** *22*, 3235-3247.

(28) Dutta, D.; Cole, N.; Willcox, M. Factors influencing bacterial adhesion to contact lenses. *Molecular vision* **2012,** *18*, 14.

(29) Ubani, U. Common bacterial isolates from infected eyes. *Journal of the Nigerian Optometric Association* **2009,** *15*, 40-47.

(30) Jones, L.; Tighe, B. Silicone hydrogel contact lens materials update. *Silicone Hydrogels Online* **2004**.

(31) Song, F.; Koo, H.; Ren, D. Effects of material properties on bacterial adhesion and biofilm formation. *Journal of dental research* **2015**, 0022034515587690.

Fangchao Song

329 Link Hall
Syracuse University
Syracuse, NY 13244

Tel: (315)560-7922
E-mail: fasong@syr.edu
https://sites.google.com/site/fangchaosong/home

EDUCATION

Ph.D. in Chemical Engineering, Department of Biomedical and Chemical Engineering, Syracuse University, Syracuse, NY *May, 2016*

- Thesis: *Effects of material stiffness on biofilm infection and the physiology of attached bacterial cells*.
- Research Advisor: Dr. Dacheng Ren.

M.S. in Chemical Engineering, Department of Chemical and Biological Engineering, Zhejiang University, Hangzhou, China *September, 2010*

- Thesis: *Kinetics and Modelling of Melt/Solid polycondensation of poly(L-lactic acid)*.
- Research Advisor: Dr. Linbo Wu.

B.S. (with the honor of outstanding graduate) in Chemical Engineering, Department of Chemistry and Chemical Engineering, Shandong University, Jinan, China *June, 2007*

- Thesis: *Synthesis and characterization of carbosilane dendrimers used as silica-based stationary phases in high performance liquid chromatography (HPLC)*.
- Research Advisor: Dr. Shengyu Feng.

RESEARCH EXPERIENCE

Effects of material stiffness on bacterial adhesion and biofilm infection. (*03/2013 - present*)

- Firstly reported the effects of surface stiffness on the physiology of attached bacterial cells, phagocytosis, and the possible pathway of bacterial surface stiffness sensing.
- Two papers have been published in Langmuir and Journal of Dental Research, respectively; three papers are in preparation.
- Parts of the results will be summarized as my Ph.D. thesis.

Controlling bacterial persister cells and biofilms by synthetic brominated furanones. *(02/2012 - 3/2013)*

- Found that the brominated furanones (BFx), in particular, (*Z*)-4-bromo-5-(bromomethylene)-3-methylfuran-2(5*H*)-one (BF8) could be an anti-infective drug through inhibiting the persisters and biofilm formation.
- Two papers have been published in Bioorganic & Medicinal Chemistry Letters and Applied Microbiology and Biotechnology, respectively.

Persister formation in *Candida albicans* biofilm and the effects of Granulocyte macrophage colony-stimulating factor (GM-CSF) on fugal persisters. *(08/2012 - 1/2013)*

- Indicated that the diffusion of anti-fungal drug in biofilm is the more critical than the persister formation in *C. albicans* biofilm infection.

Effect of environmental factors on *E. coli* persister formation. (*02/2011 - 6/2012*)

- Reported the effects of medium viscosity, pH, oxygen, and nutrients on *E. coli* persister formation.

Process and kinetics of melt/solid polycondensation of poly(L-lactic acid). (*09/2007 - 07/2010*)

- Optimized the process of melt polycondensation, investigated the catalystic mechanism, developed the model of melt and solid processes, obtained kinetic parameters, optimized and simulated the melt and solid processes. The model was used in the scale-up of poly(lactic acid) manufacturing.
- Two papers have been published in Journal of Applied Polymer Science and *Industrial &*

Engineering Chemistry Research, respectively; two patents have been granted; two papers are in preparation.
- The results were summarized as my master thesis.

Kinetics and modeling of melt polycondensation reaction for synthesis of poly(butylene succinate-co-butylene terephthalate). (*09/2008 - 05/2010*)
- Constructed a model of melt polycondensation and simulated the melt polycondensation processes.
- One paper has been published in Macromolecular Reaction Engineering.

Synthesis and characterization of carbosilane dendrimers used as silica-based stationary phases in High-performance liquid chromatography (HPLC). (*02/2007 - 06/2007*)
- Synthesized the first generation carbosilane dendrimers by using methods of Hydrosilylation and Grignard Reaction, and then used it as adhesive to bond the dodecane to silica gel to synthesize silica-based stationary phases for HPLC.
- The results were summarized as my bachelor thesis.

Density function theory study and Quantitative structure-activity relationship for Lactams. (*03/2006 - 05/2006*)
- Used density functional theory (DFT) by Gaussian and Genetic Algorithm analysis by Materials studio to simulate the quantitative structure-activity relationship (QSAR) for Lactams.
- Awarded the Second Prize in Student Research Training Program.

PUBLICATIONS

■ *Published papers*

Fangchao Song, Hyun Koo, Dacheng Ren. *Effects of surface properties on bacterial adhesion and biofilm formation.* Journal of Dental Research, Volume 94, Issue 8, 1027-1034, 2015.

Fangchao Song, Dacheng Ren. *Stiffness of cross-linked poly(dimethylsiloxane) affects bacterial adhesion and antibiotic susceptibility of attached cells.* Langmuir, Volume 30, Issue 34, 10354-10362. 2014.

Jiachuan Pan, **Fangchao Song**, Dacheng Ren. *Controlling persister cells of Pseudomonas aeruginosa PDO300 by (Z)-4-bromo-5-(bromomethylene)-3-methylfuran-2(5H)-one.* Bioorganic & Medicinal Chemistry Letters. Volume 23, Issue 16, 4648-4651. 2013.

Jiachuan Pan, Xin Xie, Wang Tian, Ali Adem Bahar, Nan Lin, **Fangchao Song**, Jing An, Dacheng Ren*. (Z)-4-bromo-5-(bromomethylene)-3-methylfuran-2(5H)-one sensitizes Escherichia coli persister cells to antibiotics.* Applied microbiology and biotechnology, Volume 97, Issue 20, 9145-9154. 2013.

Bo Peng, Hongbing Hou, **Fangchao Song** et al. *Synthesis of high molecular weight poly(L-lactic acid) via melt/solid state polycondensation: II. Effect of pre-crystallization on solid state polycondensation of poly(L-lactic acid). Industrial & Engineering Chemistry Research*. Volume 51, Issue 14, 5190-5196. 2012.

Fangchao Song, Linbo Wu. *Synthesis of high molecular weight poly(L-lactic acid) via melt/solid polycondensation. I: Intensification of dehydration and oligomerization during melt polycondensation.* Journal of Applied Polymer Science. Volume 120, Issue 5, 2780-2785. 2011.

Lixia Hu, Linbo Wu, **Fangchao Song**, Bo-Geng Li. *Kinetics and modeling of melt polycondensation reaction for synthesis of poly(butylene succinate-co-butylene terephthalate) I- Esterification.* Macromolecular Reaction Engineering. Volume 4, Issue 9-10, 621-632. 2010.

■ *Papers in preparation*

Fangchao Song, Dacheng Ren*. Bacterial motility reveals motB is involved in response to material stiffness during Escherichia coli biofilm formation.*

Fangchao Song, Dacheng Ren. *oprF is involved in sensing of material stiffness by Pseudomonas aeruginosa.*

Fangchao Song, Yanrui Zhao, Dacheng Ren. *Effects of surfaces stiffness of poly(dimethyl-siloxane) on phagocytosis on E. coli biofilms.*

Yang Lu, Chunyang Wang, Wenjie Yuan, Shanshan Wei, Jiaoqi Gao, Boyuan Wang, **Fangchao Song**. *Actual measurement and analysis on microbial contamination in central air conditioning system at a venue in Dalian, China.*

Fangchao Song, Linbo Wu. *Synthesis of high molecular weight poly(L-lactic acid) via melt/solid polycondensa-tion. III: Kinetics of melt polymerization of L-lactic acid.*

Fangchao Song, Linbo Wu. *Synthesis of high molecular weight poly(L-lactic acid) via melt/solid polycondensa-tion. IV: Modelling of solid polymerization of oligo(L-lactic acid).*

■ *Conference presentations*

Fangchao Song, Dacheng Ren. *Material stiffness affects bacterial adhesion and the physiology of attached cells.* The 3rd Stevens Conference on Bacteria-Material Interactions. Hoboken, 2015.

Fangchao Song, Dacheng Ren. *Surface stiffness affects Escherichia coli adhesion, growth, and antibiotic susceptibility of attached cells.* 2014 AIChE Annual Meeting. Atlanta, 2014.

Linbo Wu, Weichao Wang, Dan Cao, Hongbing Hou, **Fangchao Song**, Zhaoqin Ma, Xiangying Sun. *Polycondensation Technologies for Synthesis of Poly(L-lactic acid) Materials.* The 4th International Conference of Technology and application of biodegradable Plastics (ICTABP4). Shanghai, China, 2010.

■ *Conference posters*

Fangchao Song, Megan Brasch, James Henderson, Dacheng Ren. *A role of material stiffness in bacterial adhesion and biofilm formation.* 7th ASM conference on biofilm. Chicago, 2015.

Fangchao Song, Dacheng Ren. *Surface stiffness affects Escherichia coli adhesion and antibiotic susceptibility of attached cells.* 114th General Meeting of American Society for Microbiology. Boston, 2014.

Fangchao Song, Linbo Wu. *Kinetics of melt polycondensation of L-lactic acid.* The 6th Chinese National Chemical and Biochemical Engineering Annual Meeting. Changsha, China, 2010.

PATENTS

Melt/solid state polycondensation preparation method for polylactic acid. **CN102040730**.
Melt/solid phase polycondensation preparation method of polylactic acid material with high molecular weight and high crystallinity. **CN102002147**.

AWARDS AND HONORS

Syracuse University Outstanding TA Award, Syracuse University *04/2015*
Best presentation of session, 2014 AIChE Annual Meeting *03/2015*
Graduate Student Organization Travel Grant, Syracuse University *11/2014*
Nunan Travel Grant, Syracuse University *04/2014*
The First-class graduate fellowship, Zhejiang University 09/2007

Outstanding Graduates, Shandong University *06/2007*
The Innovation Scholarship, Shandong University *12/2006*
The First-class Outstanding Student Scholarship (Top 4%), Shandong University *10/2006*
Student award for research and Innovation, Shandong University *12/2005*
Excellent Student Leader, Shandong University *11/2005*
The Second-Class Outstanding Student Scholarship (Top 10%), Shandong University *10/2004*

SCIENTIFIC AND TECHNICAL COMPETITIONS

The Meritorious Winner (Top 14%) in the Mathematical Contest in Modeling (MCM) *02/2007*
The Best Presentation in the Research of supercritical fluid technology and its application *11/2006*
The First Prize in Design of float valve rectifying tower for distilling alcohol *05/2006*
The Third Prize in the 5th 'Challenge Cup' Contest in Business Project *03/2006*
Honorable Mention in the Interdisciplinary Contest in Modeling (ICM) *02/2006*
The Second Prize in the Student Research and Training Program *05/2006*
The First Prize (Top 3%) in Chinese Undergraduate Mathematical Contest in Modeling *09/2005*
The Second Prize in the National Contest of Physics *09/2002*
The Third Prize in the National Contest of Chemistry *06/2000*
The First Prize in the National Contest of biology *05/1999*

CERTIFICATONS

Certification of successfully completing ExploRX Explore Statistics with R *11/2014*
Certification of successfully completing Circuits and Electronics 6.002x *07/2012*
National Computer Rank Examination Certificate (Specializing in Database) *04/2005*

SKILLS AND INTERESTS

Software: Matlab, Aspen, Lingo, Origin, AutoCAD, Microsoft Office.
Programming Languages: C, Matlab, R.
Languages: English and Mandarin.
Skills: GC, HPLC, GPC, DSC, TGA, IR, DMA, Viscometer, Optical microscopy, Electrophoresis, AFM, SEM, Photolithography, Cloning, PCR, Flow cytometer, RNA isolation, Cell cultures, Viability test, NMR.
Interests: Microbiology, Polymers, Chemical engineering, Surface engineering, Mathematical modeling, Computing, Physics, Basketball, Soccer.

TRAINING AND INTERNSHIP

Photolithography, Cornell Nanoscale Science and Technology Facility (CNF), Ithaca, NY, *12/2014*

- Joined the community of CNF, learnt and improved the skill of mask making and photolithography, especially the SU-8 photolithography.

Process Engineer, Qingdao Soda Ash Industrial Co., Ltd, Qingdao, China, *07/2006*

- Obtained the training of manufacturing sodium bicarbonate, including the process control and the technical process design.

TEACHING EXPERIENCE

Syracuse University:

Teaching Assistant: CEN/BEN 575 Process Control *Spring 2015 and Spring 2016*

- Supervised students to understand the class materials, graded the homework, and evaluated the students' performance.

Teaching Assistant: CEN/BEN 301 Biological Principle for Engineers *Fall 2014*

- Collaborated with the professor to design the lab and created the lab instructions, made the lab purchases, assessed the budget, prepared the lab stuffs, and led the lab independently, as well as evaluated the students' performance.

Teaching Assistant: CEN/BEN 341 Heat and Mass Transfer *Spring 2013*

- Created the lecture materials based on the class contents and students' questions, instructed students in the recitation for understanding the principles of heat and mass transfer.

SERVICE

Mentor, *Research mentor for Research Experience for Undergraduate, Syracuse University*, *2013*
Co-chair, *the 39th Annual northeast bioengineering conference – Modeling section, Syracuse, 2013*
Volunteer, *the 4th Chinese National Chemical and Bio- Engineering Annual Meeting, Hangzhou*, *2007*
Student Leader, *Department of Chemical Engineering at Shandong University, Jinan*, 2004-2007
Volunteer, *External Relations of Young Volunteers Association, Jinan*, *2003-2005*

PROFESSIONAL AFFILIATIONS

American Institute of Chemical Engineers (AIChE)
American Society for Microbiology (ASM)
American Association for the Advancement of Science (AAAS)
Biomedical Engineering Society (BMES)